STATE: Montana
AGENCY: Fish, Wildlife & Parks
GRANT: Grouse Food, Pollinator, and Dung Beetle Ecology - Grazing
MT TRACKING: W-164-R1

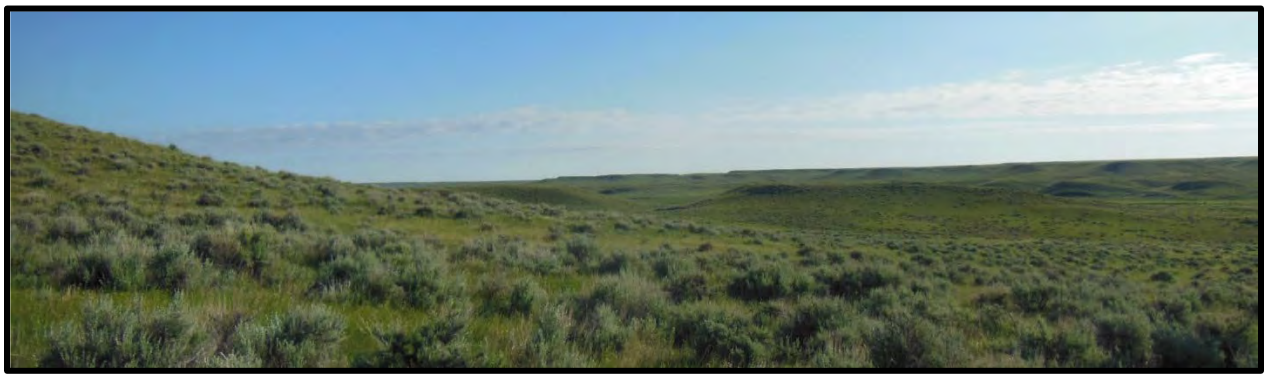

Photo by the Avian Science Center, University of Montana, Missoula

Submitted by:

Jessica Mitchell, Ph.D. and Claudine Tobalske, Ph.D.
Director and GIS Analyst / Ecologist
Spatial Analysis Laboratory
University of Montana

Lorelle Berkeley, Ph.D. and Mark Szczypinski
Wildlife Research Biologist and Science Technician
Wildlife Division, Research Bureau
Montana Fish, Wildlife, and Parks

Victoria Dreitz, Ph.D. and Jennifer Helm
Associate Professor, Director of Avian Science Center and PhD. Candidate
Wildlife Biology Program, W.A. Franke College of Forestry and Conservation
University of Montana

Predictive Spatial Layer of Invertebrate Biomass for Sage-Grouse and Songbird Grazing Studies in Central Montana

9/30/2021

Final Report

Contents

List of Figures

Predictive Spatial Layer of Invertebrate Biomass for Sage-Grouse and Songbird Grazing Studies in Central Montana

FINAL REPORT

Submitted to: Montana Fish, Wildlife, and Parks, and the U.S. Fish and Wildlife Service

Authors: Jessica Mitchell and Claudine Tobalske, Spatial Analysis Laboratory, University of Montana, Missoula, MT 59812; Lorelle Berkeley and Mark Szczypinski, Montana Fish, Wildlife and Parks, Wildlife Division, Helena, MT 59620; and Victoria Dreitz, Wildlife Biology Program and Avian Science Center, W.A. Franke College of Forestry and Conservation, University of Montana, Missoula, 59812.

Period of Agreement Date: Apr 1, 2016 – Jun 30, 2021

EXECUTIVE SUMMARY

Previous studies suggest that invertebrates are vital to sage-grouse diets when they are available, composing 10-15% of adult sage-grouse diets during the spring and summer. In particular, invertebrates compose a large part of diets for sage-grouse chicks and may be important for their survival, and also that of hens during the spring/summer. Areas with higher densities of invertebrates are preferred by hens with broods.

Little is known about the foraging habits of songbirds in central Montana. But in general, across their distributions, invertebrates are a mainstay of the diets of several of the songbird species found there that are of conservation concern including Brewer's Sparrow, Sage Thrasher, McCown's Longspur, Chestnut-collared Longspur, and Lark Bunting.

Montana Fish, Wildlife, and Park's (FWP) sage-grouse grazing project (PR grant #F15AF00490 "MT Sage-Grouse Grazing Evaluation") is estimating habitat use and survival for sage-grouse hens and chicks in

central Montana, and how these are influenced by grazing and habitat variables. In conjunction, the University of Montana – Avian Science Center is evaluating how grazing affects songbird diversity, abundance, and reproduction in the same location (PR grant #F16AF00294 "Migratory Songbird Grazing Study"). However, these projects are not measuring invertebrate availability as a food resource for birds. This agreement focuses on measuring this key resource for both projects to help evaluate the effects of grazing management on invertebrates and the implications for conservation of sage-grouse and songbird populations in this area.

Data collected through 2017 focused on evaluating the overall effect of the Natural Resources Conservation Service's Sage-Grouse Initiative (SGI) grazing management on invertebrate diversity and abundance. This work provided a foundation that describes the structure of invertebrate communities in our study area and the effects of grazing on these communities. Results from these data suggested that invertebrates, particularly those preferred by sage-grouse, responded positively to pasture rest during the early brood-rearing period. But invertebrate sampling has not yet been linked to sage-grouse demographics or songbird communities. Since 2017 under this agreement, our focus has been on evaluating the relationship of invertebrate biomass to songbird communities and sage-grouse demographics, population dynamics, and habitat use.

The objective of this project was to create a predictive spatial layer of invertebrate biomass across the sage-grouse (PR grant #F15AF00490 "MT Sage-Grouse Grazing Evaluation") and songbird (PR grant #F16AF00294 "Migratory Songbird Grazing Study") grazing project study areas in central Montana to provide invertebrate food availability data for sage-grouse grazing project vital rate, habitat use, and population models, and songbird grazing project reproduction, community, and abundance models. We completed data collection during spring/summer 2020 and herein report on the final spatial layer that was generated. This is the final report for PR #F16AF00293 "Grouse Food, Pollinator, and Dung Beetle Ecology – Grazing" on generating the predictive invertebrate biomass spatial layer for the sage-grouse and songbird study areas, but we will continue to fine-tune this layer and further analyze invertebrate biomass data for PR grant # F21AF01330 Sage-Grouse/Songbird/Bug Grazing Project.

Arthropod biomass sweep data collected between 2012 and 2018 at 59 locations in the Lake Mason area were provided to the Spatial Analysis Lab. Using a variety of land cover, remote sensing derived, and climate predictive variables, a RandomForest model was developed and extrapolated to generate a continuous surface of biomass for the entire study area. Percent bare ground, percent shrub cover, Gross Primary Productivity for 08/2014 and Mean Gross Primary Productivity for June (2012-2018) were among the most important variables; the best model explained 26.7% of biomass variance and was used to inform the 2019 field season. Between May 1 and July 30, 2019, detailed vegetation data and arthropods were collected at 47 field locations, some visited 2 or 3 times for a total of 114 visits. An additional 191 sites were visited for arthropod collection only and did not include detailed vegetation data. Despite some trends (e.g. decreasing biomass with increasing bare ground, increasing biomass with increasing herbaceous cover) these new data failed to provide a satisfactory model or improve on the first one. The 2020 field season consisted of 218 sampling sites, which served as input for new models; because

of a dramatic increase in biomass compared with previous years, these models were developed using 2020 field samples only. To spatially expand the model to a larger area covering all songbird sampling locations, new predictive variables, such as vegetation data from the Rangeland Analysis Platform and climate variables from the stand-alone program ClimateNA, were generated. Model development followed a two-step approach: a first batch of 20 models identified the most important variables from a set of 58, which served as input for a second batch of 20 models. Aside from elevation and mean litter 2011-2020, all important variables were broad-scale climate variables from ClimateNA. On average, the second batch of models explained 30.8% of arthropod variance. Additional variables such as grazing treatment and landscape metrics were tested for importance, but failed to increase predictive power.

The sampling for this project was designed to provide data for the spatial layer. However, for influential variables identified from the modeling effort, we tried to explore the relationship of these variables with invertebrate biomass. We used multiple categorizations of SGI grazing management to evaluate the relationship of this Initiative with invertebrate biomass. Our sample sizes were not large enough in some of the categories to detect differences. We did not see a relationship of SGI grazing management with invertebrate biomass, though SGI enrolled pastures tended to have increased invertebrate biomass over those that did not. However, this included pastures that were enrolled but the SGI grazing system had not yet been implemented. The relationship is not clear and further study would be helpful.

This document is a concatenation of three previous reports and presents the datasets and models generated each year.

BACKGROUND

Greater sage-grouse (*Centrocercus urophasianus*; hereafter 'sage-grouse') populations have been in decline in the western U.S. since the 1950s (Connelly and Braun 1997), and approximately 76% of sagebrush (*Artemisia* spp.) -associated songbird species are declining nationally (Saab and Rich 1997; Paige and Ritter 1999; Dobkin et al. 2008). Sage-grouse conservation is currently a priority, as this species was a candidate for protection under the Endangered Species Act (ESA) in 2010 and 2015. In 2015, the U.S. Fish and Wildlife Service (USFWS 2015) determined that listing the sage-grouse was not warranted, in part, due to collaborative conservation efforts among agencies and private landowners. The status of sage-grouse is currently being re-evaluated by USFWS. Information on the effects of grazing on sage-grouse and their habitat, which includes food sources such as invertebrates, is needed to provide support for conservation efforts.

Sage-grouse share their habitat with several migratory songbird species that breed in Montana's sagebrush systems and are also of conservation concern, including: Brewer's sparrow (*Spizella breweria*), sage thrasher (*Oreoscoptes montanus*), thick-billed longspur (*Calcarius mccownii*), chestnut-collared longspur (*Calcarius ornatus*), and lark bunting (*Calamospiza melanocorys*; Casey 2000, Rich et al. 2004). Sagebrush-nesting species make up the largest number of Species of Continental Importance within the Intermountain West (Rich et al. 2004). Songbirds are often used as indicators for ecosystem health in sagebrush steppe habitat because of their mobile and conspicuous nature (Bradford et al. 1998). Therefore, it is important to

understand the big picture of sagebrush ecosystem status and the several species that rely on it, and how our conservation efforts affect the ecosystem.

Declines in sagebrush-associated avian species are congruent with significant losses of sagebrush habitat (Braun et al. 1976, Knick 1999). Conversion of sagebrush to agriculture (Connelly et al. 2004, Smith et al. 2016); fragmentation resulting from energy (Naugle et al. 2011) or subdivision development (Leu and Hanser 2011); conifer invasion (e.g., in Oregon and western Montana; Crawford et al. 2004, Beck et al. 2012); and modifications, such as prescribed fire, herbicides, and some grazing practices that lead to exotic, annual grass establishment are significant stressors on sagebrush systems (Rich et al. 2005, MTSWAP 2015).

Livestock grazing is a land use that is receiving much scrutiny regarding its effects on wildlife populations because it is so prevalent in sagebrush systems. It is the largest land management practice in the world (Krausman et al. 2009) and the dominant land management practice in sagebrush habitat, affecting 70% of land in the western United States (Fleischner 1994). Thus, this land use is not likely to disappear, and is one of the many land uses we must learn how to manage for desired stakeholder and wildlife management goals.

Livestock grazing affects sagebrush habitat by altering its vegetation structure, composition, and productivity (Beck and Mitchell 2000, Hormay 1970, Krausman et al. 2009). There is growing recognition that livestock grazing can be manipulated to positively affect sagebrush-associated bird habitat (Holechek et al. 1998, Coppedge et al. 2008). However, heavy livestock grazing can have negative effects on bird habitat, such as decreasing invertebrate biomass (Krausman et al. 2009), an important food source for several bird species including sage-grouse and migratory songbirds.

The Sage-Grouse Initiative (SGI) Program

The SGI grazing program in central Montana focuses on improving livestock production and rangeland health while simultaneously alleviating threats to and improving habitat for greater sage-grouse (USDA 2015). The SGI program occurred on private ranches containing potential sage-grouse habitat as defined by topography and sagebrush canopy cover ≥5% (NRCS pers. comm.) within sage-grouse core areas (Figure 1a). Montana Fish, Wildlife and Parks (FWP) designated core areas in Montana as locations of highest conservation value for sage-grouse based on habitat and number of breeding males (Figure 2). FWP estimated that the core areas included ~76% of the displaying males in Montana as of 2013. The NRCS enrolled more than 400,000 acres of pasture lands in the SGI grazing program across Montana (NRCS pers. comm.).

Livestock producers enrolled in the SGI program implement an approximately three-year grazing regime developed with NRCS range management specialists. Range management specialists could suggest pasture rest, pasture deferment, changing the number of animal units, or installing fences or water sources to adjust pasture size or livestock distribution. SGI grazing regimes were tailored to each ranch and varied by needs of the producer or with pasture condition while following the NRCS Conservation

Practice Standard for Prescribed Grazing (NRCS 2017, Smith et al. 2018). Additionally, plans align with four minimum criteria intended to support sage-grouse habitat:

1. Grazing utilization rates of ≤50% of the current year's key forage species growth,
2. ≥20-day shift annually in the timing of grazing,
3. A plan to address unexpected circumstances like drought or fire,
4. ≤45-day continuous grazing durations within any one pasture (Smith et al. 2018).

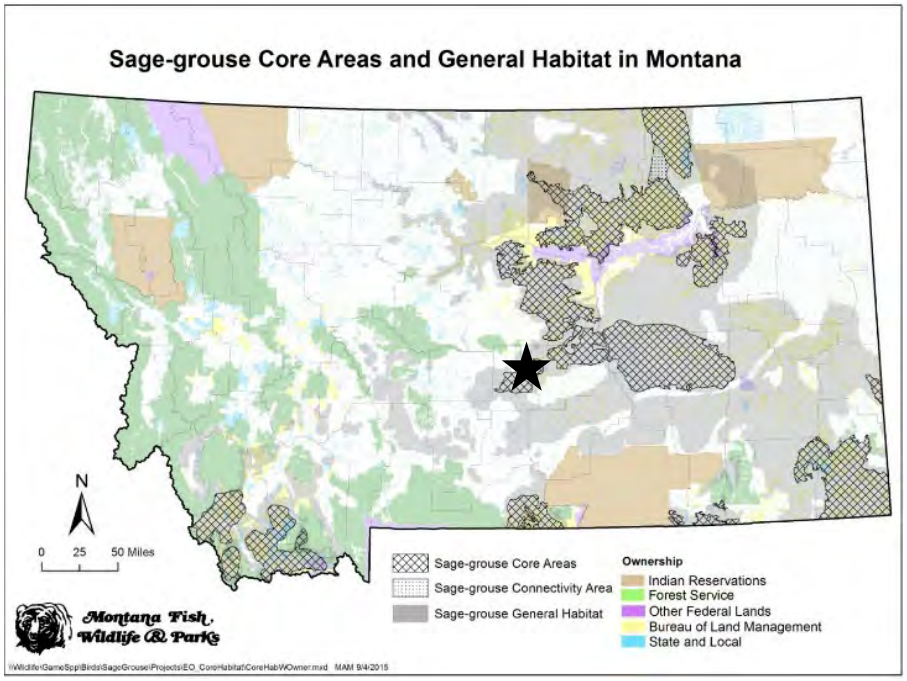

Figure 1. Greater sage-grouse core areas as defined by Montana Fish, Wildlife & Parks in 2013. The black star represents the location of the study area for this project in Golden Valley and Musselshell Counties, Montana, USA.

SGI grazing regimes are rotational and use a combination of rest and deferment to increase vegetation cover for nesting birds (Doherty et al. 2014, Smith et al. 2018), in addition to other strategies. But a component of functional habitat for sage-grouse includes food resources such as invertebrates. Even though our goal was to model invertebrate biomass, we attempted to evaluate relationships between SGI grazing management and invertebrate biomass.

Chick survival is the most concerning demographic rate in sage-grouse (Aldridge and Boyce 2007, Gregg and Crawford 2009, Dahlgren et al. 2010, Guttery et al. 2013) and is relatively low compared to adult female (hereafter 'hen') survival and nest success in FWP's central Montana sage-grouse grazing project (PR grant #F15AF00490 "MT Sage-Grouse Grazing Evaluation"; Berkeley et al. 2019). Dahlgren et al. (2016) suggest that invertebrates may be important for sage-grouse chick survival, especially during the early brood-rearing period (<21 days), and important for nesting hens. They are a rich source of protein, particularly during the spring when plants have not begun growing and energetic needs for nesting hens are high. Johnson and Boyce (1990) suggest that invertebrates are vital to sage-grouse chick survival and

that invertebrates compose a large part of diets in chicks (see also discussion and references in Drut et al. 1994 and Thompson et al. 2006). Fischer et al. (1996) suggest that areas with higher densities of invertebrates are preferred by hens with broods. Invertebrates, orthopterans (grasshoppers, crickets, katydids) in particular, have also been shown to be an important food source for other species in the grouse taxanomic subfamily Tetraonidae including greater prairie chickens (*Tympanuchus cupido*) (Londe et al. 2021).

Little is known about the foraging habits of songbirds in central Montana. But in general, across their distributions, invertebrates are a mainstay of the diets of several songbird species found in this area and mentioned above as species of conservation concern including Brewer's sparrow, sage thrasher, thick-billed longspur, chestnut-collared longspur, and lark bunting (Rodewald 2015). These species eat a combination of ground-dwelling and above-ground invertebrates (Rodewald 2015).

FWP's sage-grouse grazing project is estimating habitat use for sage-grouse hens and chicks and how these are influenced by grazing management and habitat characteristics in central Montana. The University of Montana – Avian Science Center's songbird grazing project (PR grant #F16AF00294 "Migratory Songbird Grazing Study", Dreitz et al. 2019) is evaluating how grazing affects songbird diversity, abundance, and reproduction in the same location. However, these projects are not measuring invertebrate availability as a food source for birds. Our goal is to measure this key resource for both projects to help evaluate the effects of grazing management on invertebrates and the implications for conservation of sage-grouse and songbird communities in this area.

Objective

Our primary objective was to create a spatial layer that predicts invertebrate biomass for the sage-grouse and songbird grazing project study areas.

METHODS

The study area covers 250,389 ha mostly in the Golden Valley and Musselshell counties of central Montana (Figure 1b), near the town of Roundup in big sagebrush steppe habitat. Big sagebrush steppe is the most widely distributed sagebrush system in Montana, and is typically characterized by Wyoming big sage (*Artemisia tridentata* ssp. *wyomingensis*) with perennial grasses and forbs dominating at least 25% of cover (Montana Natural Heritage Program 2011). The area is also dominated by privately held agricultural areas. We accomplished our objective by sampling invertebrates at stratified random points (see description, next paragraph) throughout the study areas in central Montana. These samples were then dried and weighed (see above) to obtain a biomass value for each sampling point.

Our sage-grouse and songbird study areas included ranches enrolled in SGI as well as ranches that were not enrolled. Both categories included private and public land. All public land was leased by producers and managed as part of larger ranches. We were able to obtain grazing data from producers with both enrolled and not enrolled ranches. There were a few producers for which we were not able to access their land or obtain grazing data, and this is why we have some unknowns in the data.

We sampled invertebrates at stratified random sites, rather than at sage-grouse nest and brood locations, to reduce sampling effort. Instead we focused on adequate sampling across the study area and in areas of higher uncertainty to accomplish our objective of creating a predictive spatial layer by modeling invertebrate biomass as a function of habitat predictors. This strategy enabled us to use a model to predict the biomass of food insects available to sage-grouse and songbirds at locations we did not sample. In addition, this effort made use of the data already collected for the grazing aspect of this project from 2012-2017. We provide a general summary of our methods and results below.

MODELING THE DISTRIBUTION OF INVERTEBRATE BIOMASS

FINAL REPORT

CLAUDINE TOBALSKE AND JESSICA MITCHELL
SPATIAL ANALYSIS LAB, THE UNIVERSITY OF MONTANA

Invertebrate Biomass Model – 2012-2018 Data

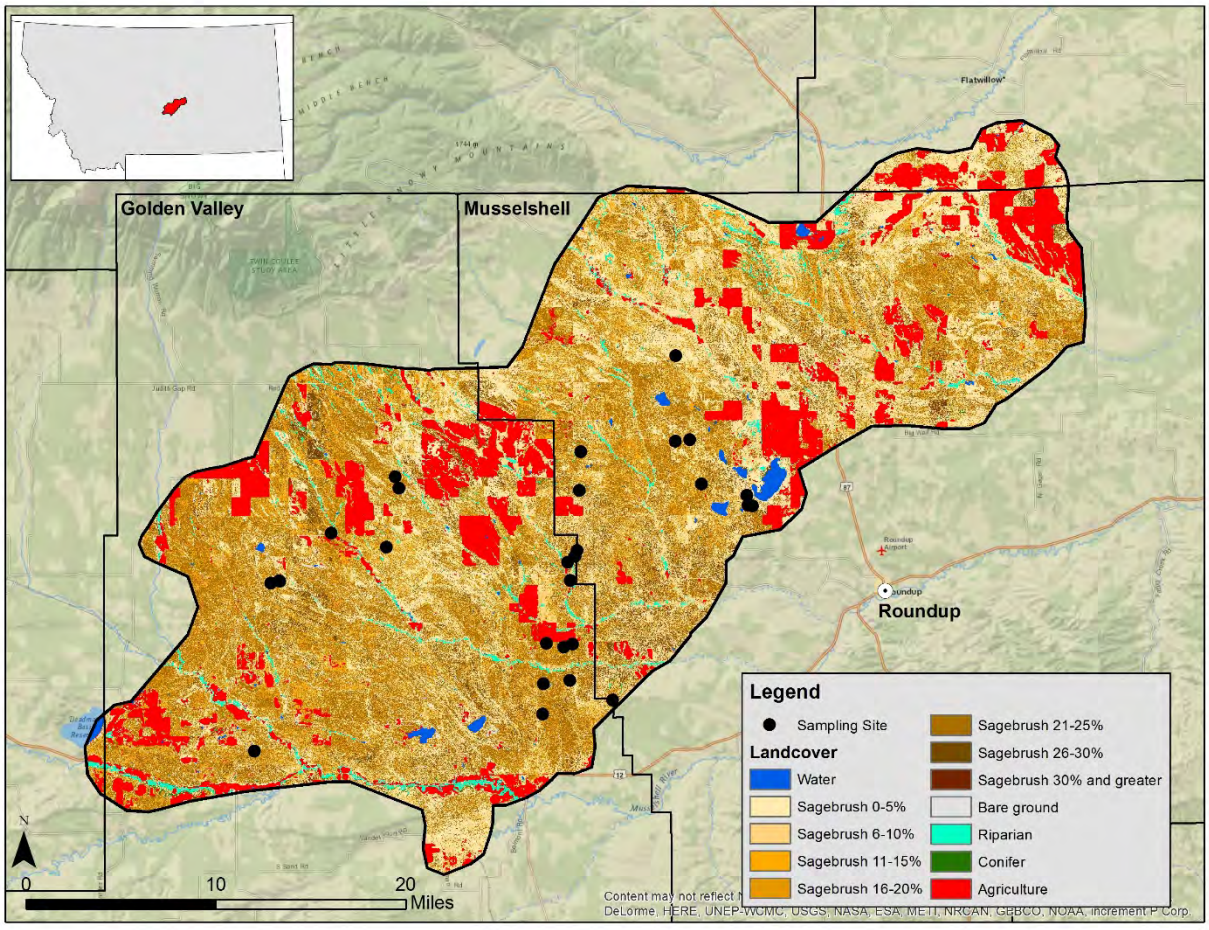

Figure 1b. Study area location in Montana and land cover composition.

METHODS

Biomass Data

A total of 2,541 samples of arthropod biomass (dried, grams) were collected between May 31, 2012 and June 30, 2017 at 30 different geographic locations within the study area; however, one site (Lehfeldt E1N) was eliminated from analysis due to missing x-y coordinates. Arthropod sampling methods included sweeps (all sites) and pitfalls (12 sites), with method also listed as "Not recorded" for some samples at nine sites. Comparison of biomass values from these "Not recorded" samples with those of sweep samples showed no significant difference (Figure 2), so they were considered "sweeps" and used in the analysis. On the other hand, pitfalls samples resulted in much higher biomass values than sweeps samples for the 12 sites where they were also collected at (although with a large standard deviation, Figure 3), so the Random Forest model was run using only sweep samples (n = 1,641).

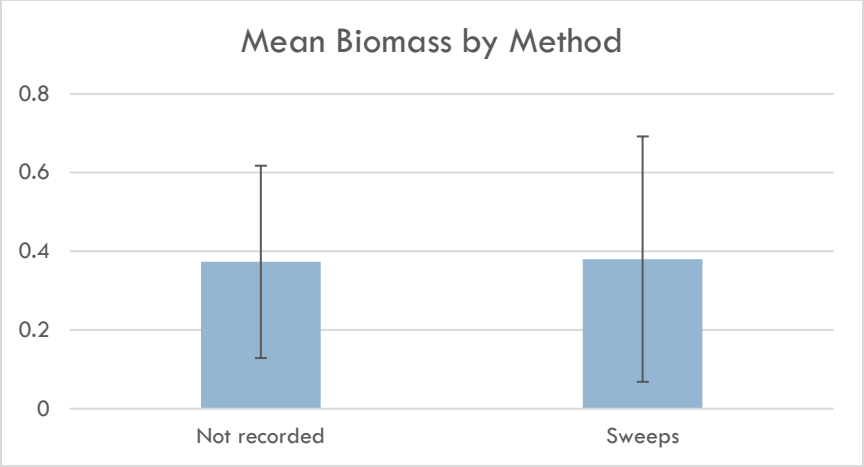

Figure 2. Mean arthropod biomass comparison at nine sites from two different methods.

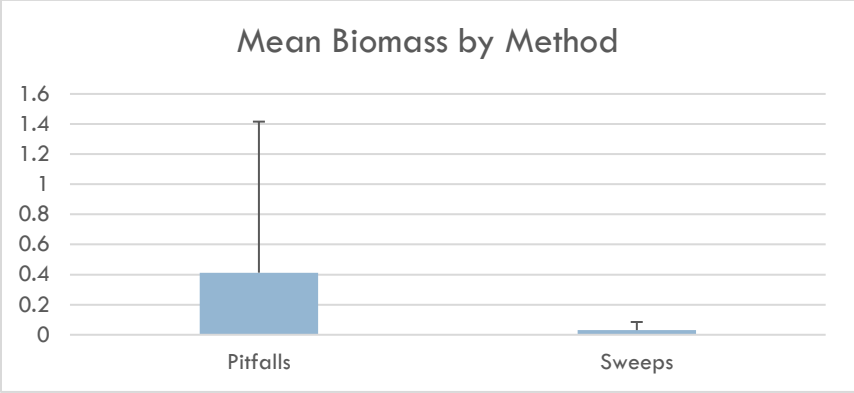

Figure 3. Mean arthropod biomass comparison at twelve sites from two different methods.

An additional 30 new sites were sampled in 2018, using sweeps as well as shrub litter and shrub brushing in a quadrant design. Despite similar biomass between "Shrub" and "Sweep" methods (Figure 4), only those samples collected by the sweep method were included in the analysis to maintain consistency in sampling and to put more effort into sampling more sites rather than using multiple, more intensive methods at fewer sites.

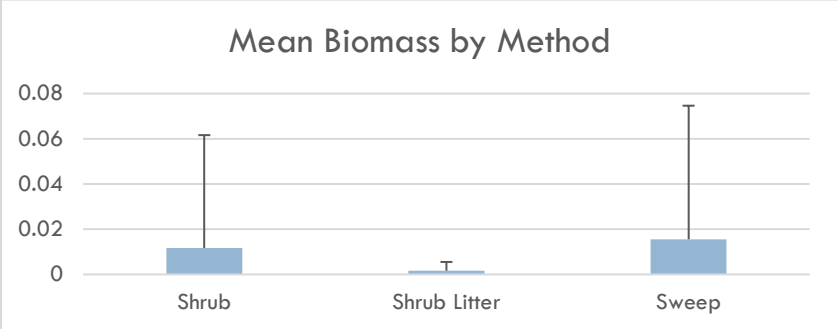

Figure 4. Mean arthropod biomass comparison at 30 sites from three different methods.

Arthropod order was collected for all but 105 samples, 58 of which used the sweep method; a single biomass measurement was provided for each date, most likely the summed biomass at the site for that day. To make biomass data comparable among all sites, the 2012-2017 biomass entries were summed by site ID and collection date, then total average biomass was calculated for each site. Values averaged 0.193 gram/site and ranged from 0.0036 grams at site 32092 to 0.8409 grams at site 33018, with the majority of sites averaging less than 0.1 gram (Figure 5). These biomass averages became the "dependent" variable of the model. Because the largest biomass value was an outlier that influenced model outcome, two versions of the model are considered: one including the outlier, one excluding it. This approach maximized the number of sample sites; there was not a large enough sample size to support grouping by arthropod order, or by early season vs late season biomass.

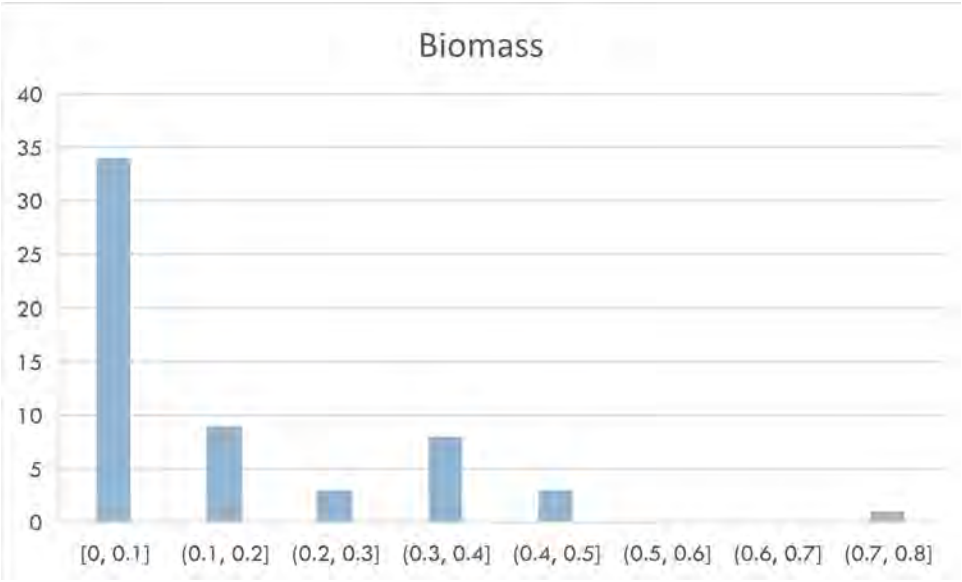

Figure 5. Mean arthropod biomass distribution at 59 sites in the Lake Mason area, 2012-2018.

Predictive Layers

Four different vegetation layers were generated at 1m pixel resolution by Open Range Consulting (2015) by classifying 2013 NAIP imagery: land cover (categorical variable, Figure 1), percent herbaceous cover, percent ground cover, and percent shrub cover (all three continuous variables). Because most land cover classes were differentiated by percent sagebrush cover, and to simplify the analysis, the land cover layer was treated as a continuous dataset by basing it on percent sagebrush, and assigning 0 to all non sagebrush classes.

Landsat Gross Primary Production data (GPP; Robinson et al. 2018; https://developers.google.com/earth-engine/datasets/catalog/UMT_NTSG_v2_LANDSAT_GPP) (30m pixel resolution) were extracted in Google Earth Engine for May, June, July, August and September 2012 through 2018 and averaged by month. Monthly minimum, maximum and mean temperature rasters (800m pixel resolution) were downloaded from the Montana Climate Office website (http://climate.umt.edu/products/meteorology/temperature.php) for May through September 2002-2012 (the most recent year available) and averaged by month, resulting in 15 variables. Finally, open water and wetlands were extracted from the Montana NWI database (http://geoinfo.msl.mt.gov/home/msdi/wetlands) and rasters of continuous Euclidean distance to the nearest polygon were generated for each. All GIS analyses were conducted using ArcGIS 10.6, unless noted otherwise.

Since the pixel size for the predictive variables varied greatly (1m to 800m), predictive layers were resampled to 30m using the DEGRADE command in Erdas Imagine for the continuous 1m NAIP percent cover rasters and the RESAMPLE command in ArcGIS for all other non-30m rasters (NAIP land cover and temperature rasters). In addition to considerably reducing processing time, this pixel size matched that of field vegetation plots, which are the same type of plot used for arthropod sampling.

Predictive Model

Values for the resampled variables were extracted at each of the 59 sites in ArcGIS and exported to a .csv. For biomass modeling, I used the R package ModelMap (Freeman et al, 2019) in R 3.3.2. This package constructs predictive models of continuous or discrete response variables using Random Forest, allowing for validation with an independent dataset and creation of graphs and tables of basic model validation diagnostics, as well as extrapolation of the model to create prediction surfaces – including map measures of uncertainty such as standard deviation and coefficient of variation for each pixel.

Several versions of the models were run, with and without the outlier biomass, but also with different sets of variables. For example, one run included only mean monthly GPP (5 GPP variables) and another also used individual month/year values (5 + 35 GPP variables).

Other variables were considered (e.g. soil data from SSURGO, Relative Annual Effective Precipitation) but their inclusion did not improve model prediction abilities.

ModelMap offers the possibility of randomly splitting the dataset into training (80%) and validation (20%) sets, based on a user-input seed value. Although this approach gives a better indication of model performance than statistics resulting from within-set substitutions, the small number of samples resulted in quite different outcomes based on what seed number was used. To make sure that both training and validation sets contained similar proportions of smaller and larger biomass values, I split the dataset into training (N = 47) and validation (N = 12) after stratifying by biomass.

The other seed input, for Random Forest proper, also resulted in small variations among models. For each dataset (with and without outlier), I ran models while increasing seed value by 5 (i.e. 5, 10, etc, through 45) and compared model performance and variable importance based on percent increase mean square error (mse; the increase in mse of predictions as a result of the variable being permuted). Model performance was evaluated by percent variance explained and Pearson's and Spearman's correlation coefficients between observed and predicted values of the validation dataset.

New Sampling Sites

A lattice of potential sampling points was automatically generated in ArcGIS, with points regularly spaced by 200m (the minimum distance between two sampling points for the 2018 field season). Cadastral data for Golden Valley and Musselshell counties were downloaded from the Montana Geographic Information Clearinghouse (http://geoinfo.msl.mt.gov/msdi/cadastral) and points overlapping parcels with denied access were deleted. Points falling within the Department of Revenue Final Land Unit agricultural parcels (https://mslservices.mt.gov/Geographic_Information/Data/DataList/datalist_Details.aspx?did={0d715638-eef4-4c69-8d26-a83aff6c7cf2}) were also deleted because, for the goals of the project, we were only sampling sagebrush habitat. Finally, points located within 200m of a site sampled previously (for arthropod biomass and bird data) were deleted, leaving 42,026 to select from. A 1ha circular buffer was centered on each point and percent bare ground (the most important biomass predictor, see results below, also the variable used to stratify sampling in 2018) was extracted for each, along with mean predicted biomass and mean biomass coefficient of variation. Continuous percent bare ground was classified into 4 categories (0-10%, 10-25%, 25-50% and >=50%).

The Sampling Design Tool (NOAA/NOS/NCCOS/CCMA/Biogeography Branch) was used to randomly select 50 points in each of the bottom three bare ground classes; because only 21 points had over 50% bare ground, they were all selected. Mean biomass and mean coefficient of variation (a measure of model uncertainty) were computed at the randomly selected sites and compared to point population values.

RESULTS

Predictive Models

Models developed without the outlier data yielded better percent variance explained, yet no model explained more than a quarter of the variance in the data (Figure 6).

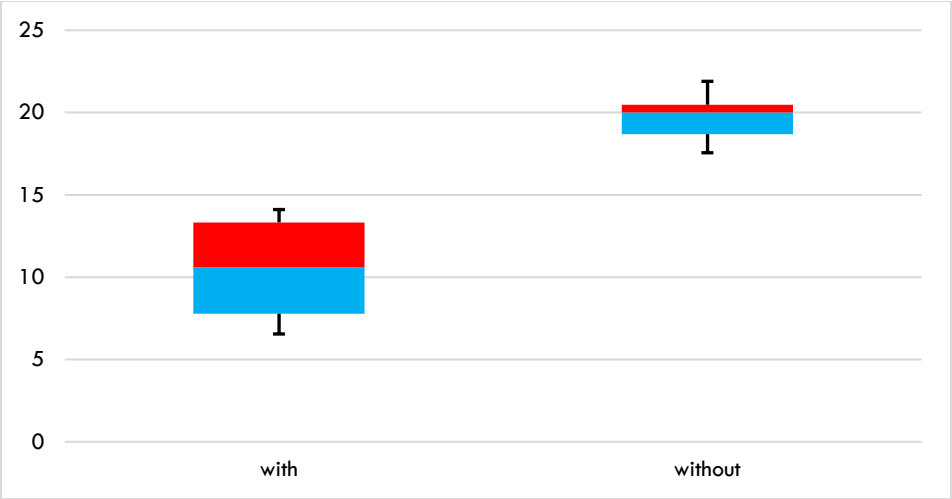

Figure 6. Boxplot comparison of Random Forest models of arthropod biomass generated from nine seed values for data including or excluding an outlier biomass value.

For both datasets, most Pearson and Spearman correlation values between observed and predicted were greater than 0.75. Among the top 6 most important variables regardless of model type, Percent Bare Ground, Percent Shrub Cover, Gross Primary Productivity for 08/2014 and Mean Gross Primary Productivity for June (2012-2018) consistently came at the top (Table 1). Comparing percent variance explained, correlation coefficients and most important variables among the nine models for each dataset, a "best model" was selected then applied to the entire dataset (i.e., no splitting into training and validation). For the dataset with outlier, this full model explained 17.15% of the variance; for the dataset without, it explained 26.7%. Pearson's and Spearman's plotted coefficients for the full models are presented in Figure 7, and percent increase in MSE in Figure 8.

Table 1. Comparison of nine Random Forest model characteristics (Percent variance explained, Pearson's and Spearman's coefficients for validation sets, and top 6 most important variables) for two datasets of arthropod biomass, including or excluding an outlier value. The models highlighted in yellow were selected for running on the full datasets.

WITH

seed	%Var	Pearson	Spearman	var1	var2	var3	var4	var5	var6
5	10.6	0.79	0.74	bare	shrub	GPP0814	GPP06	GPP0618	GPP05
10	7.72	0.75	0.76	bare	shrub	GPP06	GPP0814	Tmin08	GPP05
15	13.84	0.81	0.75	bare	shrub	GPP0814	GPP06	GPP0618	Tmin08
20	6.55	0.79	0.74	bare	GPP0814	shrub	GPP0618	GPP07	Tmin08
25	13.33	0.81	0.73	bare	shrub	GPP0814	Tmin08	GPP0618	GPP0817
30	7.9	0.78	0.76	shrub	GPP0814	bare	GPP0618	GPP05	GPP0516
35	11.23	0.77	0.73	bare	shrub	GPP06	GPP0814	Tmin08	GPP0618
40	7.78	0.77	0.74	bare	shrub	GPP0814	Tmin08	GPP05	GPP0618
45	14.11	0.84	0.73	bare	shrub	GPP0814	GPP0618	Tmin08	GPP0817

WITHOUT

seed	%Var	Pearson	Spearman	var1	var2	var3	var4	var5	var6
5	20	0.76	0.74	shrub	bare	GPP0814	GPP0618	Tmin08	GPP06
10	19.04	0.78	0.76	GPP0814	bare	shrub	GPP0516	Tmin07	GPP06
15	21.9	0.77	0.78	shrub	bare	GPP0814	Tmin08	GPP0618	GPP06
20	20.48	0.77	0.77	GPP0814	shrub	bare	GPP0618	Tmin09	GPP0918
25	20.72	0.78	0.72	bare	shrub	GPP0814	Tmin08	GPP0618	GPP06
30	17.56	0.79	0.77	GPP0814	bare	GPP06	shrub	GPP07	GPP0918
35	18.29	0.75	76	GPP0814	Tmin08	GPP0618	GPP05	GPP0516	GPP07
40	20.15	0.74	0.77	GPP0814	bare	GPP06	shrub	GPP0618	GPP0918
45	18.69	0.78	0.77	GPP0814	bare	shrub	GPP06	GPP07	GPP0618

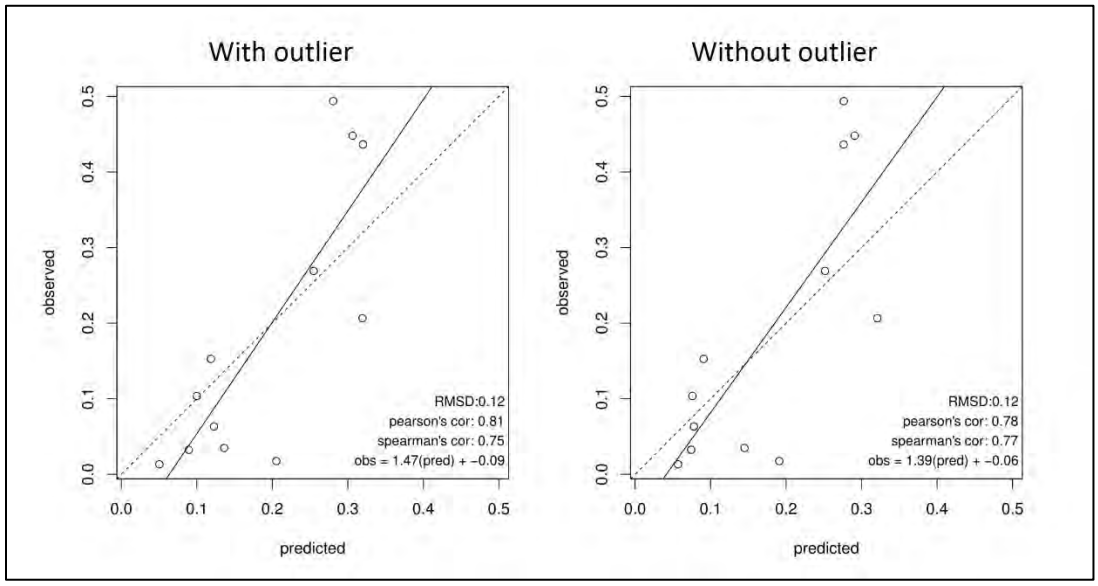

Figure 7. Scatterplot of predicted vs observed values, and Pearson's and Spearman's coefficients, for two models of arthropod biomass from datasets including or excluding an outlier value.

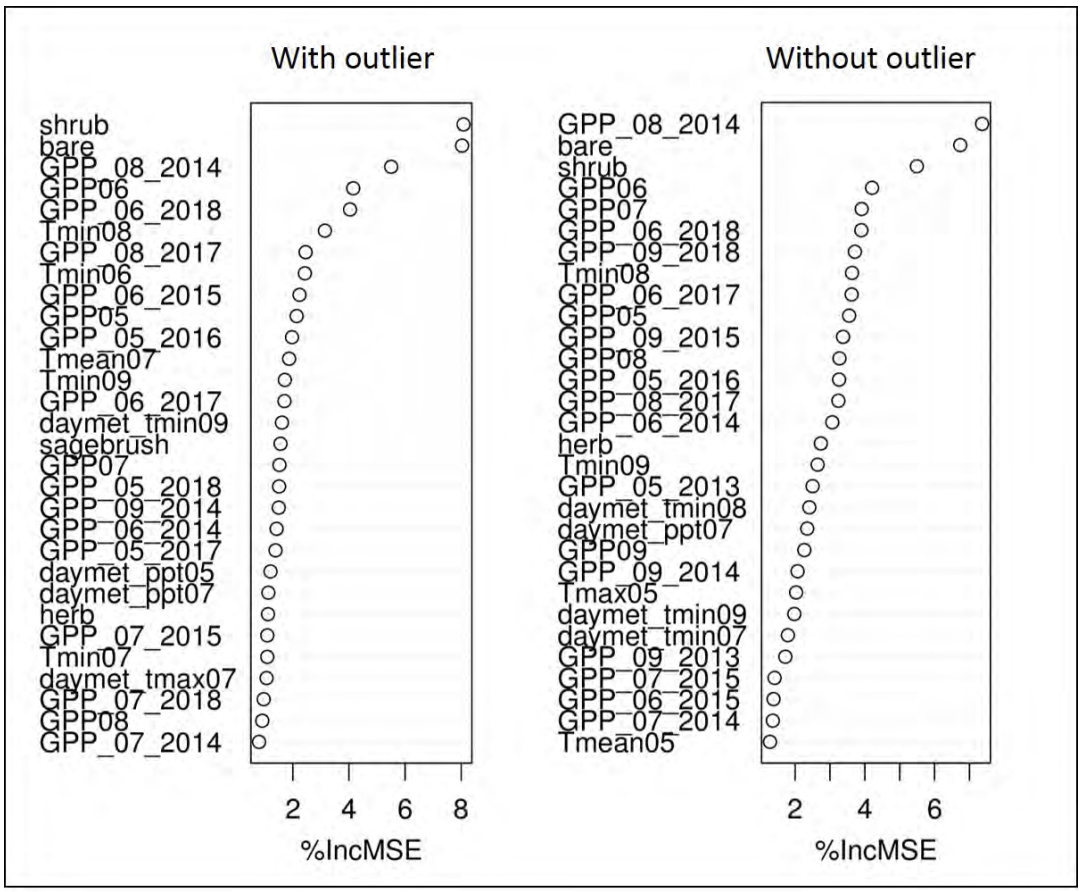

Figure 8. Percent increase in Mean Square Error for the top 30 variables, for two models of arthropod biomass from datasets including or excluding an outlier value.

Extrapolation of both models to continuous surfaces raster allows for visualization and identification of areas predicted to have higher arthropod biomass (Figures 8a and 8b). It is interesting to notice that the inclusion of the outlier with its large biomass value has a strong influence on model output, with a larger proportion of the study area predicted to have higher arthropod biomass.

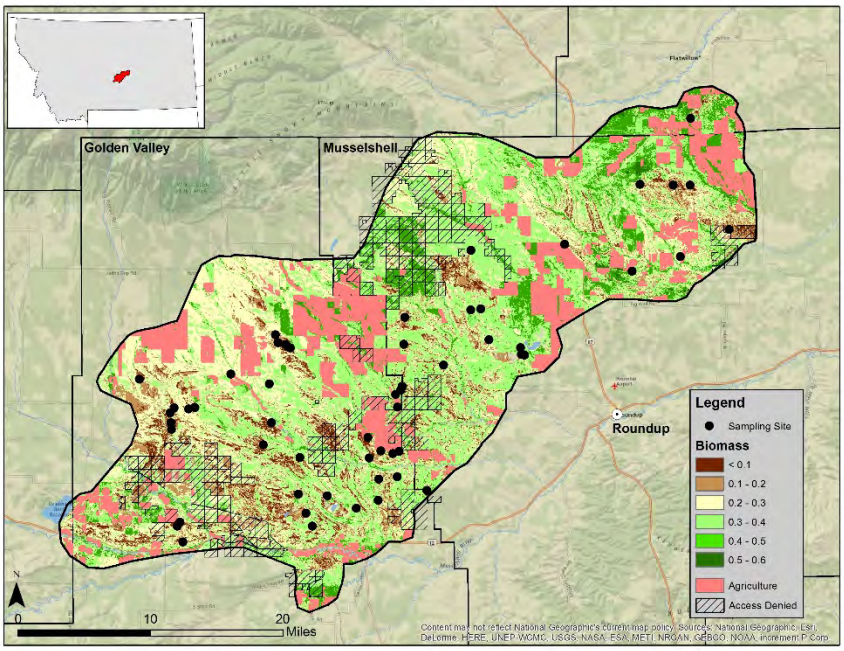

Figure 8a. Predicted arthropod biomass (grams) from dataset including a high value outlier.

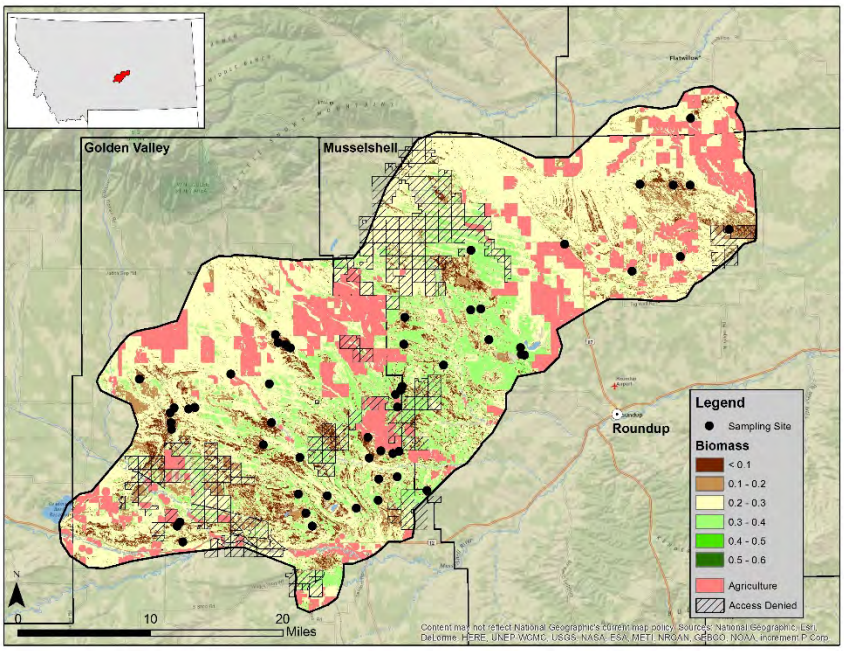

Figure 8b. Predicted arthropod biomass (grams) from dataset excluding a high value outlier.

That said, predicted biomass values at the actual sampling sites did not vary much between models (Figure 9).

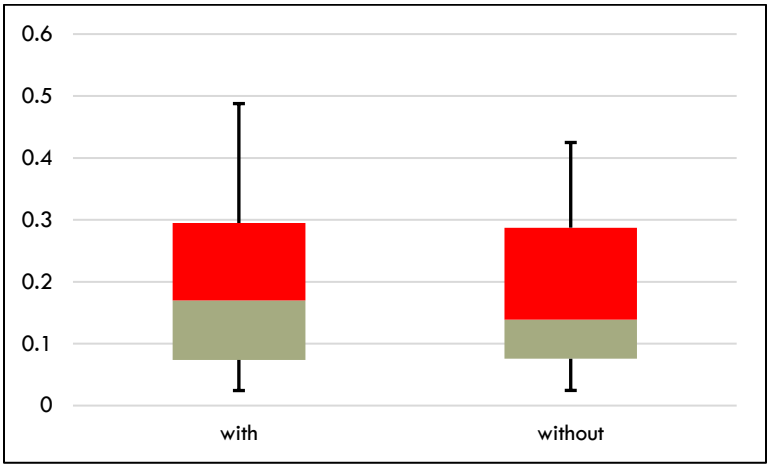

Figure 9. Boxplot comparison of predicted arthropod biomass at 59 (with) and 58 (without) sampling sites based on two Random Forest models, one including a high value outlier, the other excluding it.

Pixels with higher model uncertainty (coefficient of variation greater than 1) were almost five times more numerous for the model including the outlier (N = 55,009 or 2.03% of study area) than for the model excluding it (N = 11,295 or 0.42% of study area), but areas of higher uncertainty overlapped for 4.56% (11,114 ha) of the study area (Figure 10).

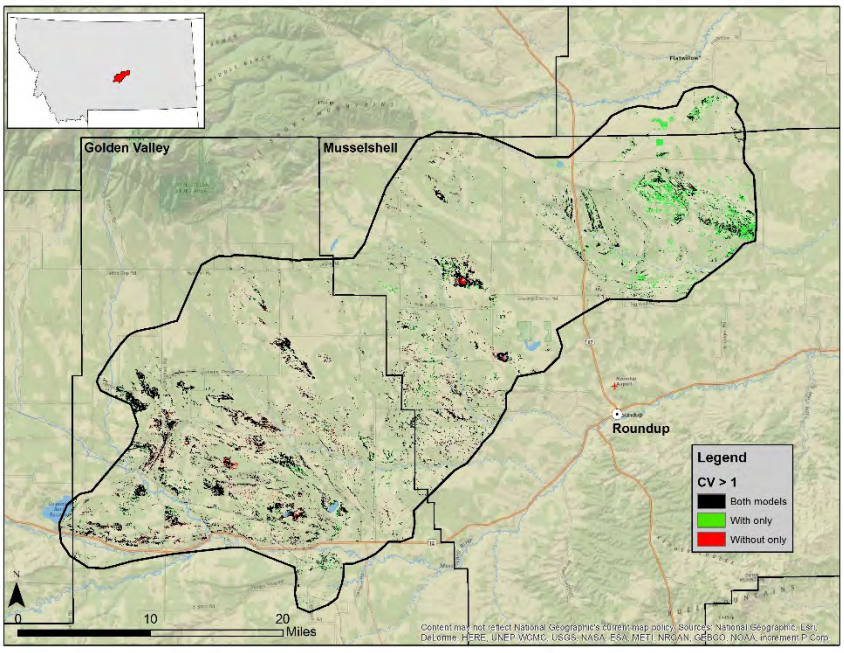

Figure 10. Location of areas of higher model uncertainty (coefficient of variation > 1) for two model of predicted arthropod biomass, including or excluding a high value outlier.

There also appears to be a correlation between model uncertainty and percent bare ground, with higher uncertainty values in areas where bare ground is more prominent; this was visible when looking at the raster datasets, and a moderate positive correlation was obtained when plotting percent bare ground versus coefficient of variation at the sample points (R^2 = 0.4947 for model with outlier, R^2 = 0.5424 for model without outlier; Figure 11).

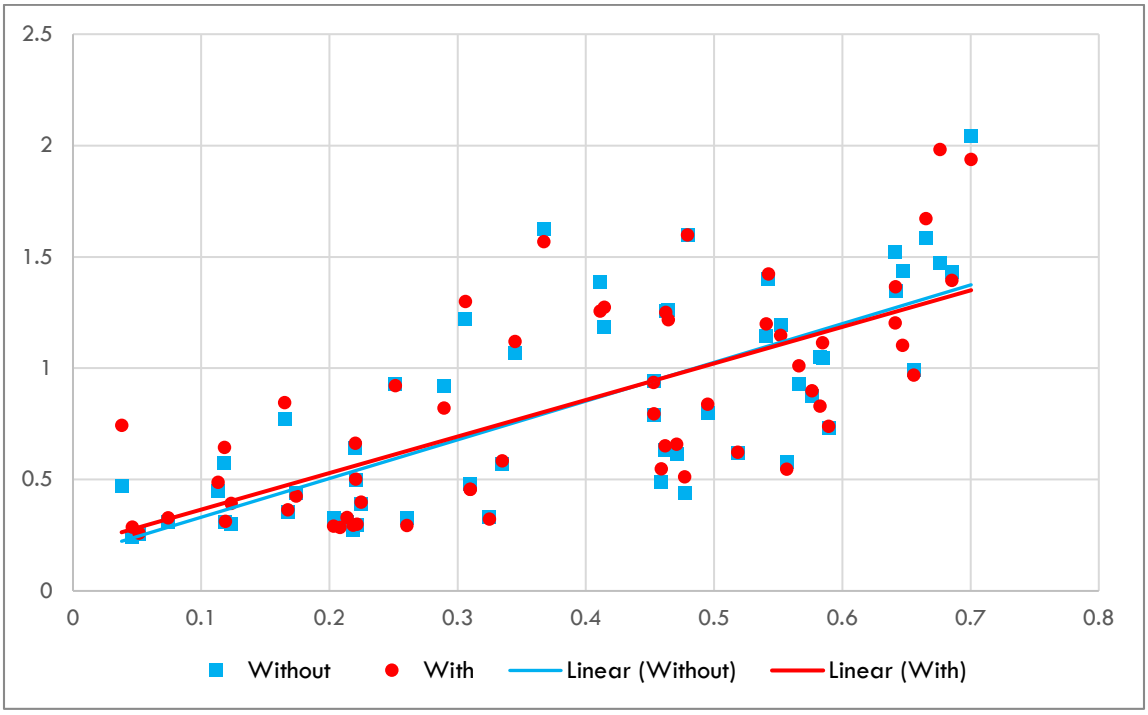

Figure 11. Regression equation of coefficient of variation by percent bare ground for two arthropod biomass models at 59 (with outlier) and 58 (without outlier) sampling points.

Random Sampling Points Selection

According to the 1m land cover layer generated from NAIP 2013, the Lake Mason study area is dominated by sagebrush of various density, and is composed of only 1.74% bare ground (Table 2). The 2018 selection of sampling sites was stratified by percent bare ground within 100m square cells (1ha), with more sites assigned to the less common patches of high bare ground cover. Such a stratification worked well for the 2019 sampling season, as the biomass models, both with and without the outlier value, were strongly driven by the Percent Bare Ground variable. In addition, selecting sites with higher bare ground cover resulted in sampling areas of higher model uncertainty, because of the correlation between these two parameters.

The continuous percent bare ground value within the 42,026 potential sampling circles generated in ArcGIS was reclassified into four categories: 0-10%, 11-25%, 26-50%, and >50%. This classification differed from the original stratification used for the 2018 sampling sites based on the proportion of sites in each

category; this stratification of bare ground provided better sampling of bare ground within the different categories as well as areas of model uncertainty. Only 21 circles contain more than 50% bare ground; all were selected. To these, 60 circles were randomly selected in each bare ground class, for a total of 201 new sampling sites. Of these, 92 (45.8%; with outlier) or 84 (41.8%; without outlier) encompass areas of higher model uncertainty (CV >1). The distribution of predicted arthropod biomass is also well represented, with biomass values ranging from 0.05g to 0.46g per circle (with outlier) and from 0.04g to 0.35g per circle (without outlier). Figure 12 presents the distribution of the potential 2019 sampling sites, along with that of previous sampling sites.

Table 2. Composition of the Lake Mason study area based on classification of 1m 2013 NAIP imagery.

Land cover class	Area (ha)	Percent
Sagebrush 0-5%	64,544	25.83
Sagebrush 6-10%	22,517	9.01
Sagebrush 11-15%	37,960	15.19
Sagebrush 16-20%	11,364	4.55
Sagebrush 21-25%	51,796	20.73
Sagebrush 26-30%	14,020	5.61
Sagebrush 30% and greater	1,802	0.72
Bare ground	4,344	1.74
Riparian	4,289	1.72
Conifer	223	0.09
Water	2,004	14.00
Agriculture	34,970	0.80

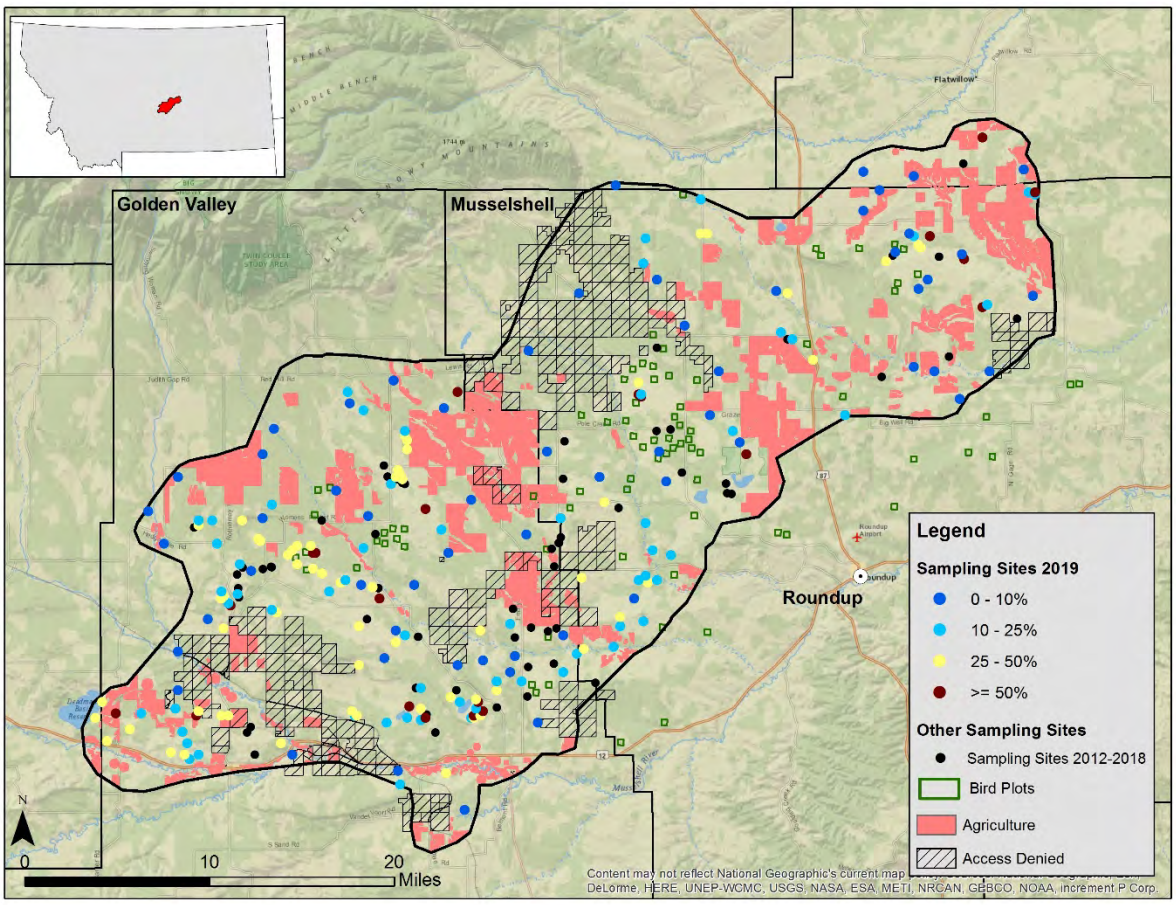

Figure 12. Location of 201 potential arthropod sampling sites for the 2019 field season colored by percent bare ground within a 1-ha circle; and location of previous years' sampling sites, in the Lake Mason study area.

Conclusions

Several factors may have contributed to the low percent variance explained by the models. Although Random Forest is known for being well suited to small sample sizes, there were only 59 geographically distinct locations in the whole study area. The 30 samples collected in 2018 did improve percent variance explained, bringing it up from close to zero (for test models developed using 2012-2017 samples only) to the mid-20s; new sample sites in 2019 will hopefully continue this trend. In terms of predictive variables, the main issue is the coarse scale of all the climate variables (800m or 1000m); unfortunately, there are no study-area wide fine-scale climate variables available.

This is a first attempt to model the distribution of arthropod biomass in the Lake Mason area; it will be interesting to see how the 2019 samples conform to model prediction, and to use their data to improve the model. One of the biggest limitations of the current model is the prediction of average biomass over the course of the growing season; if enough data are collected through repeat sampling, it may be possible to run separate models for early vs late growing season.

Invertebrate Biomass model – 2019 Data

This part of the report is composed of five sections:

1. A review of arthropod biomass data and a correlation analysis between field biomass and vegetation data (47 plots) to identify which variables may be good predictor variables for modeling the spatial distribution of arthropod biomass in the study area;
2. A relation of remotely sensed land cover characteristics to vegetation data collected in the field data (e.g. bare ground, grass and shrub cover);
3. A correlation analysis between arthropod biomass samples and a suite of spatial variables available for the entire study area (e.g., land cover, climate, ecosystem productivity), even if no equivalent information was collected in the field;
4. A validation of the 2012-2018 spatial biomass model using 2019 arthropod biomass data; and
5. The creation of new spatial models using several approaches (adding 2019 biomass to 2018 data; using 2019 biomass data only; using 2019 biomass data on a monthly basis; developing order-specific models).

Invertebrate Biomass Analysis

General Biomass Patterns

Arthropods were collected using sweeping nets ("sweep" samples) and vacuums ("shrub" samples); although, this latter approach was eventually discarded on account of unreliable biomass estimates. The collated data containing Dave Stagliano's identification by arthropod order were therefore simplified to retain only sweep data for modeling biomass patterns.

Arthropods were identified to the order level, with twelve orders present in the study area and average biomass measurements ranging from 0.003g/sample (Ephemeroptera; e.g., Mayflies) to 0.092g/sample (Orthoptera; e.g., grasshoppers) (Figure 1.1). In addition to being the heaviest on average, the Orthoptera order also makes up the heaviest individual samples, as the top 35 heaviest biomass sweeps are grasshoppers).

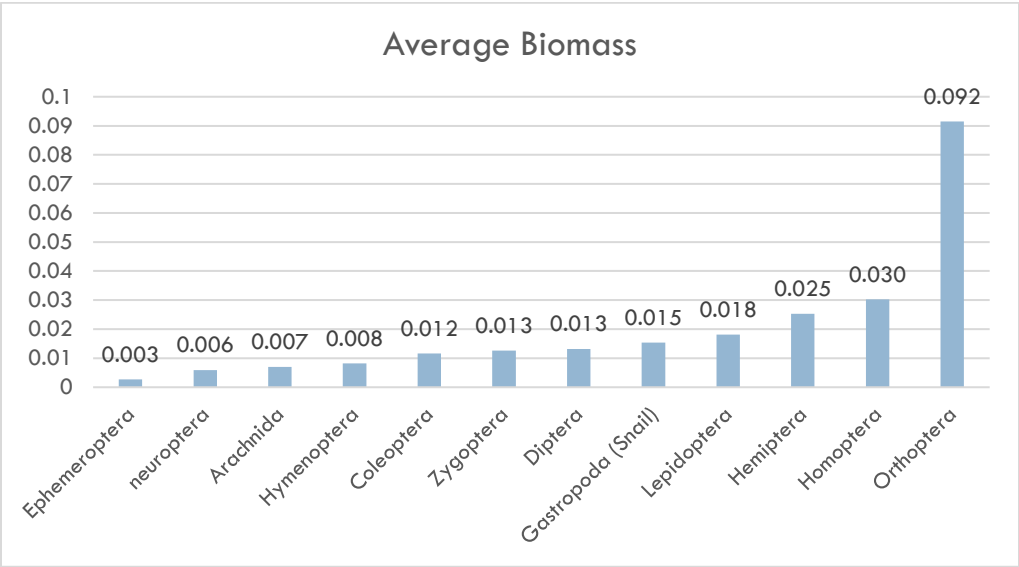

Figure 1.1. Average biomass (grams) by order from sweeps collected during the 2019 field season.

An analysis of seasonal trends (April 23rd - July 30th) in total biomass, grouped by sampling date, indicates an overall increasing trend (R2 = 0.097) as the season progresses; although, there are obvious outliers (Figure 1.2). Outliers were caused by the inclusion of heavier grasshoppers in sweep samples. When Orthopteran samples are removed from analysis, the trend is stronger, with an R^2 value of 0.282 (Figure 1.3).

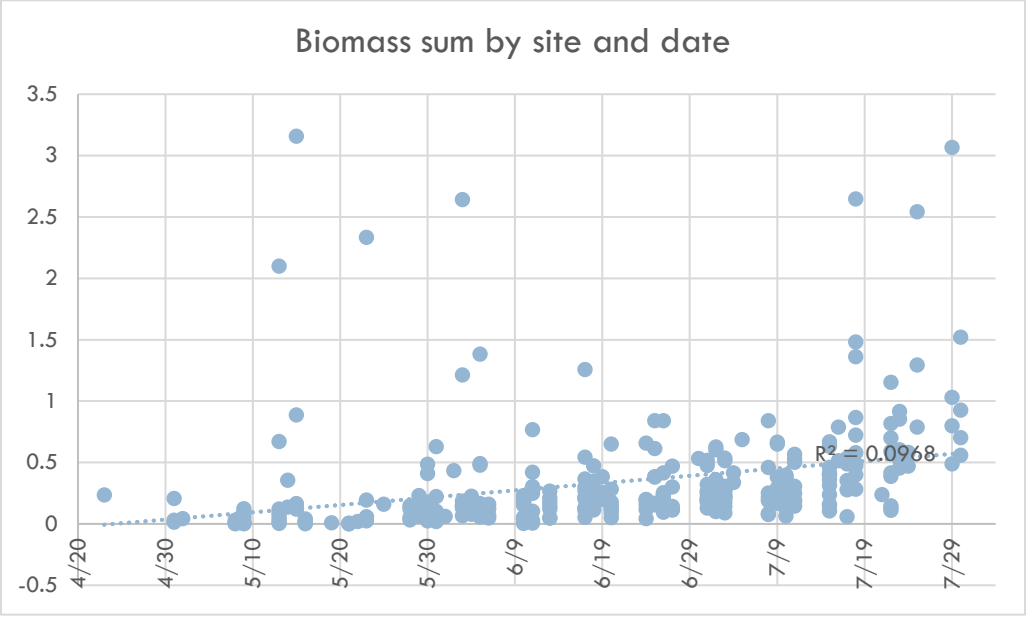

Figure 1.2. Temporal distribution of arthropod biomass for the 2019 field season.

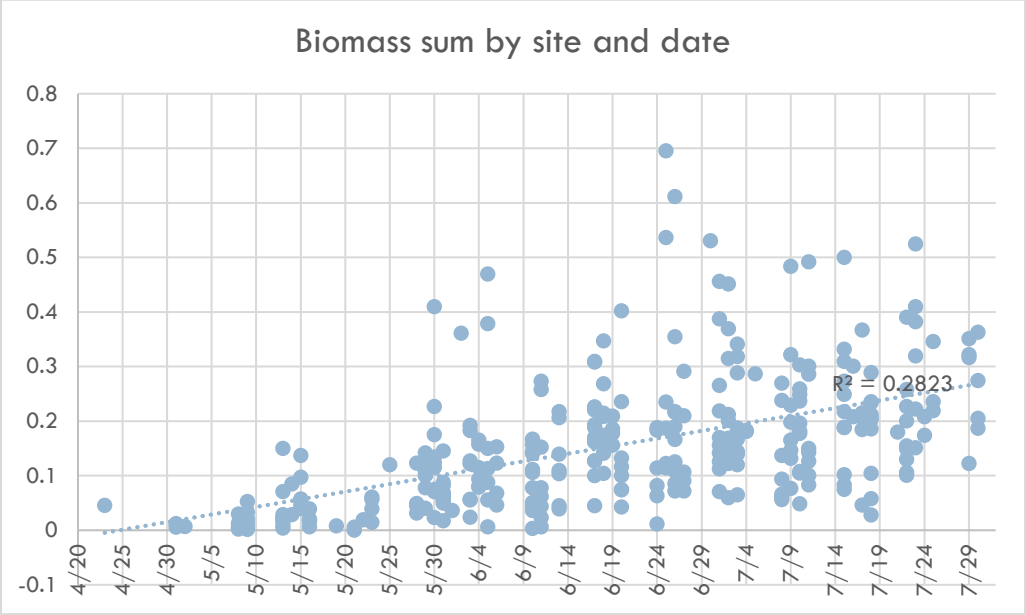

Figure 1.3. Temporal distribution of arthropod biomass for the 2019 field season, excluding orthopteran.

When looking at the evolution of biomass over time by order, Homoptera present the highest R^2 value (0.221), with all other orders having R^2 values lower than 0.1; however, there is clearly a trend of increased biomass as the season progresses (e.g. Hemiptera, Figure 1.4). Homoptera is part of Hemiptera, and both include cicadas, aphids, plant hoppers, and leaf hoppers. In both figures, there is also evidence of trends in biomass variability, which tends to peak in late June to early July and then slightly decrease. Should a spatial interpolation model such as kriging be considered in the future, additional exploratory data analysis should include frequency distributions (histograms), normality tests, and exploration of heteroscedasticity patterns in the residuals of biomass totals versus day of the year, which would suggest trend removal (normalization) and other transformation options.

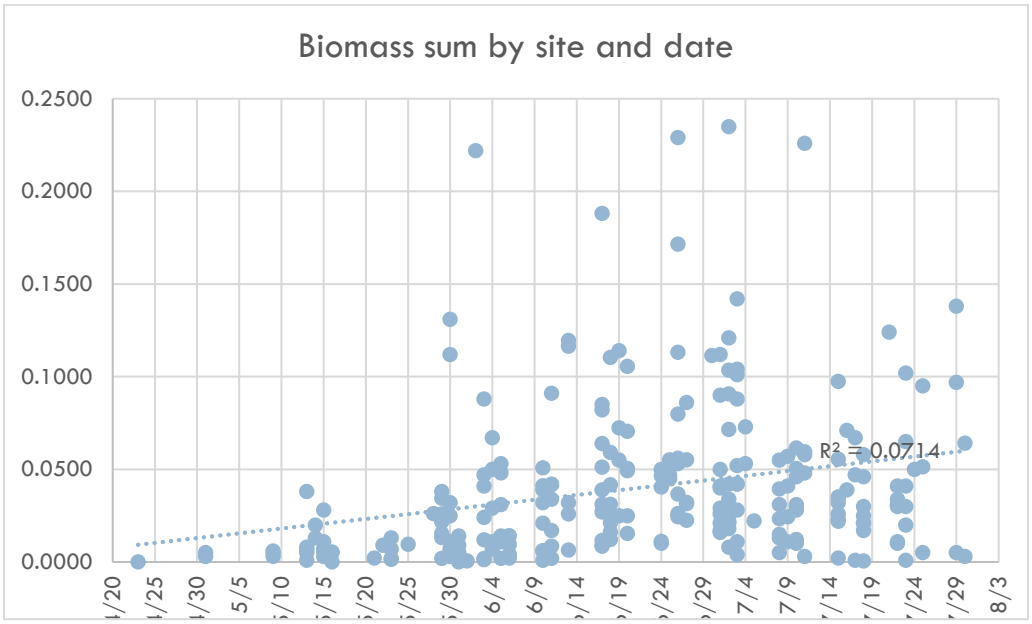

Figure 1.4. Temporal distribution of hemipteran biomass for the 2019 field season.

Thirty-five field sites were visited more than once during the field season (14 twice, 21 three times); in all cases, later samples weighed more than earlier ones at the same site, with the largest difference observed at sites W83 (2.03g), W84 (1.97g) and W87 (2.13g).

Correlation Between Biomass and Field Vegetation Plot Data

The combination of unique site ID and sampling date was used to relate sweeps of insect biomass to field sampling sites and their associated vegetation data. A total of 105 out of 319 unique combinations could be related to detailed vegetation plot data (the remaining samples were collected as validation data and did not include the detailed vegetation sampling protocol).

Biomass and Bare Ground

In the spatial model derived from 2012-2018 arthropod samples, bare ground and shrub cover were identified as important predictive variables of arthropod biomass. Regressing arthropod biomass from the 2019 field data against average percent bare ground from the 2019 field plots showed a weak correlation ($R2 = 0.025$); however, R^2 increased to 0.211 when outliers (biomass >1g) were removed (figures 1.5 and 1.6).

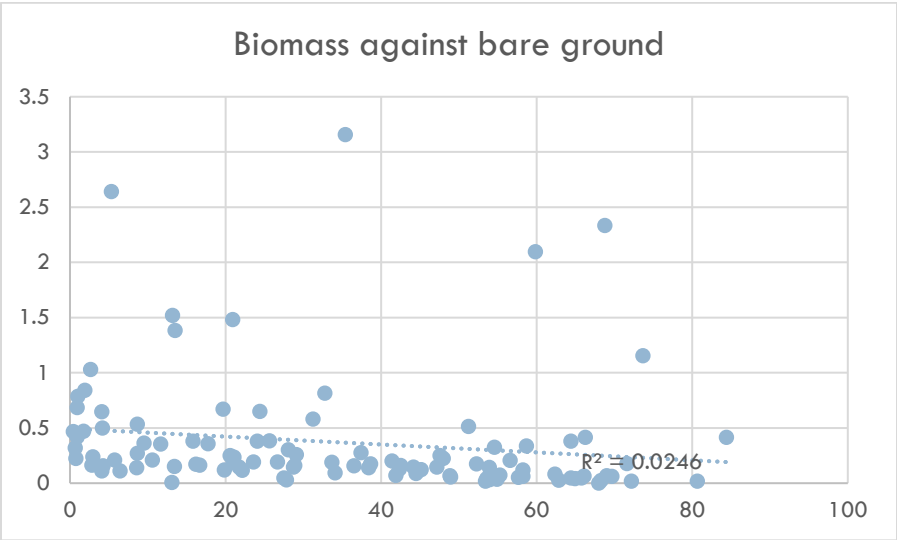

Figure 1.5. Regression of arthropod biomass (g) against average bare ground in plot.

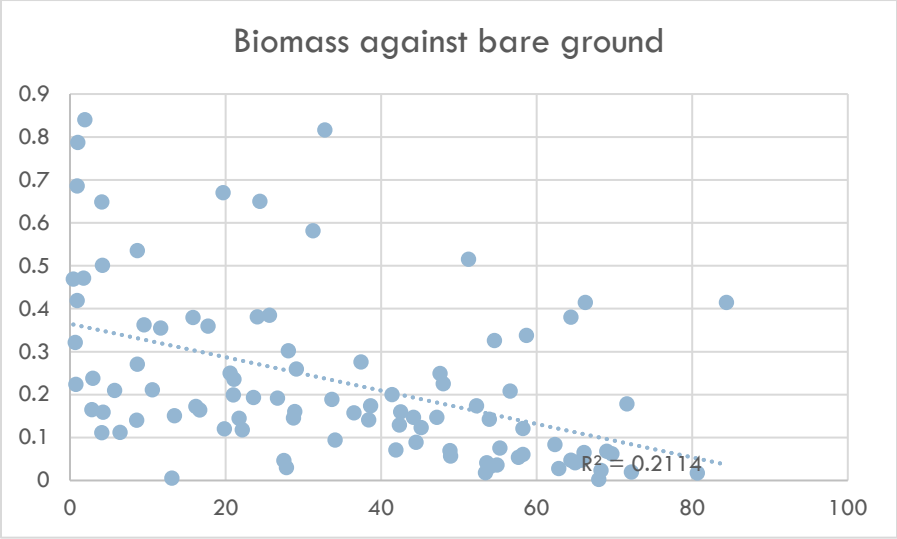

Figure 1.6. Regression of arthropod biomass (g) against average bare ground in plot after removing biomass > 1g.

Biomass and Other Variables

I ran regressions between biomass and distance to water, sagebrush cover, shrub cover, grass cover, and litter; only grass cover showed any trend, with an R^2 value of 0.222 once the heaviest outliers were removed from the dataset (Figure 1.7).

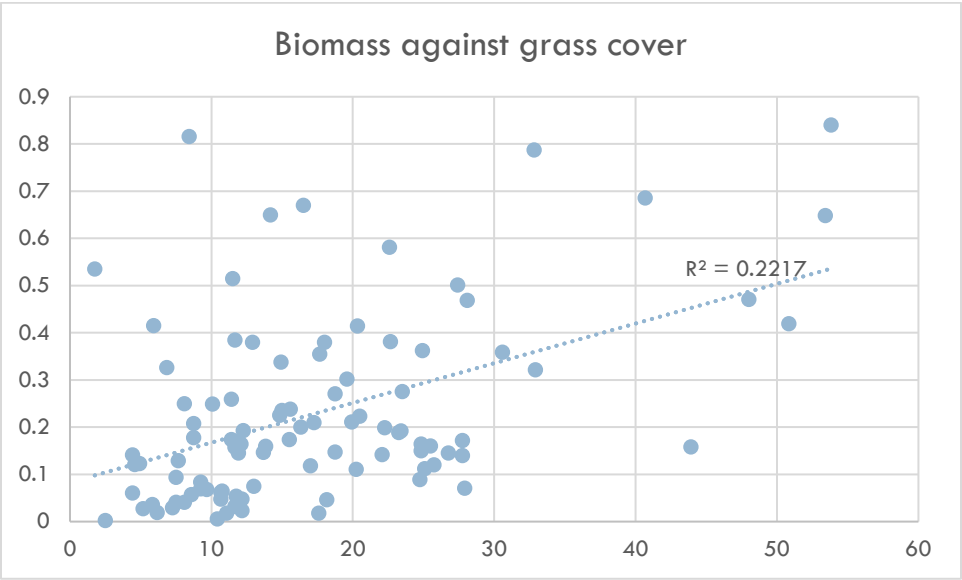

Figure 1.7. Regression of arthropod biomass (g) against average grass cover in plot after removing biomass > 1g.

Despite a week regression between biomass and shrub cover, a bar chart of summed biomass by shrub cover class seems to indicate a preference for lower shrub cover (Figure 1.8).

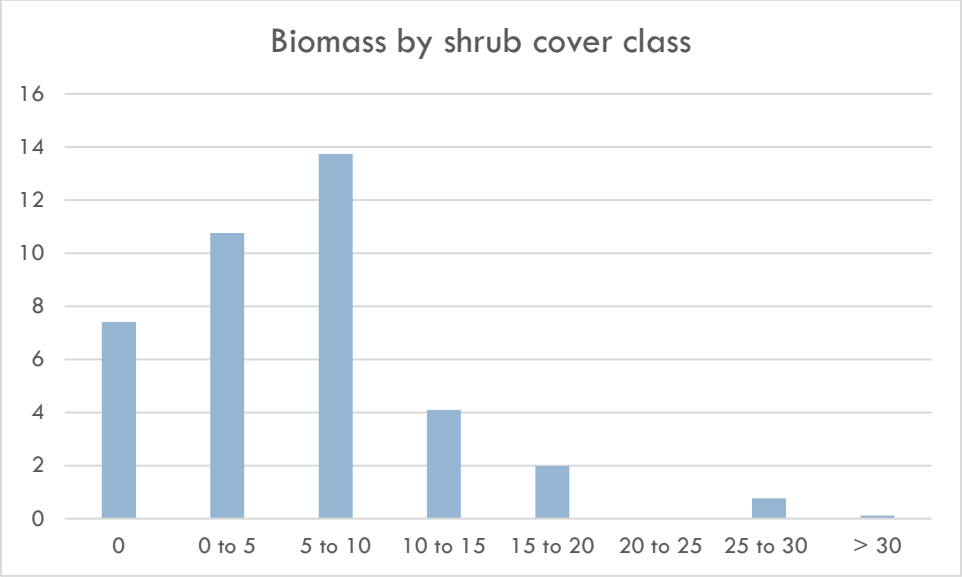

Figure 1.8. Summed arthropod biomass (g) by shrub cover class (%).

Bare ground, herbaceous cover and possibly shrub cover may be better predictors of arthropod biomass in a spatial model (temperatures and time of day could not be included). Interestingly, bare ground and shrub cover (derived from NAIP 2011) were top predictors in the 2012-2018 model, but herbaceous cover (same source) ranked very low. Other strong predictors were June and August GPP, which could be considered proxies for overall vegetation cover in field plots.

When collecting samples in the field, the field crew noticed a definite influence of weather on arthropod abundance. Temperatures were recorded at most vegetation and validation plots. Pooling all the data together (regardless of month and including outliers) shows lower biomass for colder temperatures, and conversely heavier ones when it is hotter (Figure 1.9).

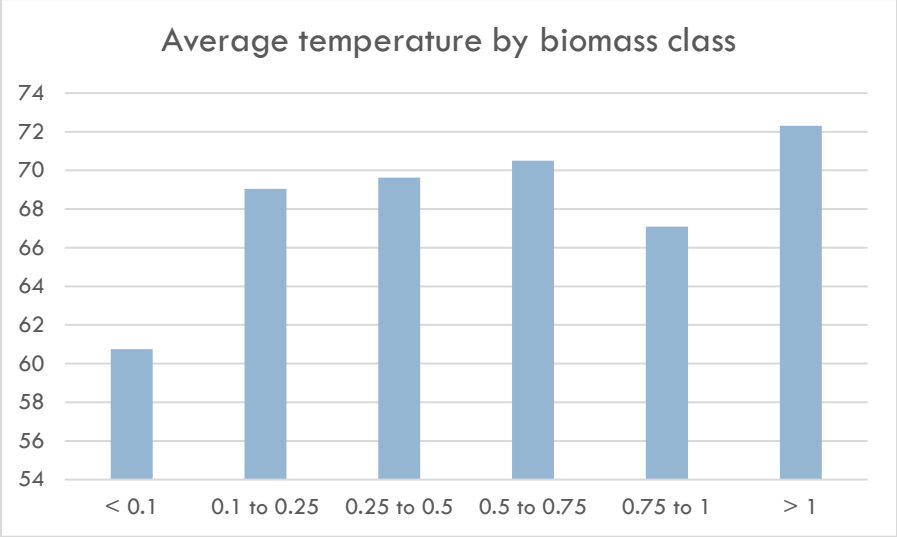

Figure 2.9. Average temperature (F) by class of biomass weight (g).

When the data are grouped by month there is a pattern of heavier biomass with warmer temperatures; although, the warmest July temperatures see a decline in average biomass (Figure 1.10).

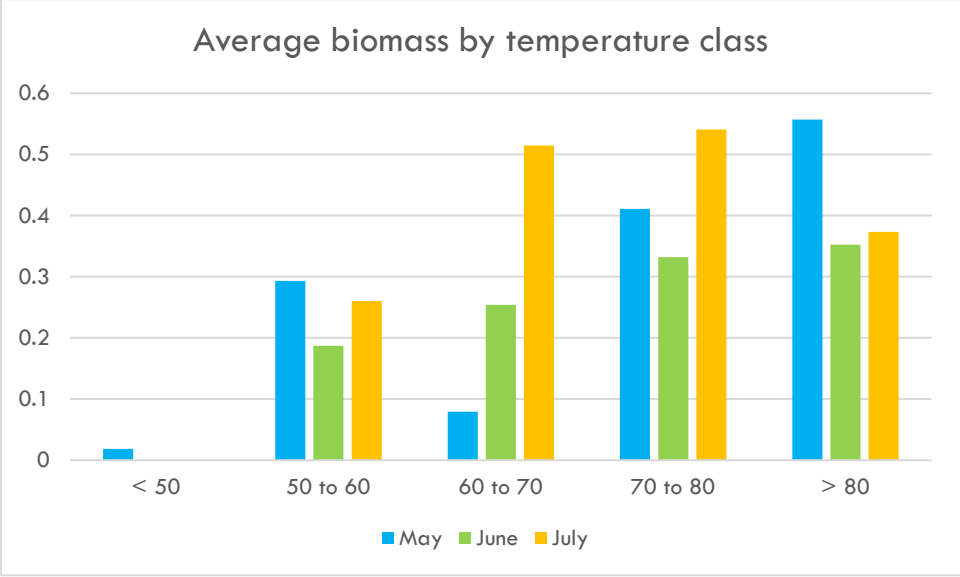

Figure 1.10. Average arthropod biomass (g) by temperature class (F).

VEGETATION ANALYSIS

Comparison with NAIP 2011

Bare Ground

The Lake Mason bare ground raster layer was generated by Open Ranch Consulting using 1m NAIP imagery collected predominantly on July 24, 2011. For the 2012-2018 arthropod biomass model, it was resampled to 30m using the DEGRADE command in Erdas Imagine because most other predictive variables were only available at coarser scales. Comparison with 2019 field data was done at both scales.

Vegetation field data from 2019 include percent bare ground, collected every 3 meters in the four cardinal directions from the plot centroid (3m, 6m, 9m). For comparison with the two raster datasets, I averaged these 12 values for each plot and used only July visit dates. For example, plot W104 was visited on May 15, June 19, and July 9; I used average percent bare ground for July 9, which is closer to the time of year the NAIP imagery was collected. I used ArcGIS Zonal Statistics as Table to calculate average bare ground from the original 1m NAIP and from the 30m resampled NAIP within the 41 July plots.

Average bare ground values range from 0.42% to 73.7% for field plots, from 4.9% to 92.5% for the 1m raster, and from 7.7% to 87.1% for the resampled 30m raster. Regressing field values against raster values resulted in an $R^2 = 0.635$ at 1m (Figure 2.1) and an $R^2 = 0.529$ at 30m (Figure 2.2).

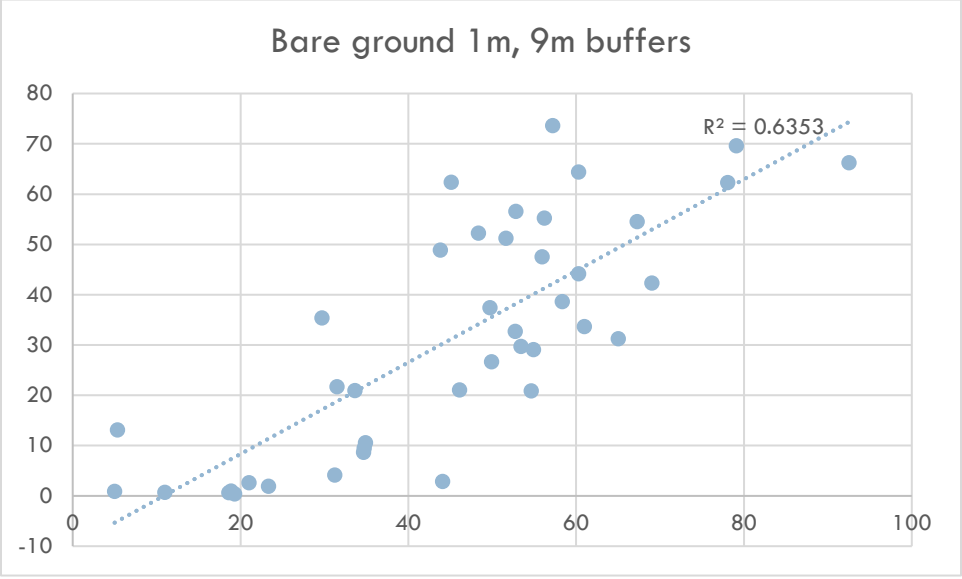

Figure 2.1. Regression plot of percent bare ground from field data against 1m NAIP imagery averaged within 9m buffers.

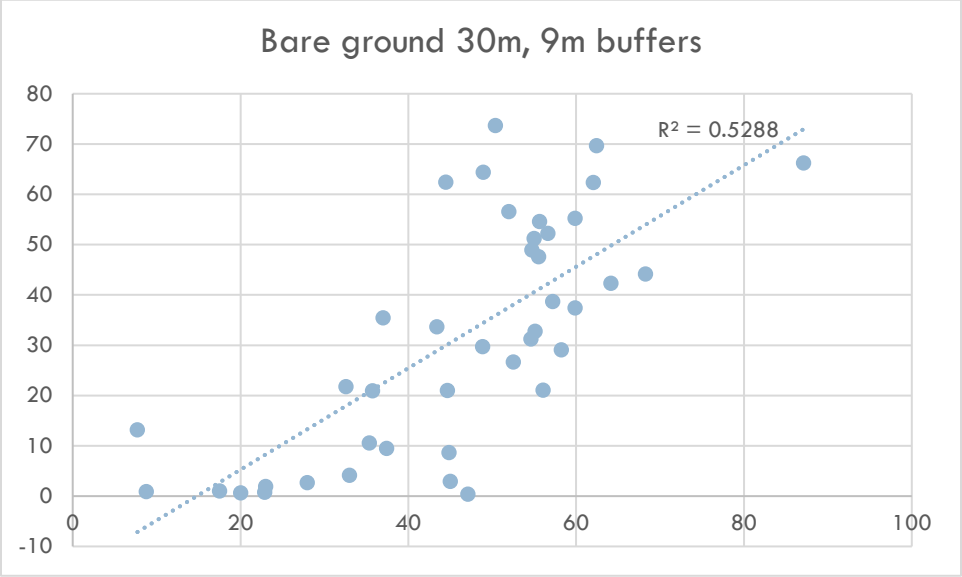

Figure 2.2. Regression plot of percent bare ground from field data against 1m NAIP imagery resampled to 30m and averaged within 9m buffers.

Shrub Cover

Shrub cover was collected along two 30m transects intersecting at the center of the field plot (one north-south and one east-west); therefore, center points were buffered by 15m. Since there is no global shrub cover value for the whole veg plot, an estimate was calculated by adding cover from individual species: ARTR, SAVE, CELA, ATRIP, CHRYS, ARCA, RHTR, and OTHER. Dead shrubs were also included.

For the 114 veg plots, shrub cover ranged from 0 (n = 14 plots) to 30.24%. Overall, shrub cover was highest for June (mean 8.23%) compared with May (6.38%) and July (6.19%); however, for the 21 plots that were visited during all 3 months, 10 had higher shrub coverage in May, 6 in June and 4 in July; I suspect that shrub cover variation is a product of the small differences in laying out the transects, as opposed to true vegetation change over time. Average shrub cover values from NAIP range from 1.6% to 21.3%.

A correlation between mean shrub cover within 30m plots from the 1m 2011 NAIP imagery and the proxy from field data shows much variation (Figure 2.3). This could be because the two datasets are not really comparable – different methods, different years.

The lack of correlation between the two datasets does not imply that NAIP shrub cover is a poor predictor of arthropod biomass; see section 3.

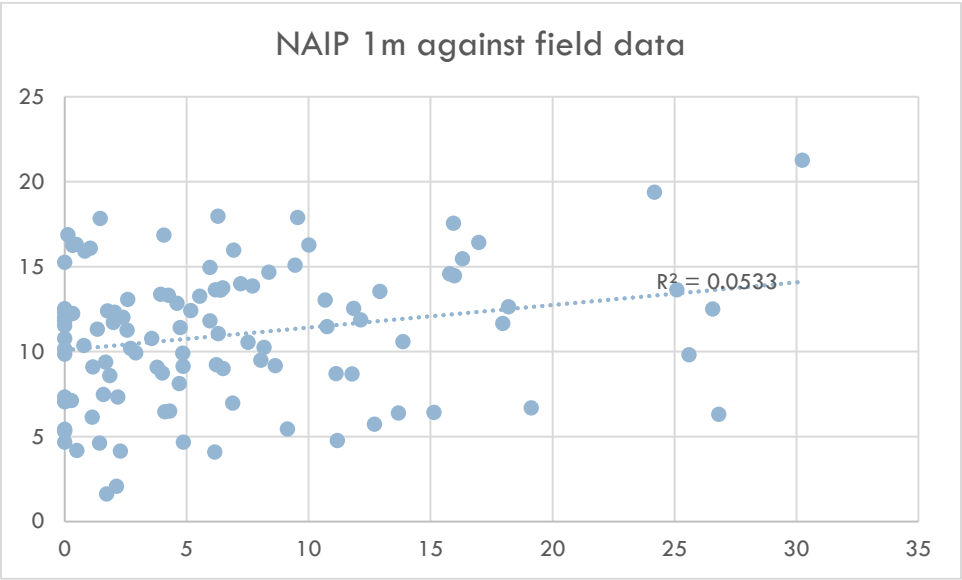

Figure 2.3. Regression of shrub coverage within 30m plots from 2011 NAIP imagery against transect shrub cover data from 2019 field work.

Grass cover

Grass cover collection followed the same protocol as bare ground, so I used the same approach for comparison between field data and NAIP (1m and resampled to 30m). In the field, average grass cover increased between May (13.7%) and June (18.4%) but remained stable in July (18.6%). Like bare ground, I opted to do comparison for July plots only (n = 41). Correlation is not as strong as with bare ground, but the pattern is there, with an R^2 value of 0.230 for 1m NAIP (Figure 2.4) and an R^2 value of 0.312 for NAIP resampled to 30m (figure 2.5).

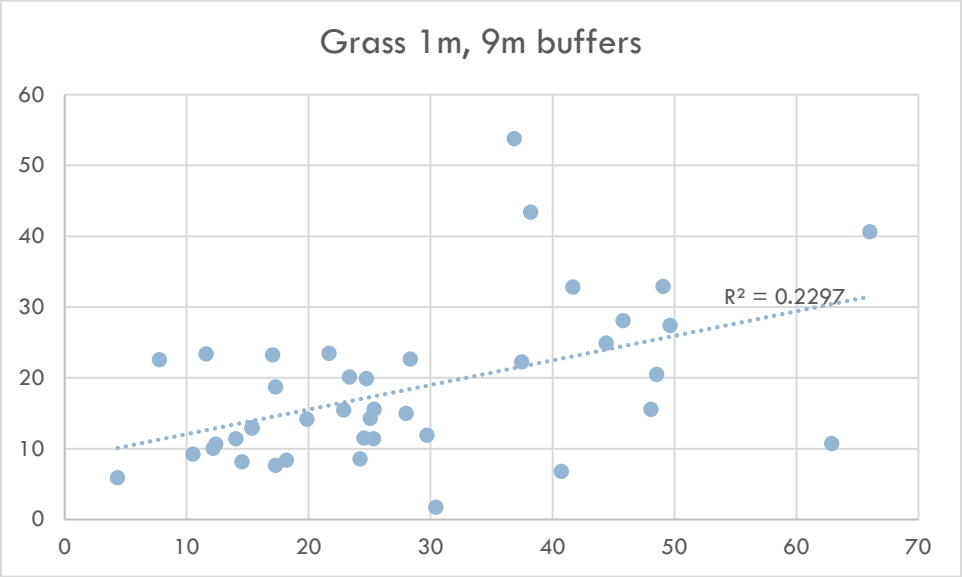

Figure 2.4. Regression plot of percent grass cover from field data against 1m NAIP imagery averaged within 9m buffers.

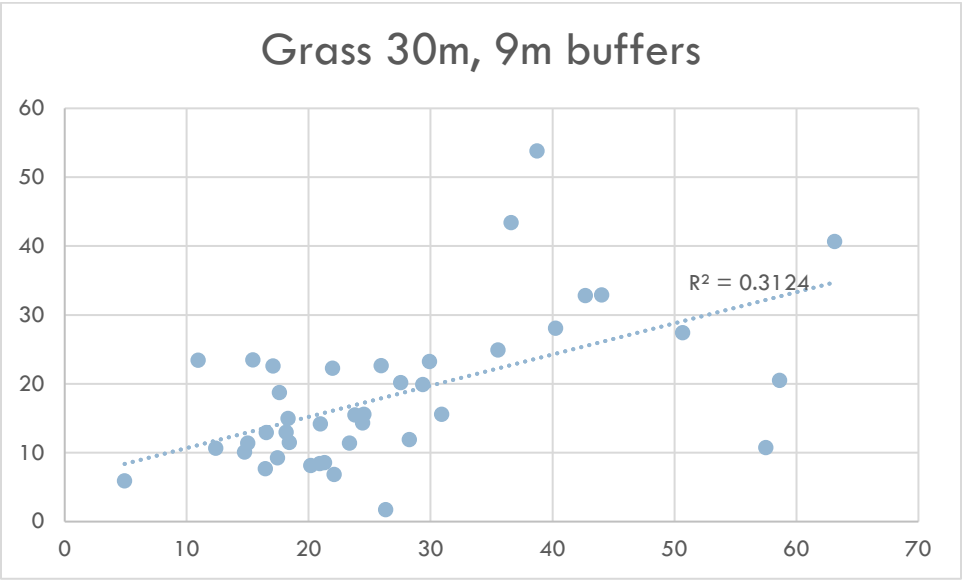

Figure 2.5. Regression plot of percent grass cover from field data against resampled 30m NAIP imagery averaged within 9m buffers.

Comparison with Sentinel 2019

Because vegetation could have changed between 2011 and 2019, Sentinel 2 imagery was downloaded from the USGS earth explorer website for two cloud-free dates, June 12, 2019 and July 22, 2019, and corrected using the Sen2Cor module of the Sentinel-2 Toolbox. A bare soil index (BSI) was calculated using the following band formula: BSI = (B11 + B4) – (B8 + B2) / (B11 + B4) + (B8 + B2) (Pal and Antil 2017). These two derived rasters have 20m pixels, which is the scale of the coarser band 11.

Correlations were calculated between average bare ground from June plots (N = 44) and mean June BSI, and between average bare ground from July plots (N = 41) and mean July BSI. However, there does not appear to be a significant correlation between BSI and percent bare ground from field data, with an R^2 of 0.009 for June and R^2 of 0.026 for July (Figures 2.6 and 2.7). Unless there is a stronger correlation between BSI and arthropod biomass, including this variable in the pool of model predictors is not expected to improve results.

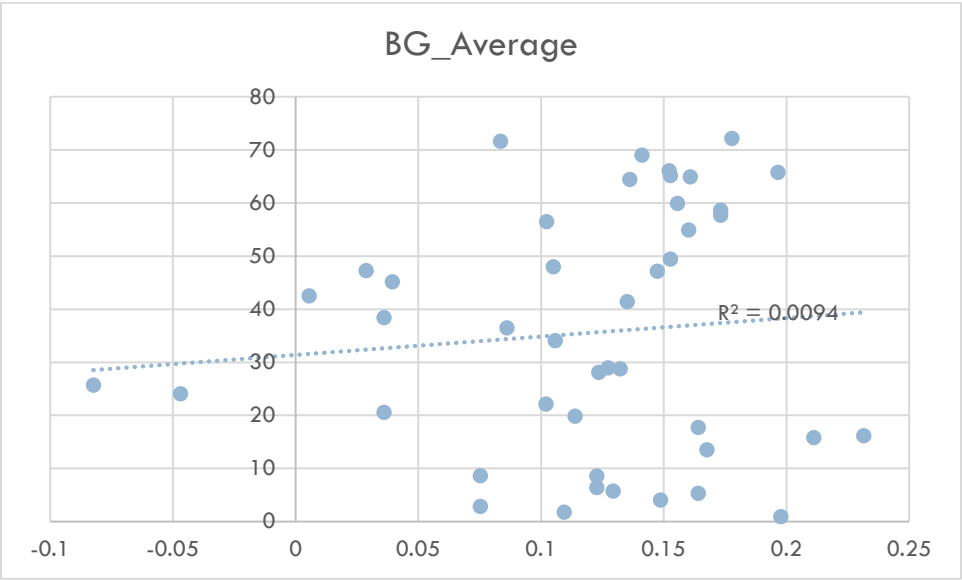

Figure2.6. Regression plot of percent bare ground from June field data against Bare Soil Index calculated from Sentinel 2 imagery.

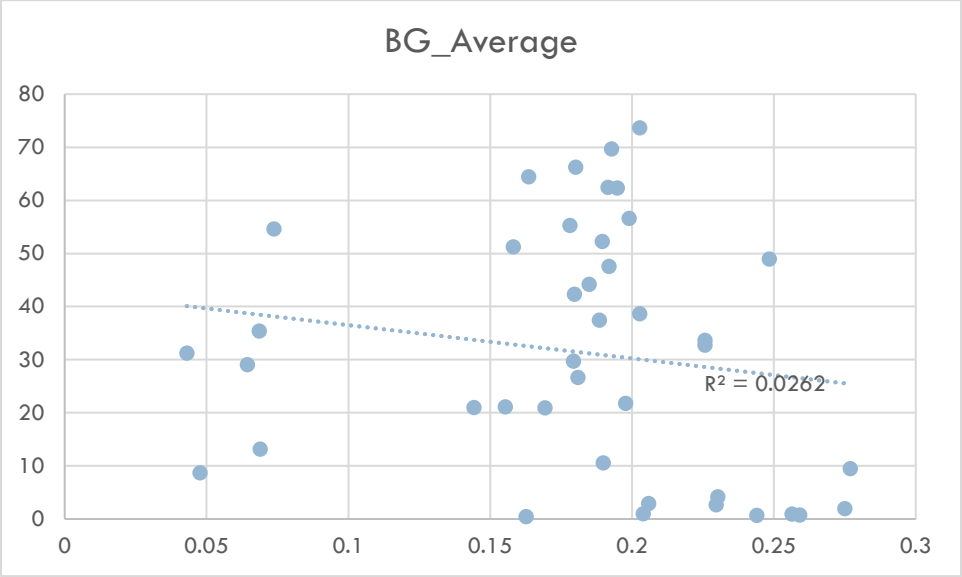

Figure 2.7. Regression plot of percent bare ground from July field data against Bare Soil Index calculated from Sentinel 2 imagery

SPATIAL ANALYSIS OF ARTHROPOD BIOMASS

Correlation patterns between arthropod biomass and site characteristics collected in the field are an important step in exploring and understanding the data; however, only those variables available for the study area in a spatial format can be used as input in a predictive distribution model. Time of day, even if

a good predictor of arthropod biomass, cannot be used as input into such a model. In this section, I explore the relationship between arthropod biomass and a variety of spatial variables.

Before any spatial analysis could be conducted, the database of insect biomass collected during the 2019 field season had to be reconciled with field sampling sites and their associated vegetation data (or simply XY coordinates in the case of validation data). The combination of unique site ID and sampling date from the resulting spreadsheet was compared with similar combinations from the vegetation field data (n = 114 points) and validation field data (n = 194). Several problems were encountered, such as field validation points with UTM coordinates either missing or having extra digits; field sites (vegetation or validation) having no corresponding arthropod sampling; or arthropod sweep samples with a combination of site ID and sampling date not found in fields sites. The field crew was able to fix some of the issues, but there remained 28 arthropod samples with no corresponding field location, and in reverse, 9 entries with Site ID and date, but no samples. Overall, 105 vegetation plots and 187 validation points could be associated with arthropod biomass data.

Arthropod sampling was done by conducting one hundred sweeps along two intersecting, 30m transects; therefore, plot centroids were buffered by 15m and pixel values were averaged within the buffer in order to give a more accurate representation of ground data than would be obtained from a single pixel (at the plot centroid).

2011 NAIP Classification

Bare Ground

Nine field sites are located outside of the classified NAIP 2011 imagery. When sites were visited multiple times (as was the case for most vegetation plots, but not for validation plots) only the one with the latest sampling date was retained and its biomass regressed against NAIP data, to avoid data duplication (since the NAIP classification is based on a single date, it was not possible to assign different NAIP values for overlapping plots collected at different dates). However in case of non-overlapping buffers, all visits were kept.

After removing overlapping buffers, 229 values remained. Regressing biomass against % bare ground from NAIP resulted in a low R^2 (0.029), even after removing outliers with biomass >1g (R^2 = 0.0297). Using only biomass collected in July slightly increased R^2 (0.0821), especially after removing outliers (R^2 = 0.1015; Figure 3.1). There is nonetheless a trend of negative relation between biomass and percent bare ground, which is confirmed by a bar graph of average July biomass by bare ground class; biomass within plots with 0 to 20% bare ground averages over twice that of plots with 60 to 80% bare ground (Figure 3.2).

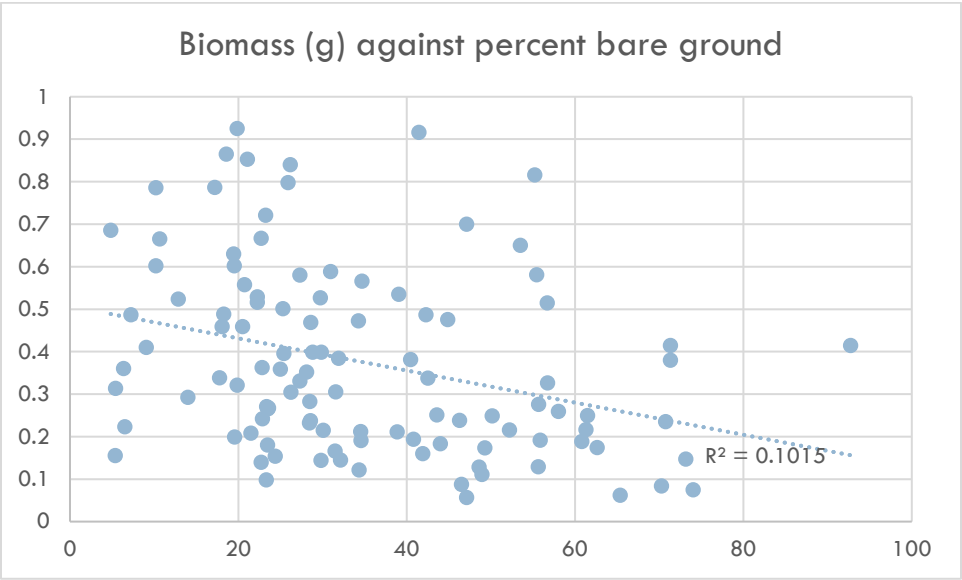

Figure 3.1. Regression plot of July arthropod biomass (g) against percent bare ground from 2011, 1m NAIP imagery within 30m plots.

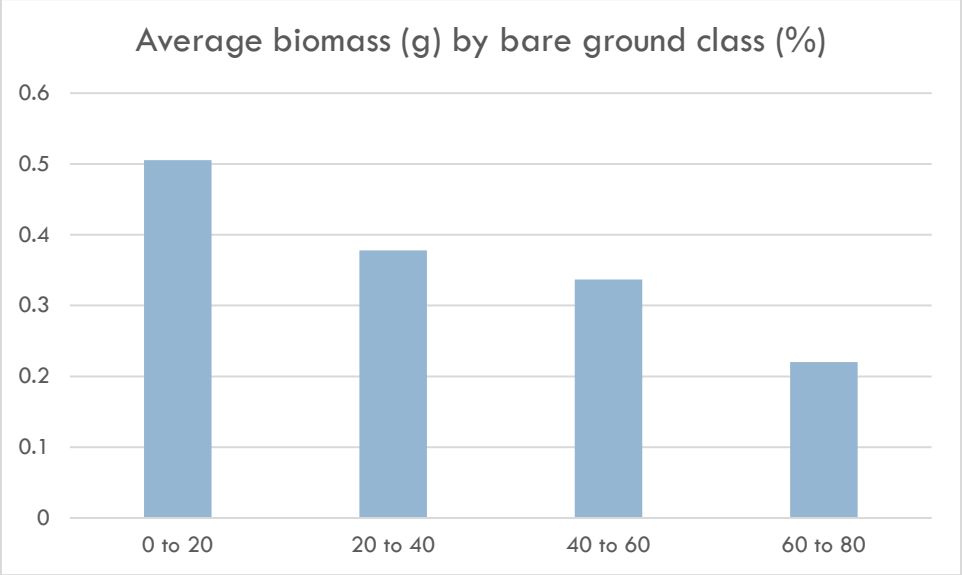

Figure 3.2. Distribution of average July arthropod biomass (g; outliers >1g removed)) by bare ground class from NAIP 2011 (% within 30m plot)

Shrub Cover

The same approach as bare ground was used to regress biomass against percent shrub cover; in this case, there was no linear correlation between the two variables, even after removing outliers and using July data only. However, a bar graph suggests lower biomass in plots with shrub cover greater than 20% (Figure 3.3).

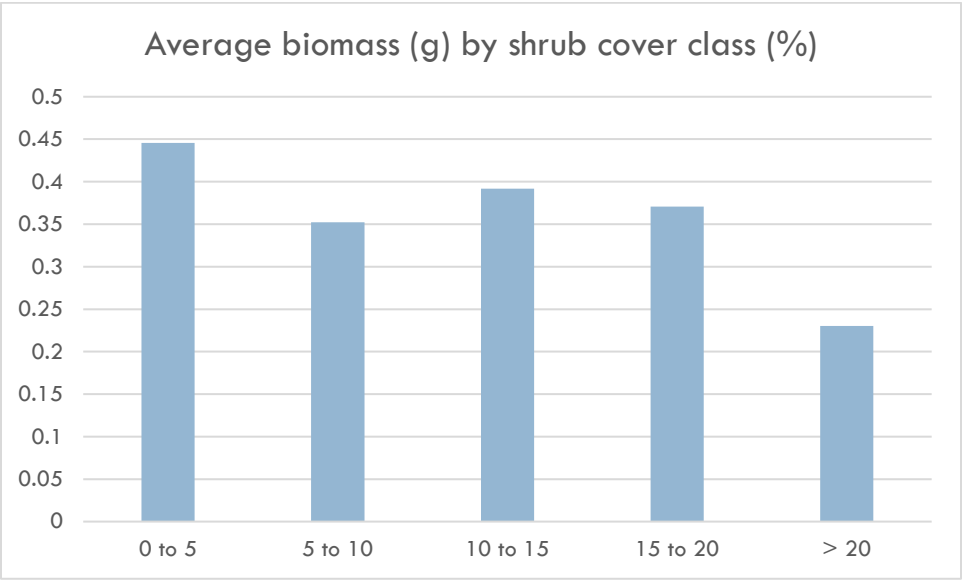

Figure 3.3. Distribution of average July arthropod biomass (g; outliers >1g removed)) by shrub cover class from NAIP 2011 (% within 30m plot)

Grass Cover

A slight positive linear correlation was observed between biomass and percent grass cover from NAIP 2011; a bar graph suggests higher biomass in plots with a higher July herbaceous coverage (Figure 3.3).

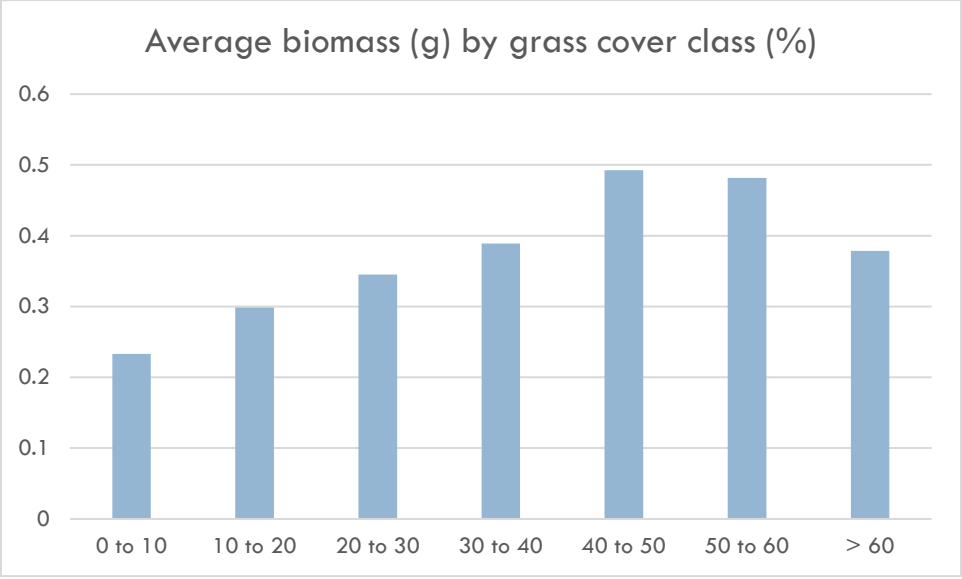

Figure 3.4. Distribution of July average arthropod biomass (g; outliers >1g removed)) by grass cover class from NAIP 2011 (% within 30m plot)

Looked at together, these data suggest higher arthropod biomass in plots with low bare ground cover, high herbaceous cover, and low to moderate shrub cover; this despite the fact that image-derived vegetation data are 8 years removed from field data.

Landsat-derived rasters

Thermal Bands 10 & 11 (June and July)

Landsat 8 imagery for 06/03/2019 and 07/21/2019 were downloaded from the USGS Earth Explorer website. Pixel values from thermal bands 10 and 11 were averaged within the 30m plots after resampling them from 30m to 1m pixels, in order to better capture possible variability within the plots (i.e., a plot overlapping several 30m pixels is assigned an average value, instead of that of the dominant pixel).

There were no linear correlations between biomass and June band 10 and band 11 values, even after removing outliers (biomass > 1g). Bar graphs did not show any obvious pattern.

For July on the other hand, a negative correlation was observed between biomass (outliers removed) and band value, for both bands; this pattern was reflected in the bar graphs (Figures 3.5 through 3.8).

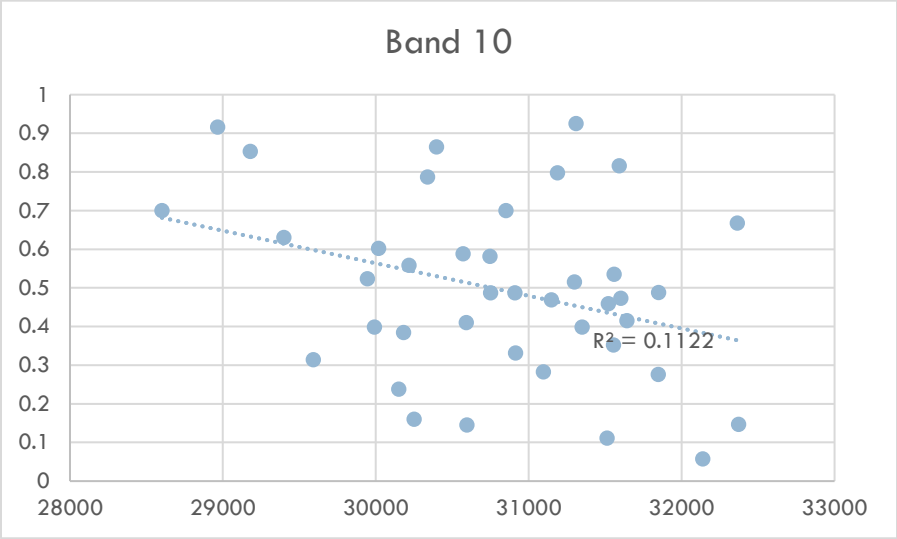

Figure 3.5. Regression plot of July arthropod biomass (g) against Landsat Band 10 values within 30m plots.

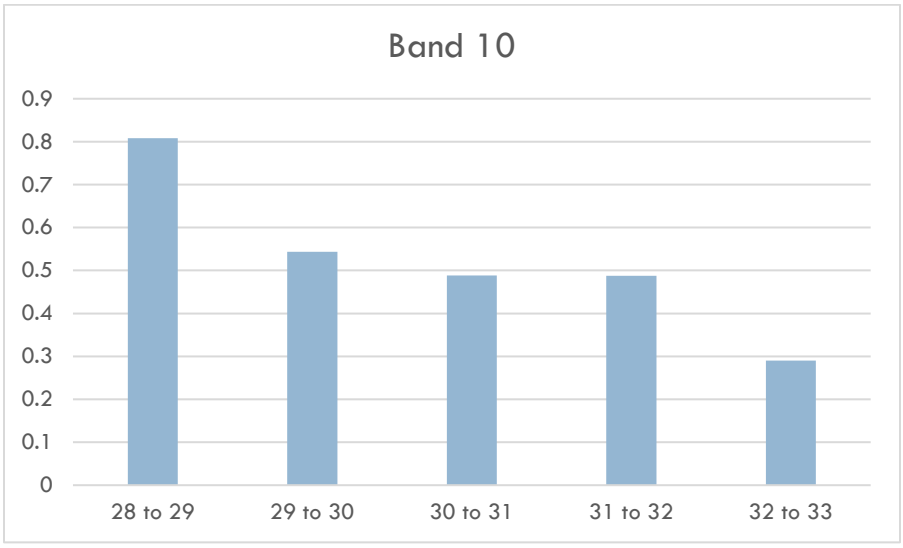

Figure 3.6. Distribution of July average arthropod biomass (g; outliers >1g removed)) by Landsat thermal band 10 classes within 30m plots.

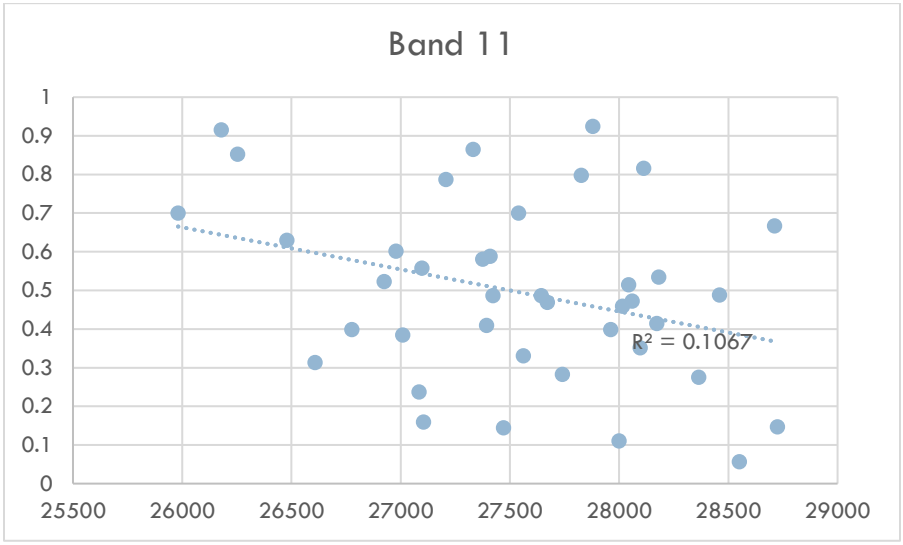

Figure 3.7. Regression plot of July arthropod biomass (g) against Landsat Band 11 values within 30m plots.

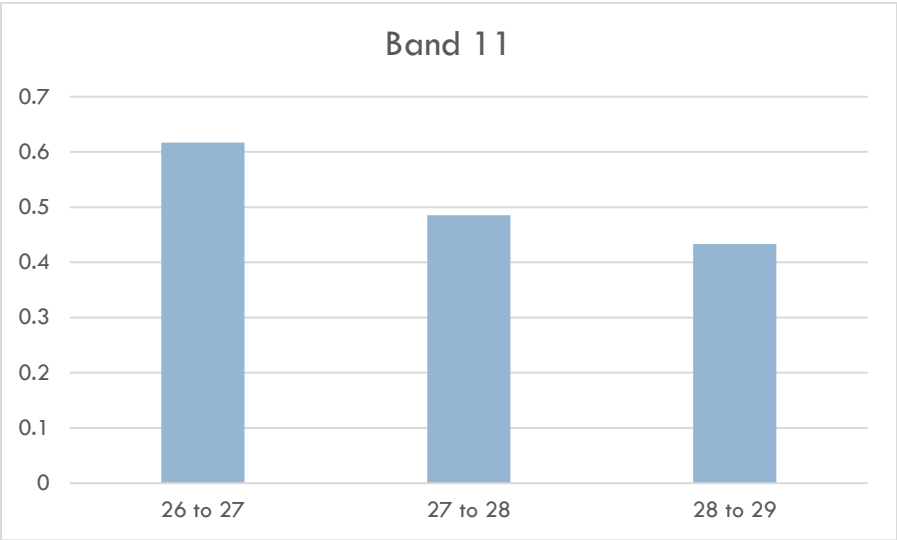

Figure 3.8. Distribution of July average arthropod biomass (g; outliers >1g removed)) by Landsat thermal band 11 classes within 30m plots.

GPP

Google Earth Engine was used to extract Landsat Gross Primary Production (GPP; Robinson et al. 2018) for June and July 2019. Biomass values greater than 1g were removed from analysis.

Even after removing outliers heavier than 1g, June variability was high (Figure 3.9); a bar graph shows heavier average biomass in the 400 to 600 June GPP values, but this could be an artifact of the data (Figure 3.10). The same variability is observed in July (Figure 3.11), although the bar graph shows a more linear, increasing trend (Figure 3.12).

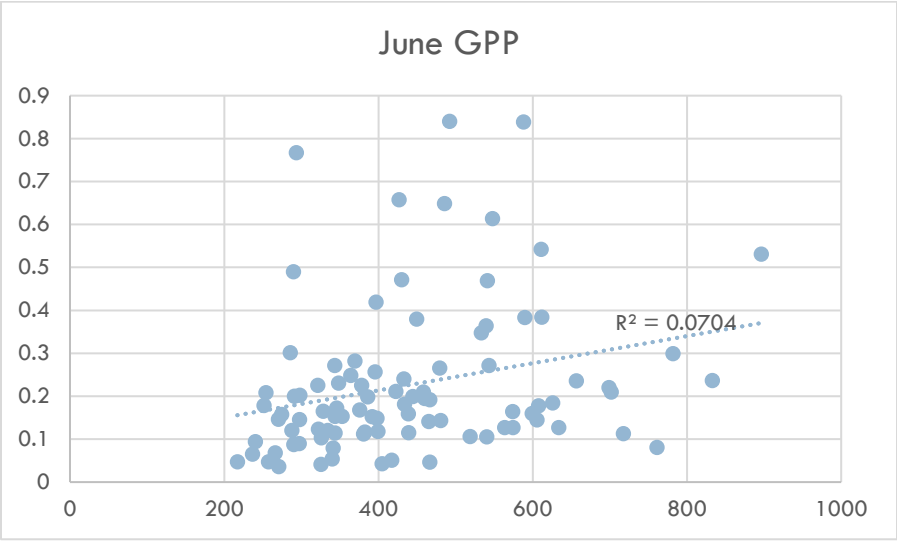

Figure 3.9. Regression plot of June arthropod biomass (g) against Landsat June GPP values within 30m plots.

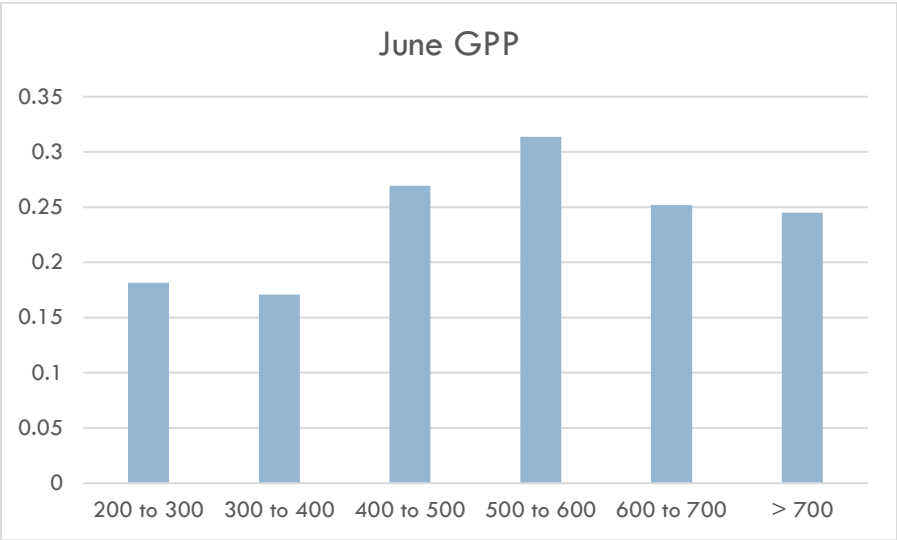

Figure 3.10. Distribution of average June arthropod biomass (g; outliers >1g removed)) by Landsat GPP classes within 30m plots.

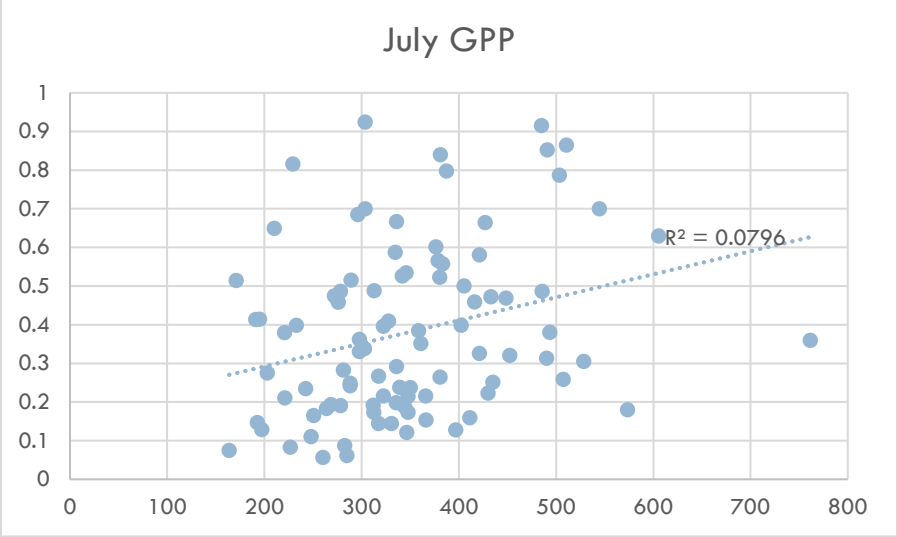

Figure 3.11. Regression plot of July arthropod biomass (g) against Landsat July GPP values within 30m plots.

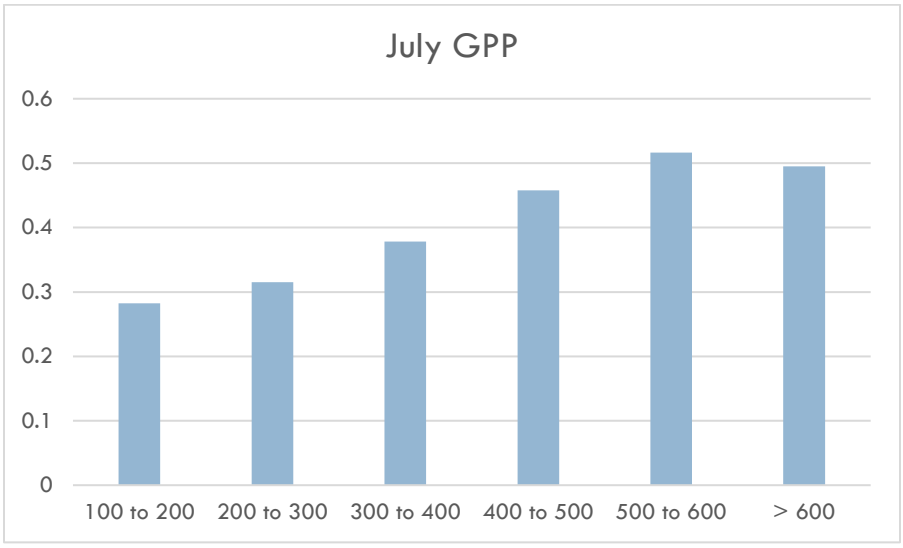

Figure 3.12. Distribution of average July arthropod biomass (g; outliers >1g removed)) by Landsat GPP classes within 30m plots.

Sentinel-derived rasters

Two cloud-free Sentinel images were downloaded from the USGS Earth Explorer website, one for June 12 2019, the other for July 22, 2019. They were atmospherically corrected to bottom-of-atmosphere using the Sen2Cor plugin of the Sentinel Application Platform (SNAP; https://step.esa.int/main/toolboxes/snap/), setting Resolution to ALL and Cirrus Correction to TRUE. Various band combinations were used to derive several indices.

NDVI

The Normalized Difference Vegetation Index was calculated from the red and NIR 10m bands using the formula (NIR - Red)/(NIR + Red), or (B8 - B4) / (B8 + B4). It ranges from -1 to +1, with higher values for live, green vegetation. As for Landsat data, imagery was resampled to 1m and averaged within each 30m plot.

As for GPP, linear correlations were weak, but bar graphs show a trend of increased biomass with higher NDVI values, for both June and July (Figures 3.13 and 3.14).

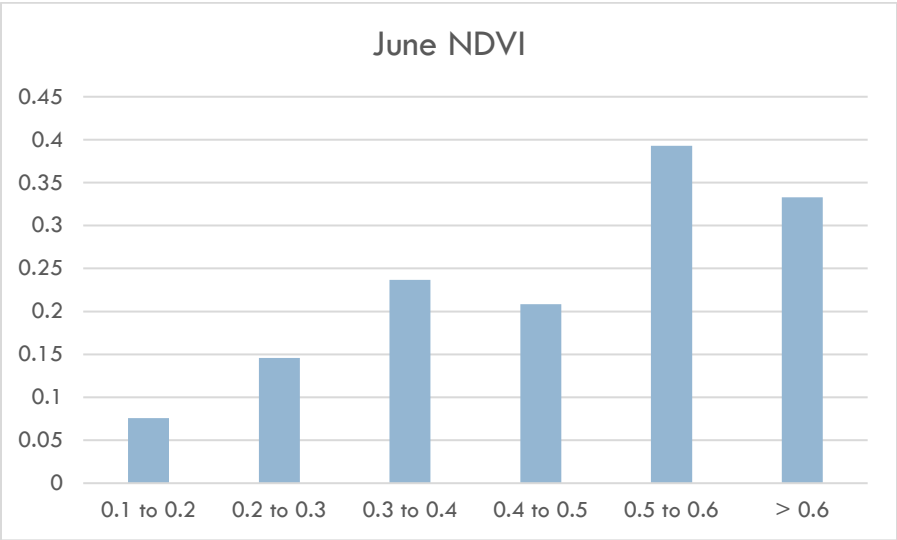

Figure 3.13. Distribution of average June arthropod biomass (g; outliers >1g removed)) by Sentinel 2 NDVI classes within 30m plots.

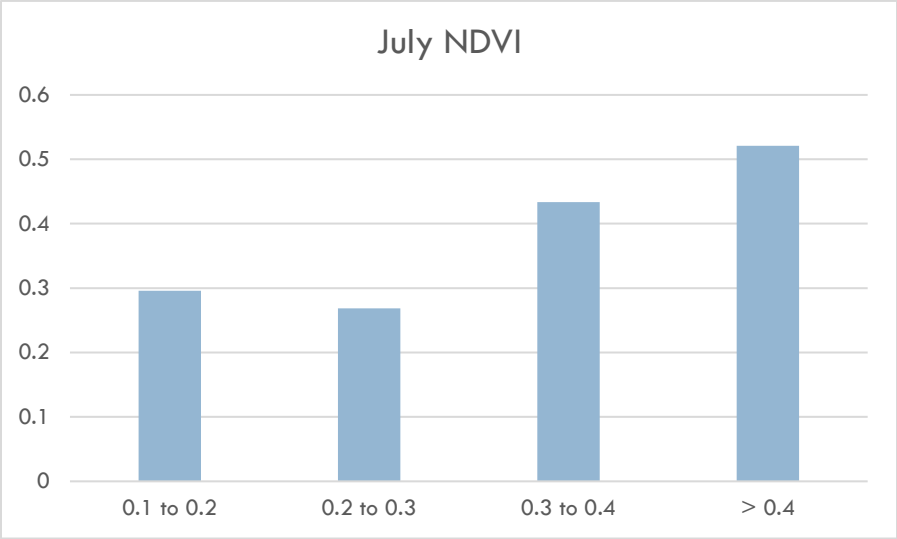

Figure 3.14. Distribution of average July arthropod biomass (g; outliers >1g removed)) by Sentinel 2 NDVI classes within 30m plots.

SAVI

The Soil Adjusted Vegetation Index is a transformation technique that minimizes soil brightness influences from spectral vegetation indices involving red and near-infrared (NIR) wavelengths. Like NDVI, it was calculated at 10m from the red and NIR 10m bands using the formula [((NIR - Red) / (NIR + Red + L)) x (1 + L)], or [((B8 - B4) / (B8 + B4 + 0.5)) * 1.5]. It ranges from -1.5 to +1.5, with higher values for live, green vegetation. As for Landsat data, imagery was resampled to 1m and averaged within each 30m plot.

Bar graphs also show a trend of increasing biomass with increasing SAVI values (Figures 3.15 and 3.16).

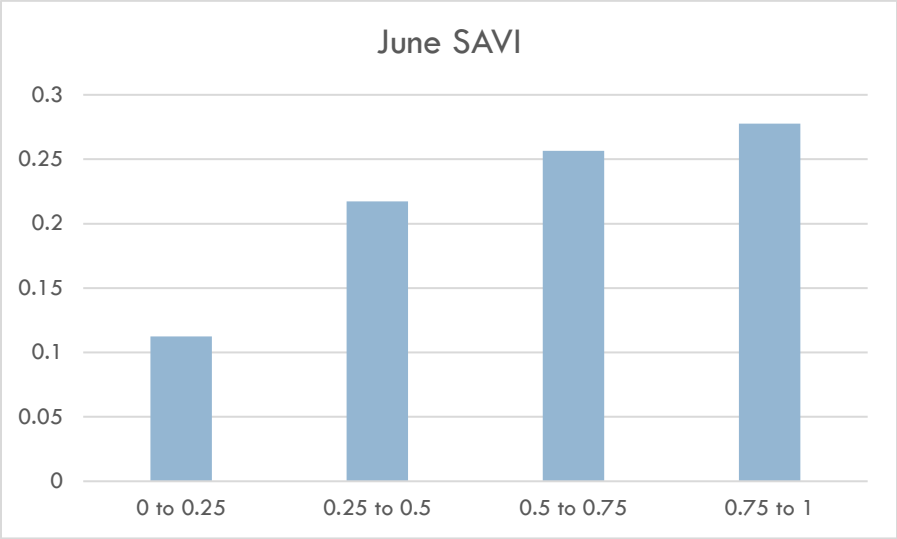

Figure 3.15. Distribution of average June arthropod biomass (g; outliers >1g removed)) by Sentinel 2 SAVI classes within 30m plots.

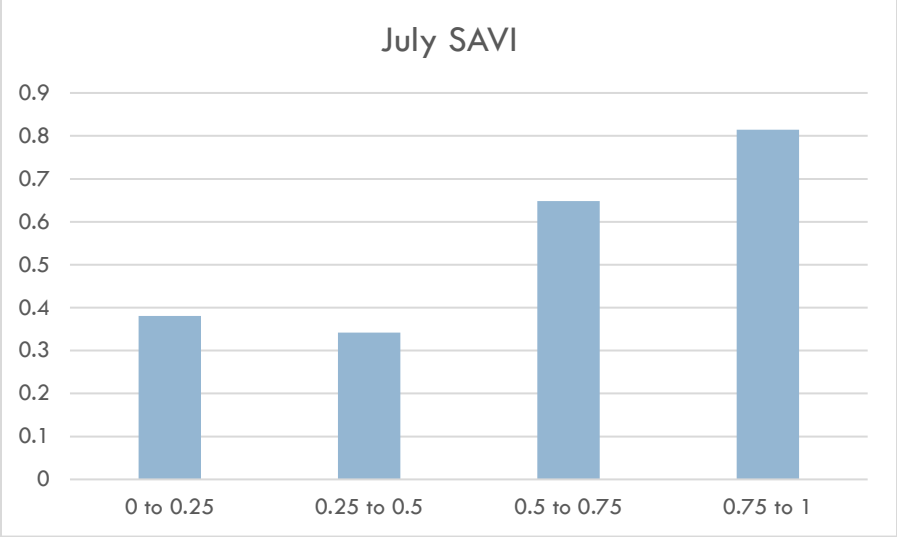

Figure 3.16. Distribution of average July arthropod biomass (g; outliers >1g removed)) by Sentinel 2 SAVI classes within 30m plots.

BSI

A bare soil index was calculated from bands 2, 4, 8 and 11 following the formula {(B11+B4)-(B8+B2)}/{(B11+B4)+(B8+B2)} (Pal and Antil 2017). Because the short wave infrared band 11 uses a resolution of 20m, the raster is at that scale.

There were no obvious patterns for July BSI; however, the June BSI bar graph shows decreasing average biomass with increasing BSI (Figure 3.17).

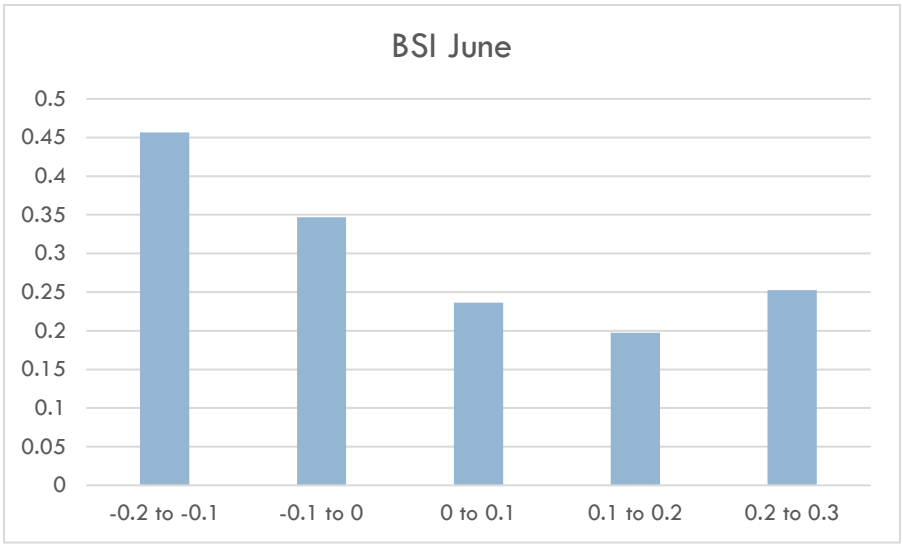

Figure 3.17. Distribution of average June arthropod biomass (g; outliers >1g removed)) by Sentinel 2 BSI classes within 30m plots.

NDMI

The Normalized Difference Moisture Index is used to determine vegetation water content; it was calculated from NIR and SWIR1, or bands 8 and 11: (B8 – B11) / (B8 + B11). Like BSI it is a 20m raster, which was resampled to 1m and averaged within 30m buffers. Both June and July NDMI bar graph shows a trend towards higher biomass with higher NDMI (Figures 3.18 and 3.19).

Overall, Sentinel-derived indices confirm patterns observed with NAIP and Landsat: a negative relation between arthropod biomass and bare ground, and a positive one with greenness/vegetation moisture content.

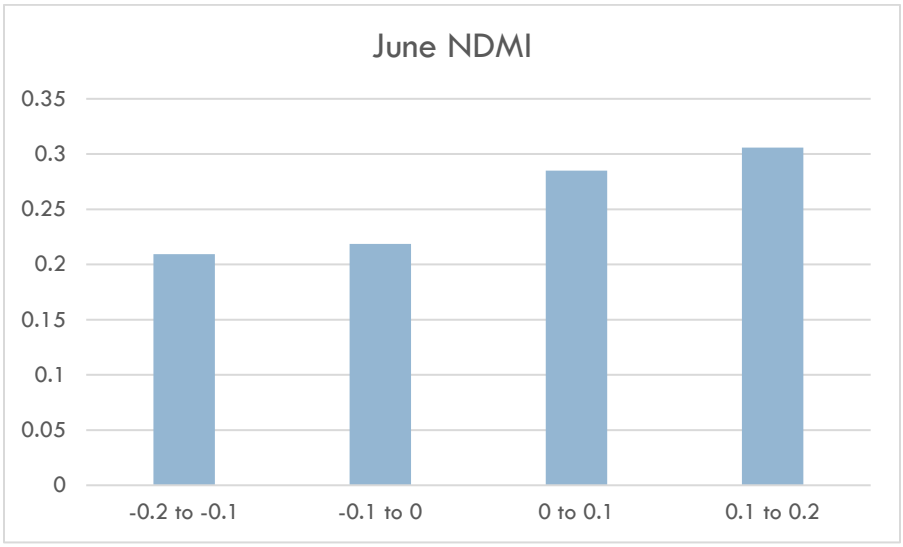

Figure 3.18. Distribution of average June arthropod biomass (g; outliers >1g removed)) by Sentinel 2 NDMI classes within 30m plots.

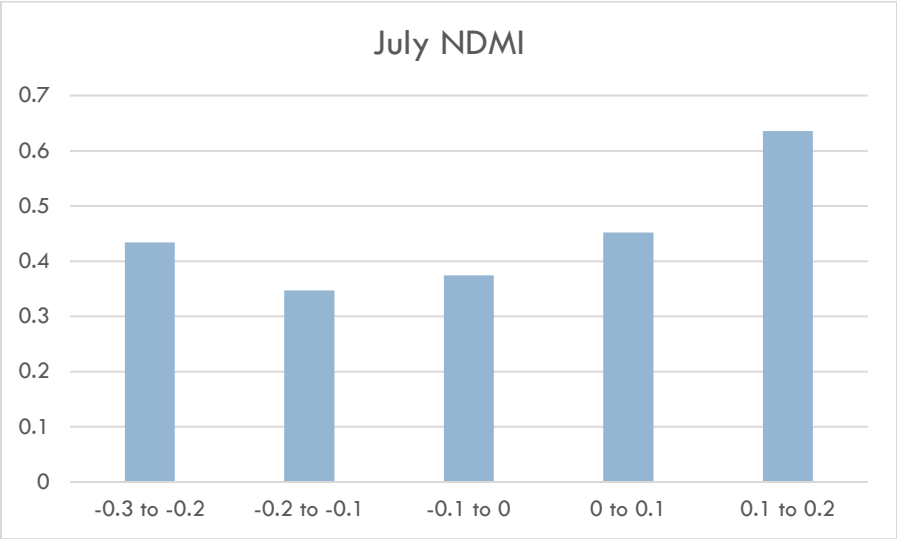

Figure 3.19. Distribution of average July arthropod biomass (g; outliers >1g removed)) by Sentinel 2 NDMI classes within 30m plots.

Solar radiation

TerraClimate

Downward Surface Shortwave Radiation was downloaded for the most recent year available (2018) from the TerraClimate website. Unfortunately, the resolution of the dataset is too coarse (4km pixels) to be meaningful within the study area; whereas values range from 0 to 467 worldwide and from 20 to 159 within the continental US, only 3 are within the Lake Mason study area (57, 58, 59; Figure 3.20).

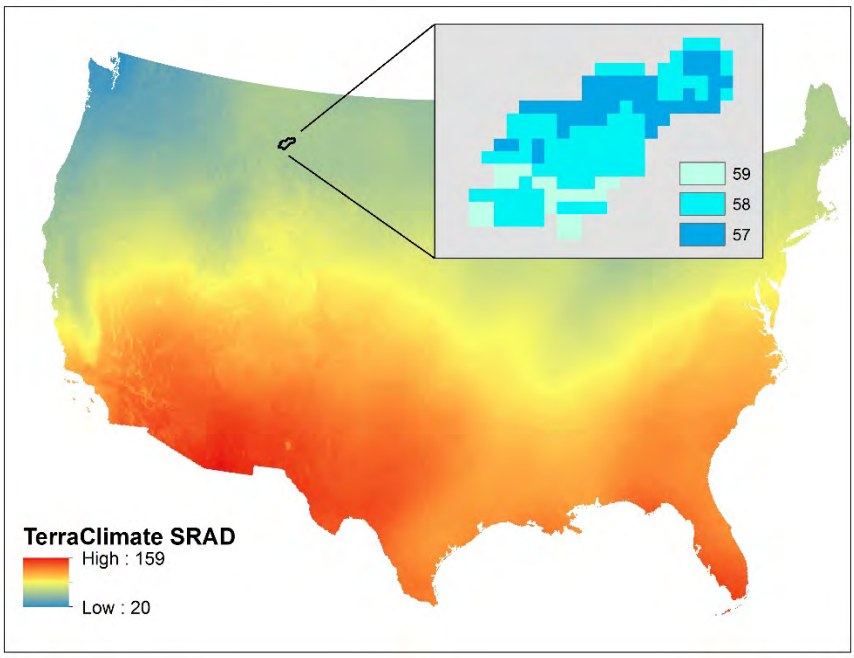

Figure 3.20. 2018 Solar Radiation from TerraClimate showing the coarse scale and lack of variability within the Lake Mason study area.

30m DEM

May, June and July solar radiation rasters were derived from a 30m DEM using the ArcGIS command Area Solar Radiation, using a 2-day interval and the default 0.5 hour interval.

Although a bar graph for May shows a steady increase of biomass with solar radiation (Figure 3.21), there is no obvious pattern for June and July (Figure 3.22).

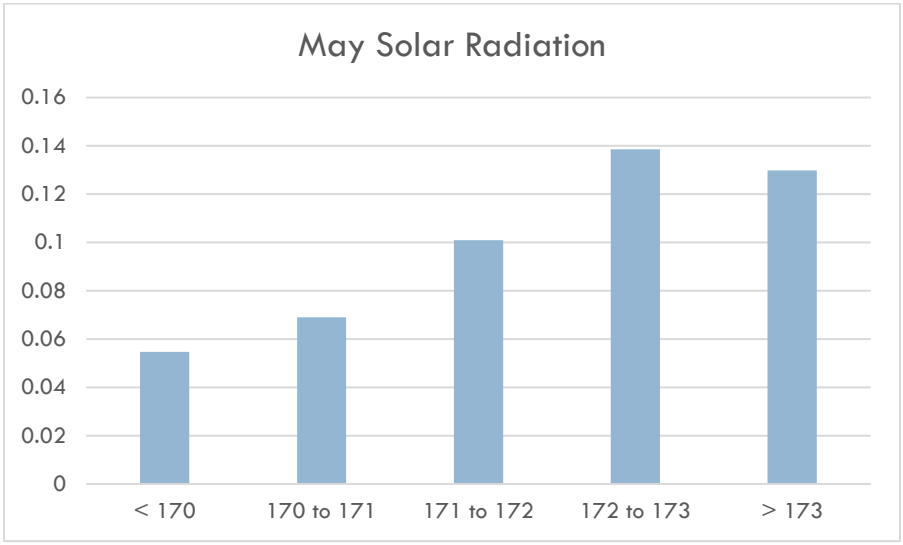

Figure 3.21. Distribution of average May arthropod biomass (g; outliers >1g removed)) by solar radiation classes within 30m plots.

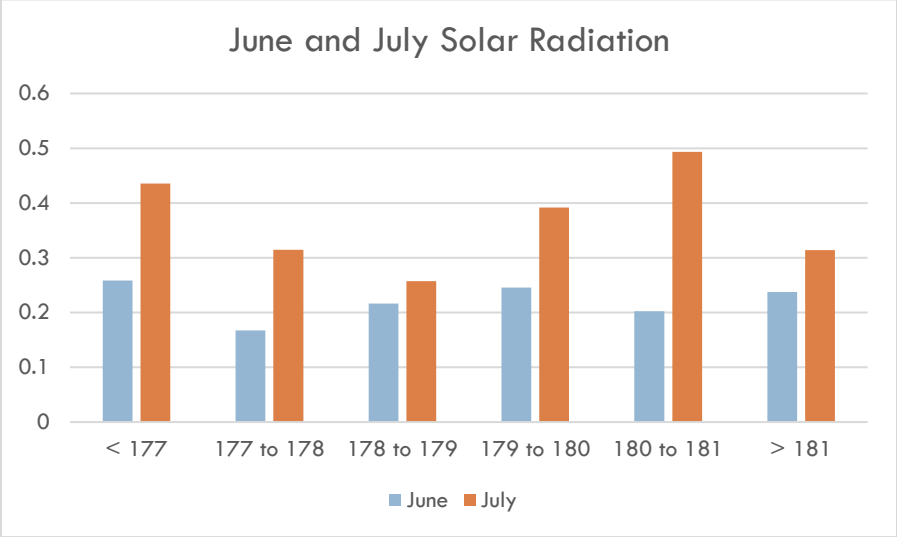

Figure 3.22. Distribution of average June and July arthropod biomass (g; outliers >1g removed)) by solar radiation classes within 30m plots.

Lidar-derived rasters

Lidar data are available for part of the study area, including the Musselshell River corridor. For simplicity and testing I used only data available from the 2010 Montana Sage Grouse Habitat Study (Figure 3.23), which provides high resolution data for 141 arthropod plots.

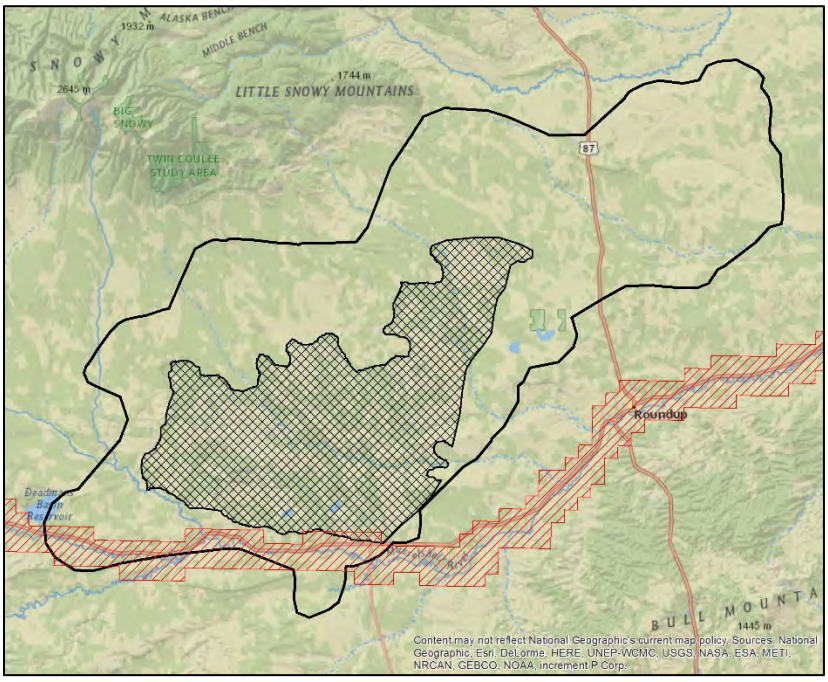

Figure 3.23. Lidar availability for the Lake Mason Study area. Black crosshatches: 2010 Sage Grouse Habitat Study; red stripes: Musselshell River corridor.

Topographic variability

The ArcGIS command Curvature was run and followed with a Focal Statistics using a circle neighborhood (15m radius) to generate a measure of topographic variability (Figure 3.24).

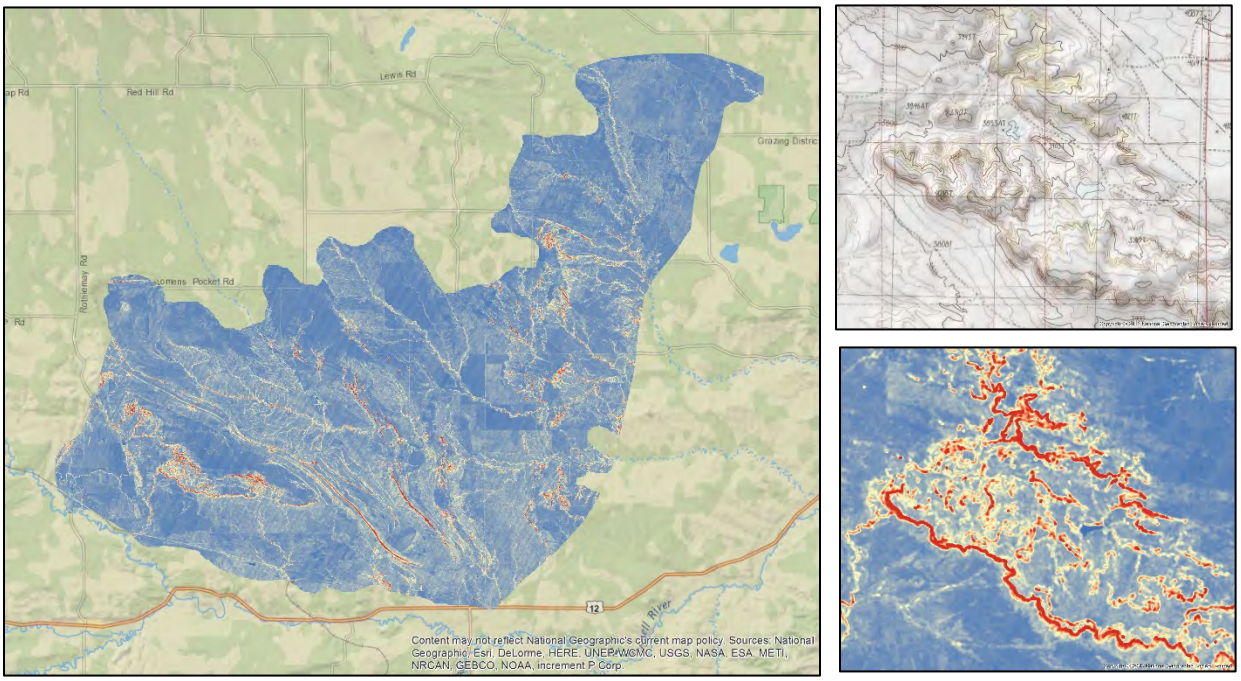

Figure 3.24. Topographic variability from LiDAR showing the more topographically varied areas in red.

In terms of distribution, the plots tend to be located on slightly more diverse terrain than what is available throughout the study area (Figure 3.25). That said, over 70% of the plots have a roughness value < 15 and only 12 (10%) have a value > 20.

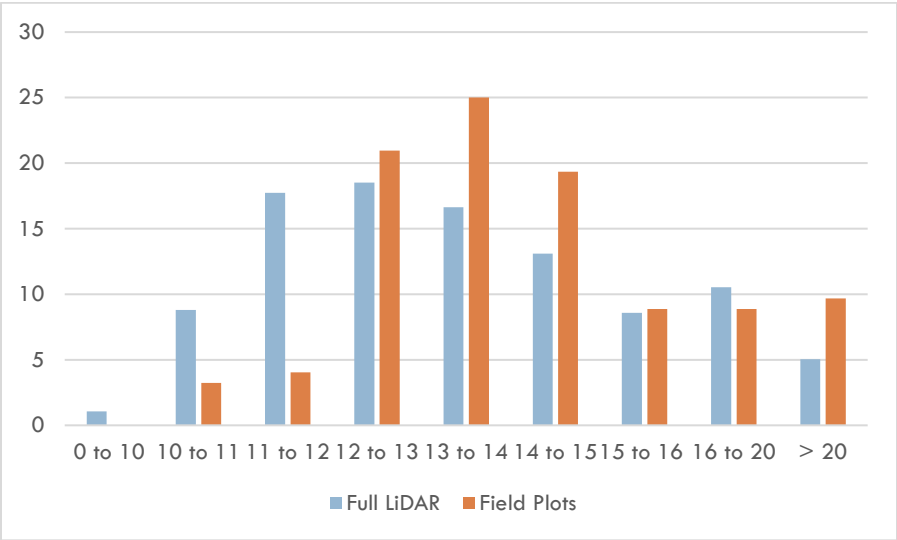

Figure 3.25. Percent composition of the area for which LiDAR is available, compared to that within 30m field plots, in terms of topographic variability.

After removing outliers, a bar graph of biomass within topographic classes shows that the lowest variability class contains heavier samples on average, although because only 5 plots compose this class, it is hard to know if this has ecological meaning or if it is just an artifact of the data (Figure 3.26).

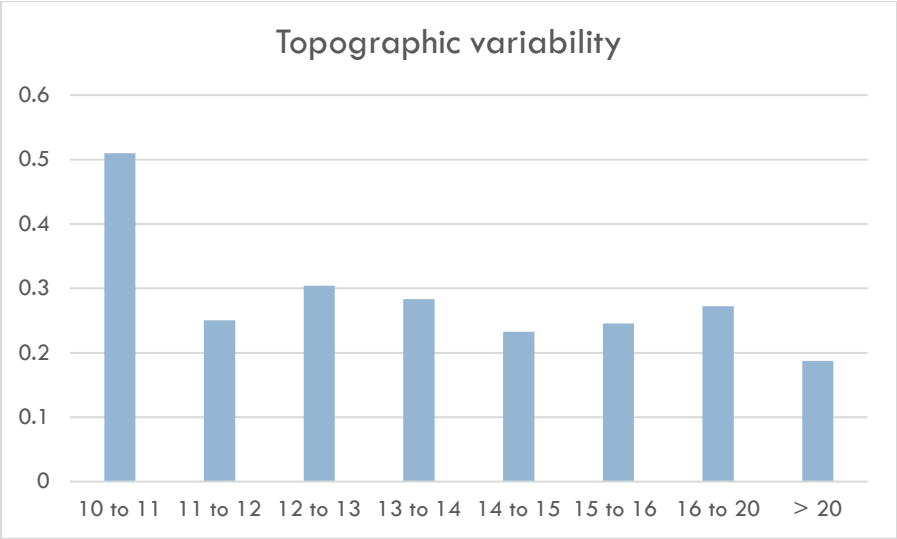

Figure 3.26. Distribution of average arthropod biomass (g; outliers >1g removed)) by LiDAR topographic variability classes within 30m plots.

2012-2018 Model Validation with 2019 Biomass Data

Two models were generated after averaging arthropod biomass data collected at 59 sites between 2012 and 2018, one including an outlier (heavier biomass), the other excluding it; in both cases, percent bare

ground was a top predictive variable, and was used to stratify the study area and generate a set of sampling points for the 2019 field season. The outlier (site ID 33018) had a biomass of 0.8409, which is on the heavier side of the 2019 data, yet would not have been considered an outlier in 2019 (for the majority of 2019 analysis, I removed sites with biomass greater than 1g; 15 sites representing 5% of the dataset). Therefore, the comparison between 2019 biomass data and model values was done with the model that includes the outlier.

Because model pixel size is 30m and the 2019 field plots are polygons with a 30m diameter, I first resampled the model to 1m then got the average biomass model value within each field plot to capture the fact that field plots likely overlap more than a single pixel. I then calculated the difference between predicted biomass and 2019 field biomass.

Two hundred and eighty-one plots overlap the model: 108 vegetation plots (47 spatially independent sites, some with repeated visits) and 173 single-visit validation plots (some with the same IDs, but non-overlapping). Differences between sampled and predicted biomass range from -0.367g (field value = 0.0246g, model = 0.391g) to 2.8g (field value = 3.157g, model = 0.355g). The heavier field samples depart most from model predictions, which is not surprising considering that the maximum pixel value for the model is only 0.57, yet 45 of the 2019 sites have an arthropod biomass larger than this value.

That said, over 40% of the field samples depart from model prediction by less than 0.1g and two-thirds of them are within 0.2g of model predictions (Figure 4.1).

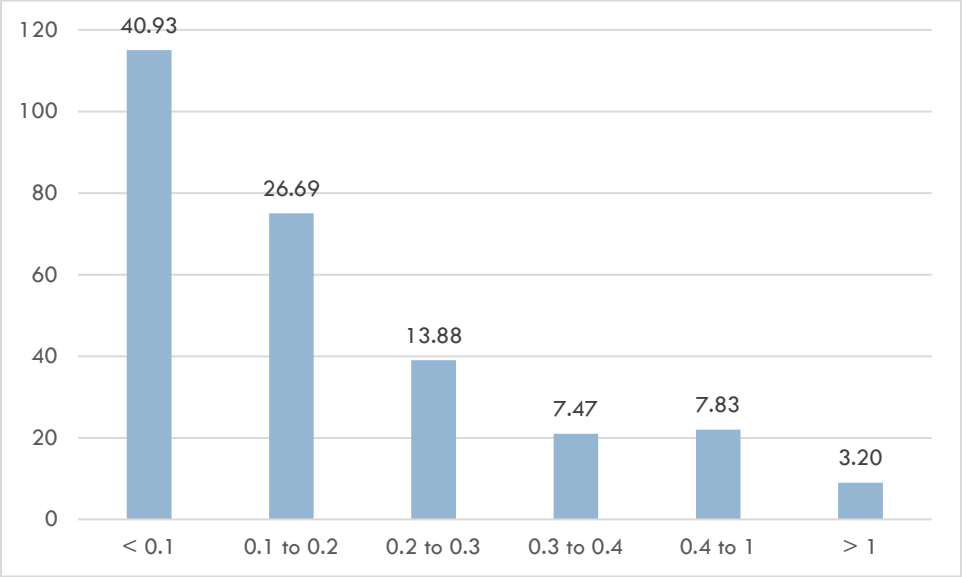

Figure 4.1. Distribution of arthropod field samples based on the difference between field biomass and predicted biomass, with percent shown atop each bar.

For those field vegetation plots sampled more than once throughout the season (N = 36), five show a within-site difference greater than 1g (plots W17, W83, W87, W84 and W133), in all cases because one of the samples is a large "outlier" biomass.

Predictive Model Using 2019 Biomass Data

RandomForest models were developed following the same methods as with 2012-2018 data; none performed well:

Model 1 used as many points as possible (all dates, but when repeated samples were collected at the same site, only July biomass data were used; N = 216).
Percent variance explained: 22.08; Pearson's: 0.36; Spearman's: 0.54; top predictor = Date.

Model 2: same as model 1 but outliers (biomass > 1g) were removed (N = 206).
Percent variance explained: 31.14; Pearson's: 0.3; Spearman's: 0.35; top predictor = Date.

Model 3: same as model 2 but Date was removed from predictors – a necessary step for spatial extrapolation to the whole study area.
Percent variance explained: 10.39; Pearson's: -0.21; Spearman's: -0.13; top predictors = SR_06 and SR_07.

Model 4: same as model 3 but Solar Radiation was removed from predictor set.
Percent variance explained: -1.05; Pearson's: -0.19; Spearman's: -0.16; top predictor = B10_06, B11_06, SAVI_07, GPP1218_05, NAIP_bare

Model 5 used data from June and July only. N = 164 (no biomass > 1g), and all variables except Solar Radiation from May and Date.
Percent variance explained: 1.17. Pearson's: 0.31; Spearman's: 0.32. Top variables: NDVI_06. BSI_06, GPP_1218_06, SR_07, SAVI_06, SR_06.

Model 6 used biomass data from July only but kept June variables (same as model 5). N = 110 (no biomass >1g).
Percent variance explained: -3.61. pearson's: 0.45; Spearman's: 0.53. Top variables: SAVI_07, NDVI_07.

Conclusions

Repeated sampling this field season made biomass data more difficult to use; best results from RandomForest were for those models including Date as a predictor (Models 1 and 2), but because Julian date cannot be turned into a spatial surface, these models could not be extrapolated to the study area. The next best model, model 3, only explained 10% of the variance in arthropod biomass. It is possible that June and July solar radiation acted as "proxy" for date.

ARTHROPOD BIOMASS MODEL – 2020 DATA

Sampling Protocol

The 2020 field season aimed at gathering biomass data for a maximum number of sites instead of detailed vegetation data at a few sites, as was done in 2019. Despite a skeleton sampling crew due to Covid limitations, around 220 sites were visited (from a regular grid of 1km points covering the study area but excluding agriculture and no-access properties) and arthropods were collected using the sweep method. Sampling consisted of two 30m perpendicular transects intersecting at the plot centroid. Reconciling the analyzed sampling bags (specimen weighed and classified by order) with actual plot coordinates resulted in 218 reliable biomass values (Figure 3).

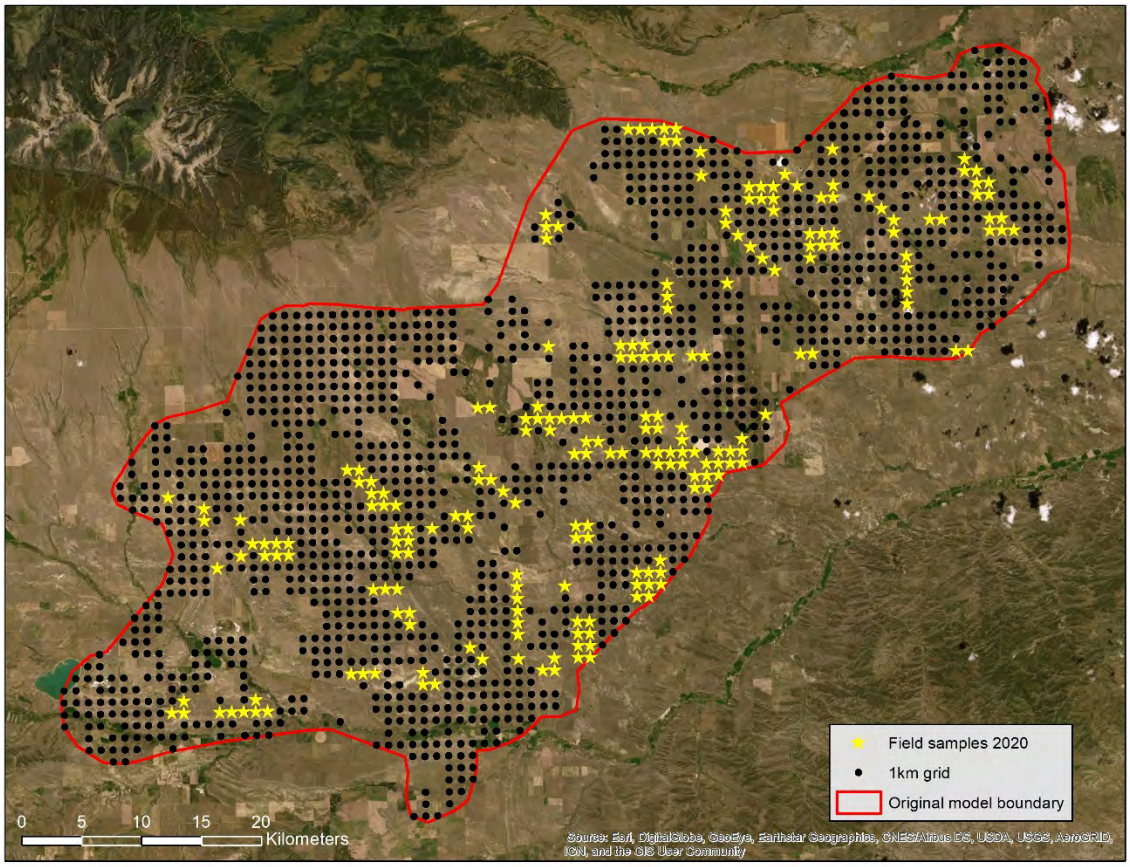

Figure 3. Distribution of 218 arthropod sampling sites during the 2020 field season in the Lake Mason area, Montana.

BIOMASS DATA ANALYSIS

Biomass data analysis was conducted after summing E/W and N/S biomass for each plot. Over the sampled period (June 8 – August 13), arthropod biomass ranged from 0.088g on June 26 to 57.44g on

July 7 (mean 6.88g, SD 8.73g). This is significantly higher than previous years. At the 59 plots collected between 2012 and 2018 and used to generate the original model, biomass ranged from 0.0036g to 0.8409g and averaged 0.193g (SD 0.189g). In 2019, for 293 unique plot/date combinations, biomass ranged from 0.0005g to 3.157g and averaged 0.347g (SD 0.435g).

Analysis by Order

Arthropods were identified, weighed, and grouped into twelve orders (Table 1). Orthoptera and Homoptera were the most common orders, sampled in all 218 plots and dominating by their number of individuals and their weights (particularly grasshoppers in Orthoptera; all weights in grams). At the other end of the spectrum, Ephemenoptera (e.g., mayflies), Dermaptera (e.g., earwigs), Neuroptera (e.g., lacewings) and Zygoptera (suborder of Odonata; e.g., damselflies) made the smallest contribution in number of individuals and weights (Table 1, Figures 2, 3, 4 & 5).

Table 1 Summary statistics of 2020 arthropod field sampling by order.

Order	Number of plots	Number of individuals	Sum biomass	Min biomass	Max biomass	Mean biomass	SD biomass
Arachnida (spiders)	191	1,250	9.35	0.0005	0.716	0.028	0.074
Coleoptera (beetles, weevils)	190	1,328	6.92	0.0005	0.552	0.022	0.049
Dermaptera (earwigs)	3	4	0.07	0.009	0.031	0.023	0.012
Diptera (mosquitos, midges, other flies)	162	2,496	3.7	0.0001	0.201	0.014	0.022
Ephemeroptera (mayflies)	1	1	0.0005	0.0005	0.0005	0.0005	0
Hemiptera (aphids, leafhoppers)	116	1,685	4.59	0.0006	0.242	0.028	0.035
Homoptera (aphids, leafhoppers)	218	10,875	40	0.001	1.151	0.096	0.131
Hymenoptera (bees, ants)	202	3,549	5.6	0.0005	0.428	0.015	0.032
Lepidoptera (butterflies & moths)	107	419	3.39	0.0005	0.571	0.022	0.056

Neuroptera (lacewings)	10	21	0.12	0.003	0.0201	0.01	0.006
Orthoptera (grasshoppers)	218	37,155	1437.2	0.005	36.944	3.274	4.766
Zygoptera (damselflies)	21	32	0.4	0.004	0.138	0.017	0.027

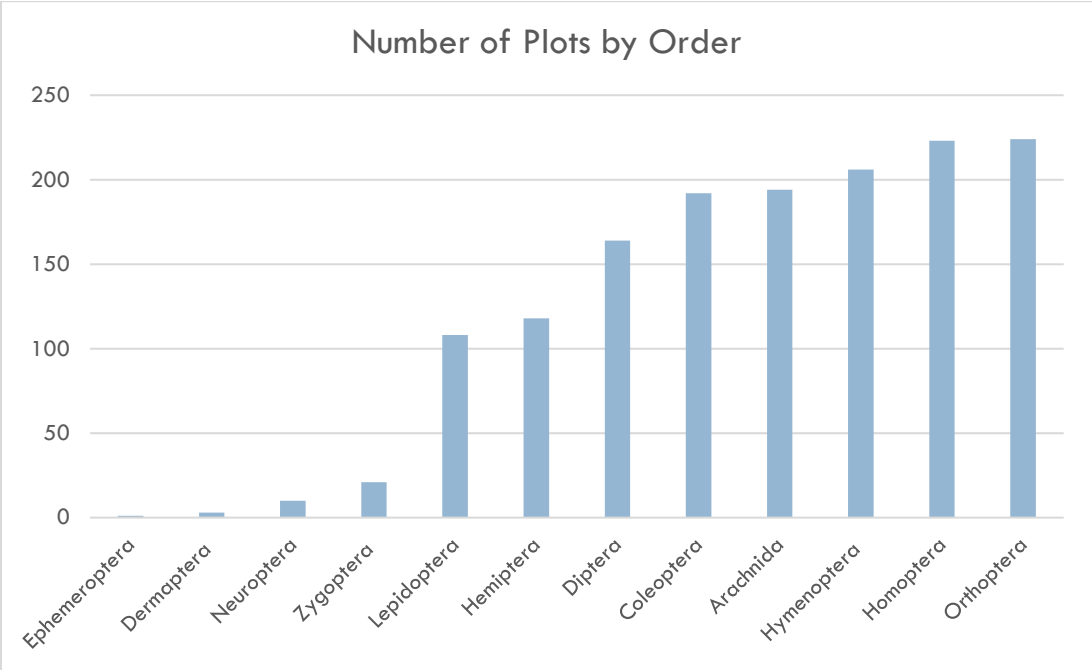

Figure 4. Distribution of number of plots by arthropod order.

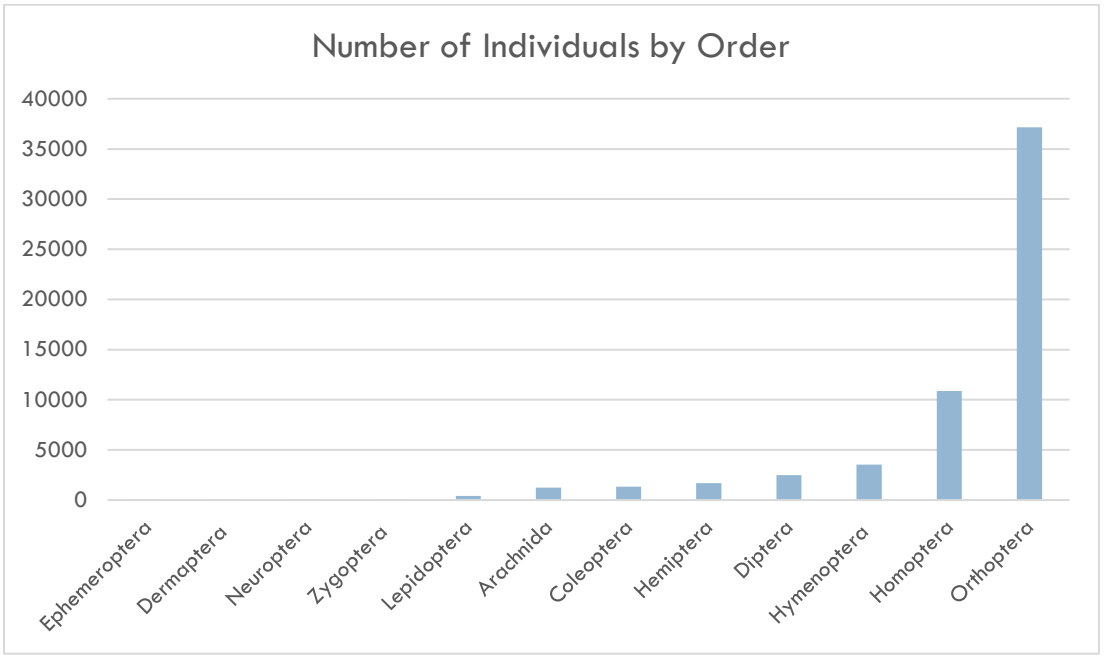

Figure 5. Distribution of number of individuals by arthropod order.

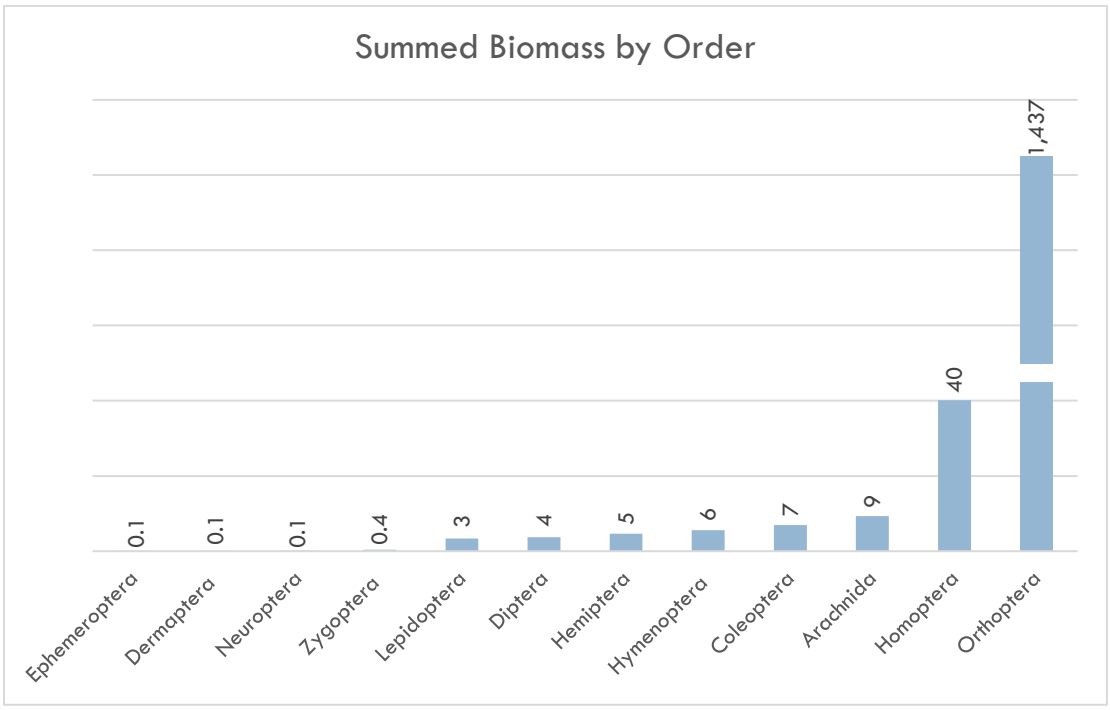

Figure 6. Summed biomass by arthropod order.

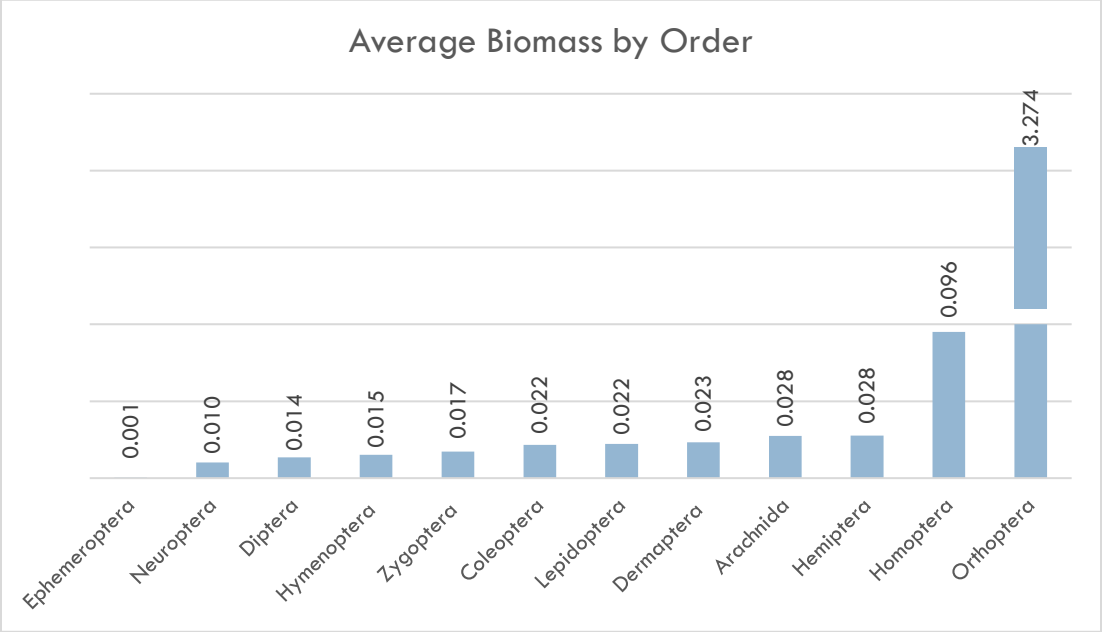

Figure 7. Average biomass (g) by arthropod order.

Temporal Distribution

Plots were visited over 30 days between June 8 and August 13. There is a trend towards increasing biomass as the season progresses (Figure 6), although when biomass is summed by date, "heavy" and "light" days are scattered throughout (Figure 7). Because there was no repeat sampling of plots this field season to prioritize maximum spatial coverage, the suitability – or unsuitability – of habitat at each plot is likely to confuse any potential temporal trend, especially after June 26 (there were clearly fewer arthropods in early June).

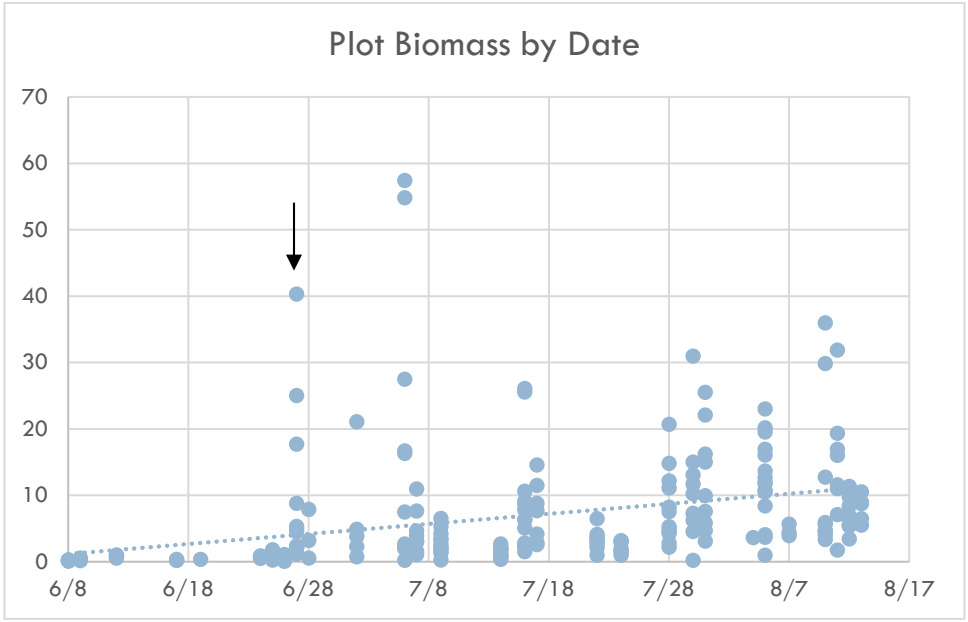

Figure 8. Temporal distribution of arthropod biomass (g) for 219 plots. Black arrow points to June 26 sampling.

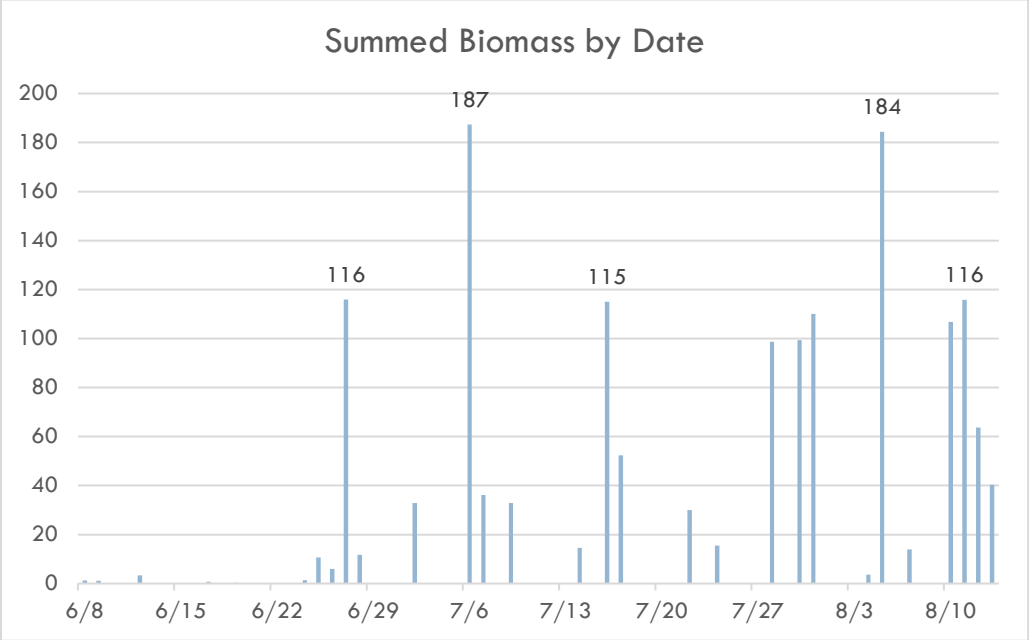

Figure 9. Temporal distribution of summed arthropod biomass (g), with labels for the "heaviest" days.

In terms of distribution by order, again, habitat suitability probably confuses potential patterns, as does uneven sampling effort (i.e., more plots collected at certain dates). Because of their heavier biomass, homoptera and orthoptera were graphed separately (Figure 8 and 9), with the remaining ten orders graphed together (Figure 10).

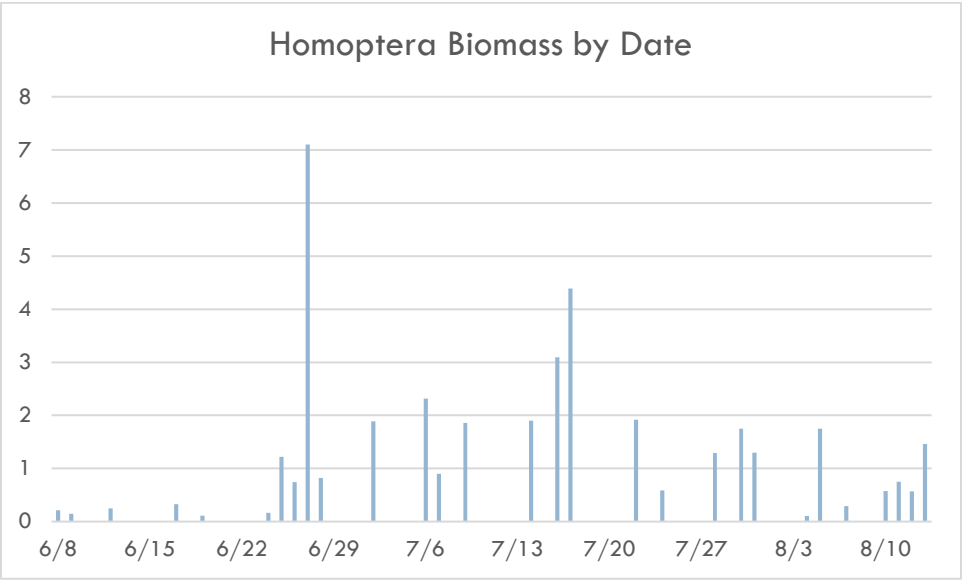

Figure 10. Temporal distribution of homoptera biomass.

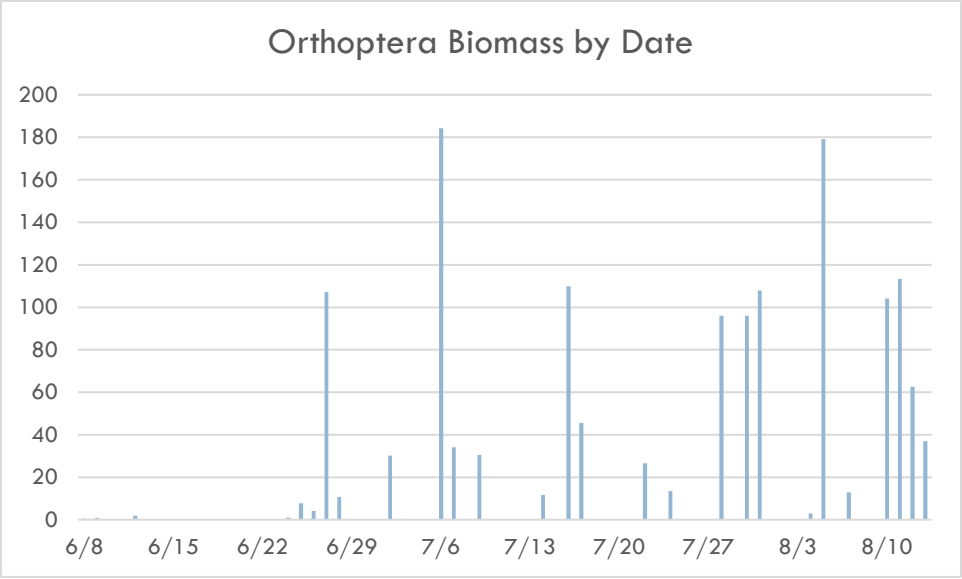

Figure 11. Temporal distribution of orthoptera biomass.

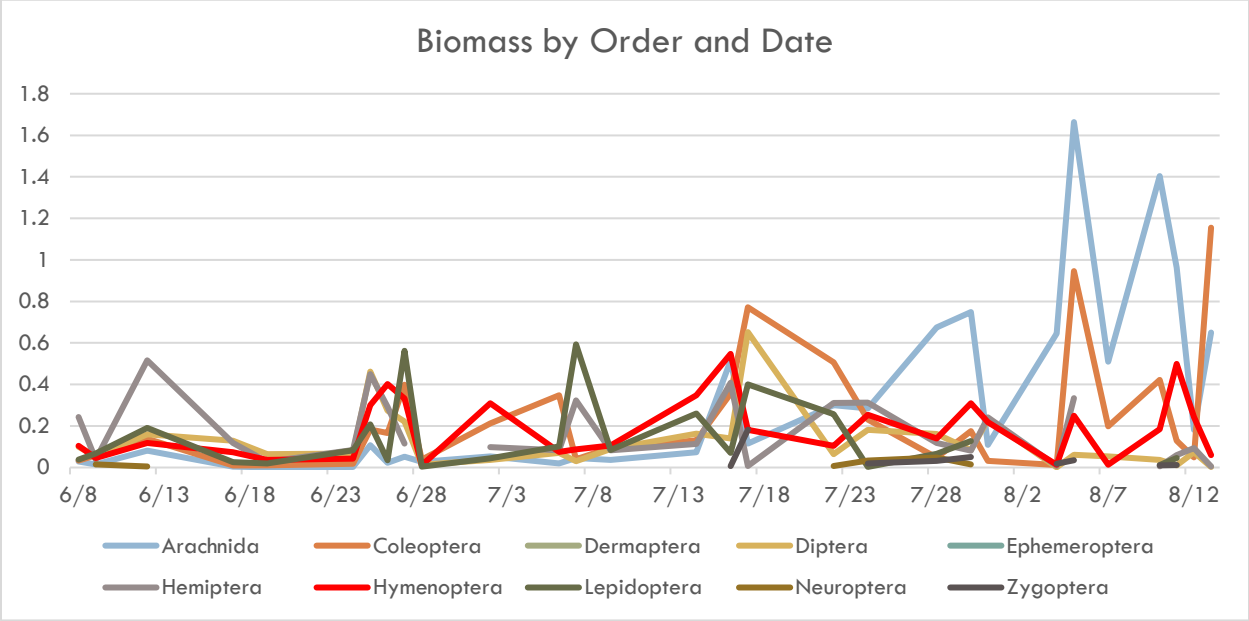

Figure 12. Temporal distribution of ten arthropod orders.

To simplify the biomass dataset, I summed all orders and grouped it by quartiles, which reveals temporal patterns previously hidden: plots with the lowest biomass (Q1) were predominantly collected in June, whereas August plots have a higher proportion of heavier biomass (Q3 and Q4) (Figure 11). Plots were sampled in clusters (several adjacent/neighboring plots sampled at the same date), which resulted in biomass plots with similar biomass often grouped together (Figure 12). There are exceptions though, with the presence of different biomass classes among plots sampled at the same date (e.g. yellow cluster on Figure 12, all 6 plots collected on July 6th).

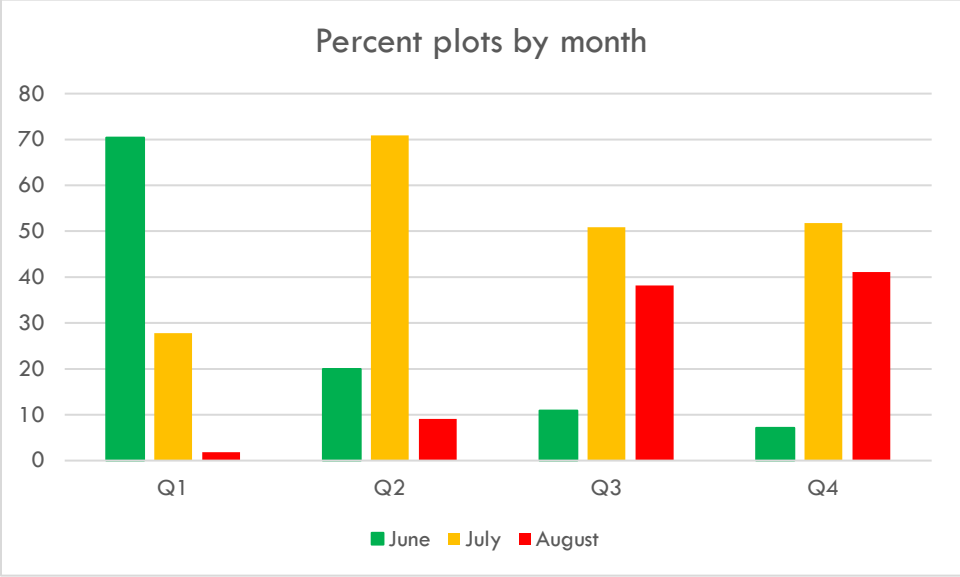

Figure 11.Seasonal distribution of arthropod biomass quartiles (percent plots on Y-axis).

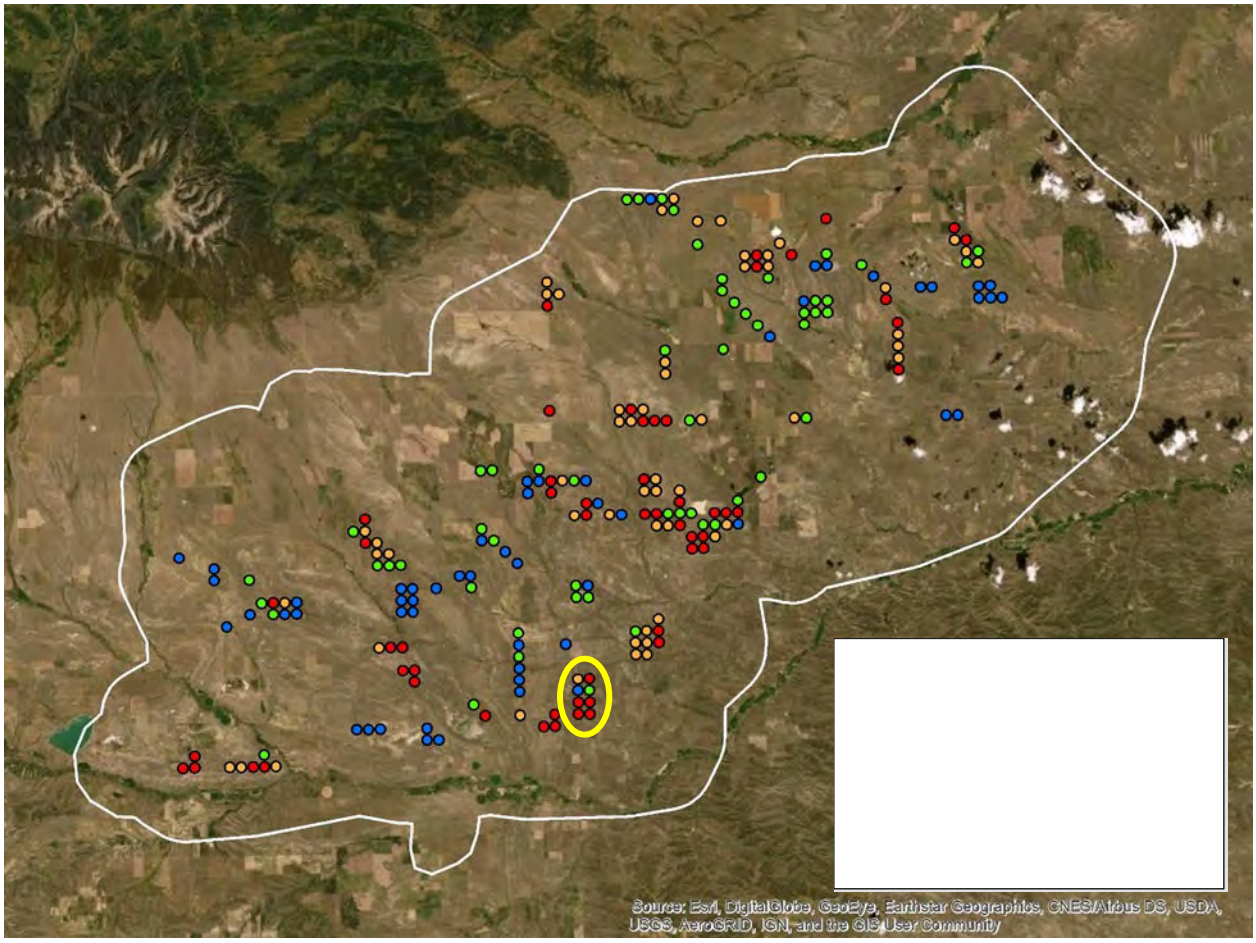

Figure 12. Spatial distribution of arthropod biomass quartiles in the study area.

Orthoptera being so overwhelming, I looked at quartile data for arthropod after removing this order. Percent plots by sampling month and biomass quartile is different when Orthoptera do not enter the biomass sum (Figure 13). July is the dominant month regardless of quartile; June does not appear as significant for Q1 as it was when Orthoptera biomass was included. There is a higher proportion of heavier plots (Q4) in August, compared to lighter plots.

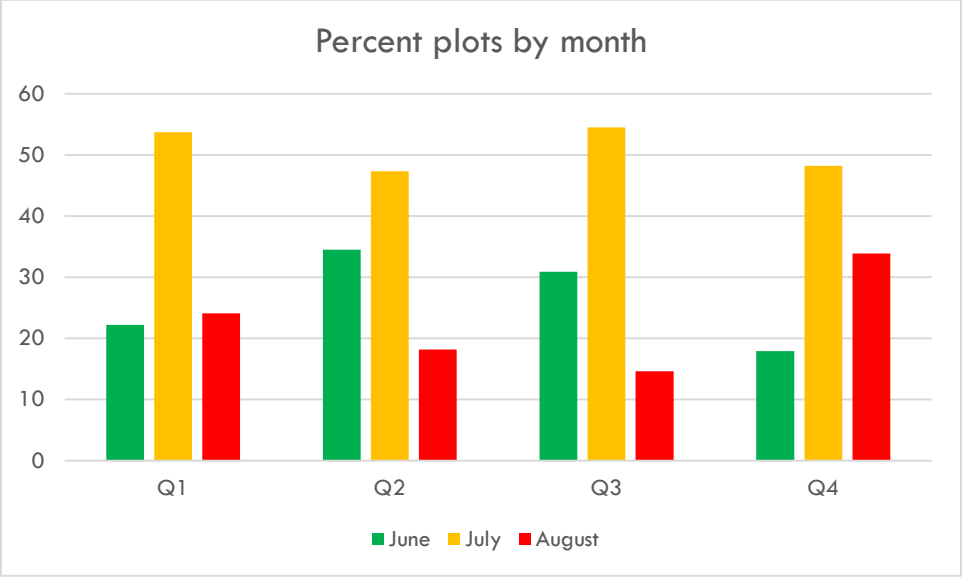

Figure 13. Seasonal distribution of biomass quartiles, no Orthoptera (percent plots on Y axis).

PREDICTIVE MODELS

Habitat Variables

Because models of arthropod biomass are to be related to other data (pertaining to bird studies), the original study area (Figure 1) was expanded to match that of songbird and sage grouse studies (Figure 14). As a result, the vegetation classification generated by Open Range Consulting using 2011 NAIP imagery could not be used as input in the 2020 models; it was beginning to be outdated anyway.

Topographic Variables

A 10m Digital Elevation Model was extracted from the statewide raster and used to derive slope (in degrees, command SLOPE in ArcGIS Spatial Analyst), curvature (command CURVATURE in ArcGIS Spatial Analyst), and solar radiation (command AREA SOLAR RADIATION in ArcGIS Spatial Analyst).

Image-derived Variables

Three sources of data were used to get vegetation-related variables for the study area:

- **Gross Primary Productivity**
  GPP rasters were downloaded from Google Earth Engine for ten years (2011– 2020); three variables were generated, average pixel value for all ten years, and the years 2019 and 2020 individually.

- **Rangeland Analysis Platform**
  RAP rasters were downloaded from Google Earth Engine for nine years (2011 – 2019); average values at the pixel level were computed for the first five bands (B1 – Annual grasslands and Forbs, B2 – Bare Ground, B3 – Litter, B4 – Perennial grasslands and Forbs, and B5 – Shrubs). These bands were also input for the year 2019 separately.

- **Tasseled Cap transformed Landsat image**
  Three bands of tasseled cap transformation (brightness, greenness, wetness) were generated for a Landsat 8 image from 08/08/2020.

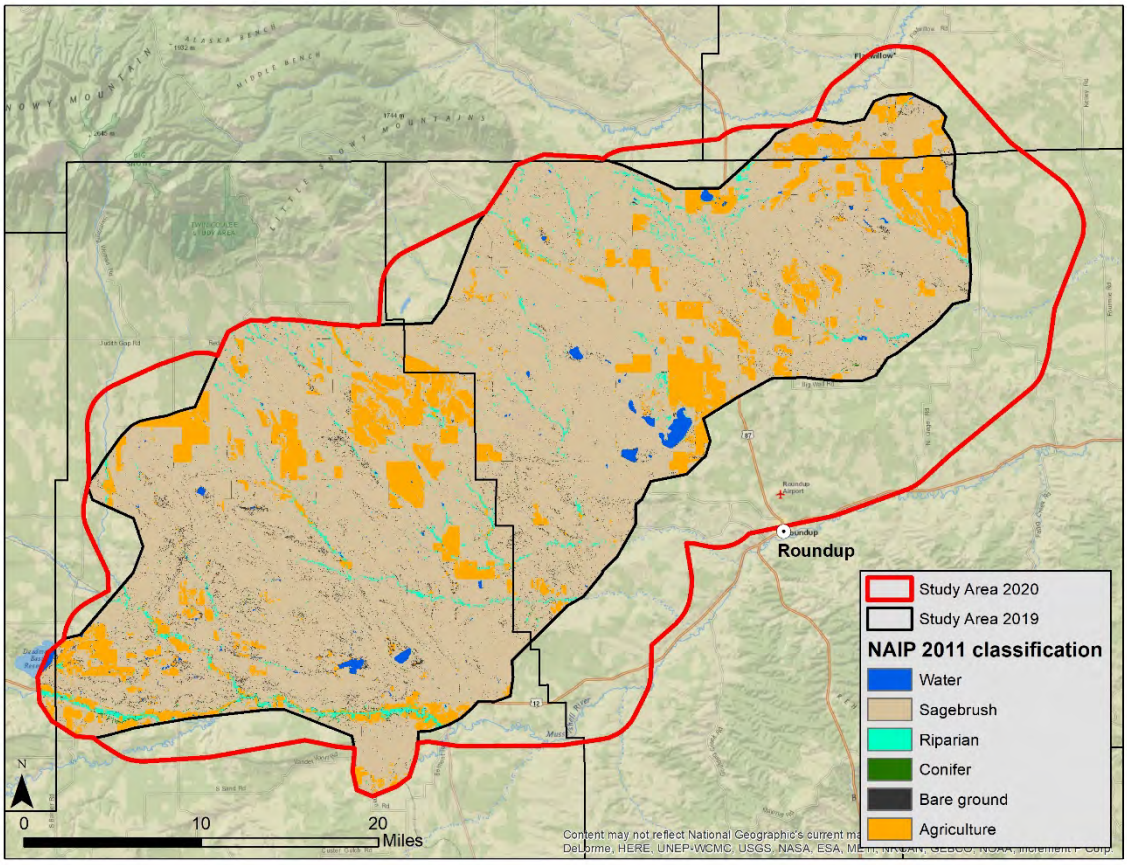

Figure 14. Comparison of 2019 study area boundary, with corresponding NAIP-based land cover classification, and 2020 study area boundary.

Climate Variables

In addition to extracting REAP (Relative Effective Annual Precipitation) from a statewide, 10m dataset, climate variables were generated through ClimateNA, a stand-alone software that can be used to estimate more than 50 monthly, seasonal and annual variables (Wang et al. 2016). A regular net of 1km points was created for the study area using the CREATE FISHNET command in ArcGIS; their XY coordinates along with elevation values at each point (N = 3,588) were input into the program, which was used to output three sets of data: annual variables for normal 1981 – 2010 (N = 25); seasonal variables for normal 1981 – 2010 (N = 59); and annual variables for 2019 (N = 25). From these 109 potential variables, 36 were deemed more important to potentially explain arthropod biomass and extrapolated to a raster surface using ArcGIS KRIGING command (Table 2).

Table 2. Climate variables generated with the software ClimateNA and extrapolated to continuous surface rasters for the study area.

Variable	Type	Source
AHM (annual heat moisture index)	Annual	Normals 1981 -
bFFP (day of the year on which frost-free period	Annual	Normals 1981 -
eFFP (day of the year on which frost-free period ends)	Annual	Normals 1981 -
CMDsp (spring Hargreaves climatic moisture deficit)	Seasonal	Normals 1981 -
CMDsm (summer Hargreaves climatic moisture deficit)	Seasonal	Normals 1981 -
CMIsp (spring Hogg's climate moisture index)	Seasonal	Normals 1981 -
CMIsm (summer Hogg's climate moisture index)	Seasonal	Normals 1981 -
CMIwt (winter Hogg's climate moisture index)	Seasonal	Normals 1981 -
DD0sp (spring degree-days below 0°C)	Seasonal	Normals 1981 -
DD18 (degree-days above 18°C, cooling degree-	Annual	Normals 1981 -
DD_18 (degree-days below 18°C, heating degree-	Annual	Normals 1981 -
DD1040 (degree-days above 10°C and below 40°C)	Annual	Normals 1981 -
DD5 (degree-days above 5°C, growing degree-days)	Annual	Normals 1981 -
NFFDsp (spring number of frost-free days)	Seasonal	Normals 1981 -
NFFDsm (summer number of frost-free days)	Seasonal	Normals 1981 -
PAS (precipitation as snow)	Annual	Normals 1981 -
PASsp (spring precipitation as snow)	Seasonal	Normals 1981 -
PASwt (winter precipitation as snow)	Seasonal	Normals 1981 -
PPTsp (spring precipitation)	Seasonal	Normals 1981 -
PPTsm (summer precipitation)	Seasonal	Normals 1981 -
PPTwt (winter precipitation)	Seasonal	Normals 1981 -
RHsp (spring relative humidity)	Seasonal	Normals 1981 -
RHsm (summer relative humidity)	Seasonal	Normals 1981 -
RHwt (winter relative humidity)	Seasonal	Normals 1981 -
SHM (summer heat moisture index)	Seasonal	Normals 1981 -
Tavesp (spring average temperature)	Seasonal	Normals 1981 -
Tavesm (summer average temperature)	Seasonal	Normals 1981 -
Tavewt (winter average temperature)	Seasonal	Normals 1981 -
Tmaxsp (spring maximum temperature)	Seasonal	Normals 1981 -
Tmaxsm (summer maximum temperature)	Seasonal	Normals 1981 -
Tmaxwt (winter maximum temperature)	Seasonal	Normals 1981 -
Tminsp (spring minimum temperature)	Seasonal	Normals 1981 -
Tminsm (summer minimum temperature)	Seasonal	Normals 1981 -

Tminwt (winter minimum temperature)	Seasonal	Normals 1981 -
DD5_2019 (degree-days above 5°C, growing	Annual	Year 2019
PAS2019	Annual	Year 2019

Variable exploration

Values for each predictive variable were extracted at the 218 sample sites to conduct exploratory analysis.

Summarizing some of the topographic and vegetation variables by biomass quartiles did not reveal any obvious pattern (Table 3).

Table 3. Mean values of 14 topographic and vegetation variables for four arthropod biomass quartiles.

	GPP	GPP	RAP	RAP Bare	RAP Litter	RAP	RAP Shrub
Q1	144	139	9.9	11.1	10.9	51.6	8.7
Q2	156	141	9.5	10.5	10.7	53.4	8.0
Q3	147	143	10.1	10.5	10.9	52.5	8.3
Q4	140	141	9.4	10.9	10.8	51.7	9.1

	Brightness	Greenness	Wetness	Elevation	Slope	Solar	REAP
Q1	0.408	-0.096	-0.245	1,145	3.3	283,698	33.8
Q2	0.411	-0.086	-0.236	1,157	3.5	284,493	34.5
Q3	0.410	-0.091	-0.244	1,144	2.9	283,540	34.5
Q4	0.405	-0.095	-0.242	1,132	2.8	282,900	34.2

Excluding Orthoptera from analysis reveals some patterns, especially when Q4 is compared with the others (Table 4). Higher GPP (both average and for 2020), larger percentage of grasses but less shrubs and bare ground. That said, there would not be much reason to generate a predictive biomass model that does not include Orthoptera, as they represent such an important proportion of the local insect biomass.

Table 4. Mean values of 14 topographic and vegetation variables for four arthropod biomass quartiles, excluding Orthoptera.

	GPP	GPP	RAP	RAP Bare	RAP Litter	RAP	RAP Shrub
Q1	141	136	8.9	12.0	11.1	50.6	9.1
Q2	138	140	9.5	11.3	10.7	51.6	8.6
Q3	149	140	10.1	11.0	10.9	51.8	8.6
Q4	157	151	10.5	8.9	10.5	55.2	7.9

	Brightness	Greenness	Wetness	Elevation	Slope	Solar	REAP
Q1	0.411	-0.095	-0.244	1,144	3.0	283,730	34
Q2	0.408	-0.093	-0.242	1,151	3.4	283,667	34
Q3	0.415	-0.094	-0.247	1,141	3.3	283,408	34
Q4	0.400	-0.086	-0.235	1,142	2.8	283,809	35

A similar analysis using climate variables generated through ClimateNA did not reveal any obvious patterns.

Model Development

Models were developed from the 218 plots attributed with the following 58 variables (values extracted at the plot centroid):

- Gross Primary Productivity (30m): 3 (average 2011-2020; GPP 2019; GPP 2020)
- Rangeland Analysis Platform (30m): 11 (average 2011-2019 for the first 5 bands: annuals, bare ground, litter, perennials, shrub; and 6 bands for year 2019)
- Tasseled Cap transformation for Landsat 08/08/2020 (30m): 3 (brightness, greenness, wetness)
- Topography (10m): 4 (DEM, slope, curvature, solar index)
- Relative Effective Annual Precipitation (10m)
- ClimateNA generated variables (10m): 36 (see Table 2 above)

Models were generated using RandomForest from the package ModelMap in R. I first generated 20 models using all 58 variables and random, model-generated seeds (the number used to initialize randomization to build RF models). The package provides two measures to evaluate variable importance: 1) %IncMSE, percent increase in Mean Standard Error as each variable is randomly permuted, i.e., how much the accuracy decreases when the variable is excluded; and 2) IncNodePurity, increase in node purity from all the splits in the forest based on a particular variable, as measured by the Gini criterion. For each model, I recorded the top 10 variables from the percent increase Mean Standard Error plot; this measure of variable importance is more robust and less biased than IncNodePurity.

To generate more parsimonious models, I selected only those variables listed in the top 10 more than once, and generated a new set of 20 models. I used an online random number generator (1-1000) to set the seeds, in order to be able to reproduce the models (the default random seed generator within ModelMap does not list what seed is used).

Results

Models based on all 58 variables

Percent variance explained by the 20 models ranged from 16.04% to 22.16% (average 19.53%); Spearman correlation ranged from 33% to 40 % (average 36.4%), whereas Pearson correlation ranged from 36% to 47% (average 41.8%) (Table 5).

Table 5. Percent variance explained, Spearman and Pearson correlation coefficients for 20 RandomForest models generated from 58 variables.

Model	% variance	Spearman	Pearson
1	21.59	37	43
2	19.99	39	42
3	17.26	40	46
4	16.04	36	37
5	21.03	36	44
6	21.31	34	35
7	19.31	37	44
8	19.06	33	40
9	22.16	37	44
10	16.54	36	44
11	18	30	36
12	19.28	39	37
13	19.89	40	47
14	19.32	35	42
15	20.5	38	39
16	19.54	39	47
17	21.82	35	43
18	17.8	33	42
19	21.51	38	44
20	18.54	36	40

Twenty-one variables are present more than once in the ten most important variables, with maximum winter temperature present in all 20 models (Table 6).

Table 6. Number of times a variable was present among the ten most important variables from 20 Random Forest models, based on percent increase in mean standard error. Only variables present at least once are listed.

Tmaxwt	Maximum winter temperature	20

PASwt	Winter precipitation as snow	18
dem	Digital elevation model	17
NFFDSp	Spring number of frost-free days	17
rap3m	Mean litter 2011-2020	17
Tavewt	Average winter temperature	17
PPTsm	Summer precipitations	14
Tminsp	Minimum spring temperature	11
PPTsp	Spring precipitations	10
RHsm	Summer relative humidity	9
DD0sp	spring degree-days below 0°C	8
PAS2019	2019 precipitation as snow	8
bFFP	Beginning of frost-free period	6
SHM	Summer heat moisture index	3
Tavesp	Average spring temperature	3
Tminwt	Minimum winter temperature	3
DD18	Degree-days above 18°C, cooling degree-	2
eFFP	End of frost-free period	2
gpp19	2019 gross primary productivity	2
PPTwt	Winter precipitations	2
RHsp	Spring relative humidity	2
CMDsp	Spring Hargreaves climatic moisture deficit	1
CMIwt	Winter Hogg's climate moisture index	1
DD5	Degree-days above 5°C, growing degree-	1
DD52019	2019 Degree-days above 5°C	1
PAS	Precipitation as snow	1
PASsp	Spring precipitation as snow	1
rap1m	Mean annuals 2011-2019	1
Tminsm	Minimum summer temperature	1

Models Based on Retained 21 Variables

Percent variance explained by the 20 models ranged from 28% to 33.56% (average 30.8%); Spearman correlation ranged from 46% to 55% (average 51.1%), whereas Pearson correlation ranged from 38% to 59% (average 53.4%) (Table 7).

Table 7. Percent variance explained, Spearman and Pearson correlation coefficients for 20 RandomForest models generated from 21 variables.

Model	Seed	% variance	Spearman	Pearson
1	256	31.84	55	57
2	750	28	46	45
3	358	31.22	52	55
4	166	29.1	51	52
5	684	31.62	50	55
6	329	31.22	55	59
7	388	29.97	48	53
8	446	33.46	54	57
9	536	31.11	49	38
10	472	29.49	49	55
11	899	32.33	51	55
12	602	29.99	52	53
13	194	30.38	50	54
14	114	31.45	47	49
15	648	28.94	55	55
16	181	30.33	51	55
17	702	31.15	55	58
18	396	32.4	53	55
19	215	29.34	46	51
20	26	32.66	53	56

Of the 21 variables used as inputs, all except two (rap1m: mean annual grasses and forbs, and eFFD: end of frost-free period) are present in at least one model (Table 8). Elevation (DEM), maximum winter temperature (Tmaxwt) and winter precipitation (PASwt) are the variables most often ranked as most important, followed by spring precipitation (PPTsp), 2019 precipitation as snow (PAS2019), spring degree-days below 0°C (DD0sp), summer relative humidity (RHsm), spring number of frost-free days (NFFDsp), and average spring temperatures (Tavesp).

Table 8. Distribution of 19 variables (rows) among the ten most important variables (columns) for 20 Random Forest models.

Variable	Var1	Var2	Var3	Var4	Var5	Var6	Var7	Var8	Var9	Var10	Sum
bFFP				1	1	2	1	2	1	1	8
DD0sp			1	1	3	2	3	3		1	14
DD18				1					1	1	3

DEM	11	8	1								20
NFFDsp					1	2	1	1	6		11
PAS2019			3	4	3	2	1		1	1	15
PASwt		1	11	2	1	3		2			20
PPTsp			1	7	3	3			2	2	18
PTTsm					1		3	1	2		7
PTTwt					1		1	1		3	6
Rap3m					1			1	1	3	6
RHsm			1	1	3	2		4	1	1	13
RHsp				1		1	2			3	7
SHM						1		2	1		4
Tavesp			2	1	1	1	3	1	1		10
Tavewt					1	1	2	2	1	2	9
Tmaxwt	9	11									20
Tminsp				1			2		2	1	6
Tminwt							1			1	2

Extrapolation to a Surface

RandomForest introduces randomization at two levels: 1) the training set for growing a tree is randomly selected from the available data, with replacement; and 2) at each node, a subset of variables are randomly selected out of the pool of available variables and the best split is used to split the node. By defining a seed, the same model can be generated each time, but any change in seed will result in a different model; therefore, the 20 models I generated are all different, both in their performance (as measured by percent variance explained) and in their composition (variables). As a result, any one of the 20 model output is different from the other; to explore spatial variability, I extrapolated each model with a percent variance explained greater than 30% to its own surface (models 1, 3, 5, 6, 8, 9, 11, 13, 14, 16, 17, 18, 20; Table 7). Figure 15 shows the average of those 13 surfaces, and Figure 16 shows model uncertainty (average coefficient of variation for those same models). The two rasters show opposite patterns, with areas of high model uncertainty corresponding to areas of low predicted biomass, and vice-versa.

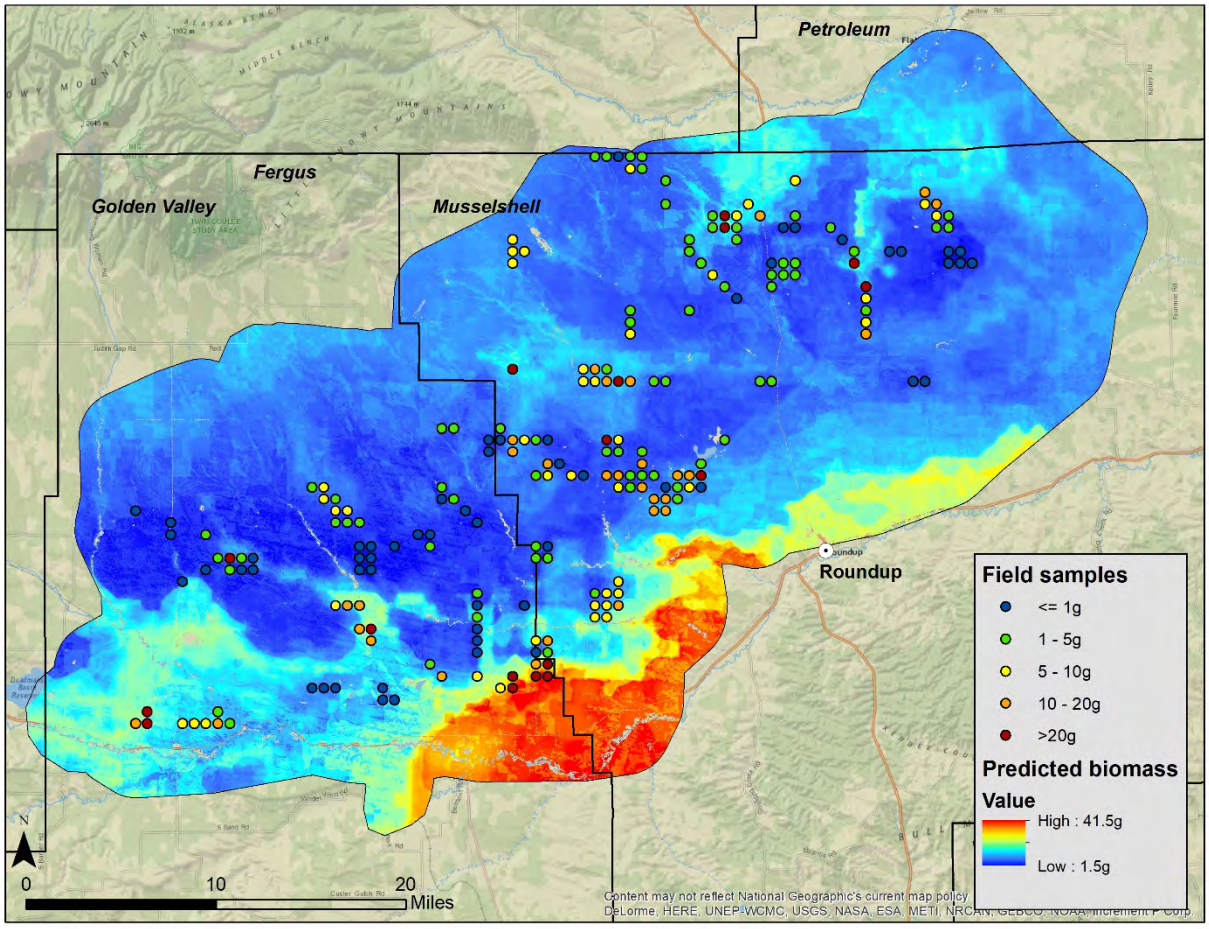

Figure 15. Continuous biomass surface extrapolated from 13 RandomForest models (averaged) based on 21 predictor variables and 218 biomass sample points.

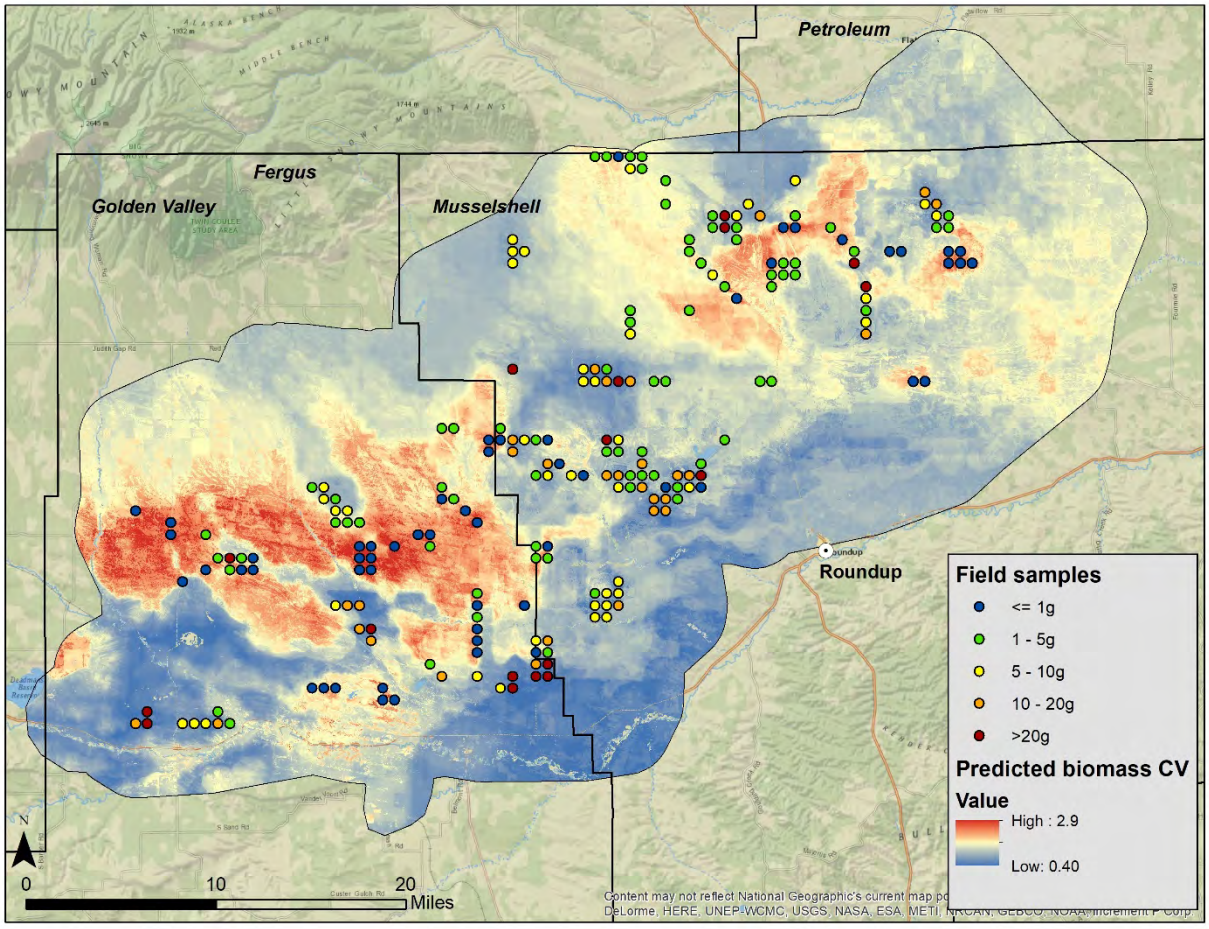

Figure 16. Model uncertainty generated by averaging the coefficient of variation of 13 RandomForest models based on 21 predictor variables and 218 biomass sample points.

Additional variables

Pasture Data

A shapefile of pastures attributed with yearly grazing treatments (2011 – 2020) was used to explore the potential effects of the following site characteristics on arthropod biomass:

- Sage-grouse initiative program:
    - yes/no for each year (N = 10);
    - last year in program;
    - ever in program.
- Treatment:
    - Code for each year (N = 10);
    - Treatment 4 (not grazed the entire year): ever in it; how many times; how many years ago;

    - Treatment 1 (grazed during nesting, April 1 – July 15): ever in it; how many times; how many years ago;
    - Treatment 2 (grazed during brood rearing, July 16 – Sept 15): ever in it; how many times; how many years ago;
    - Treatment 3 (grazed during fall/winter: Sept 16 – March 31): ever in it; how many times; how many years ago;
    - Treatment 8 (grazed during both treatments 1 and 2): ever in it; how many times; how many years ago.
- Grazing: how many days, for each year (N = 10)

Extracted pasture variables (N = 47) were added to the set of 58 variables described previously and input into an R script in RStudio, that rapidly runs 1,000 RandomForest models and generates an excel spreadsheet listing how many times each variable was selected among the top 15 most important variables. Looking at variables present in at least 10% of models (i.e., 100) shows that only treatment 2016, 2017 and 2019 get selected; all other variables, beside mean litter from Rangeland Analysis Platform, are from ClimateNA (Table 9).

Table 9. Variables present among the 15 top most important for 1,000 RandomForest models.

	Count	Percent
PAS_wt_1981_2010	1000	1
Tave_wt_1981_2010	1000	1
Tmax_wt_1981_2010	1000	1
DD_0_sp_1981_2010	995	0.995
DD18_1981_2010	994	0.994
NFFD_Sp_1981_2010	991	0.991
PPT_sm_1981_2010	991	0.991
bFFP_1981_2010	948	0.948
PAS_1981_2010	892	0.892
Tmin_sp_1981_2010	887	0.887
treatment2017	884	0.884
RH_wt_1981_2010	881	0.881
SHM_1981_2010	711	0.711

Tave_sp_1981_2010	613	0.613
RH_sm_1981_2010	552	0.552
treatment2019	407	0.407
treatment2016	290	0.29
CMI_wt_1981_2010	281	0.281
RAP3mean	130	0.13
Tmax_sm_1981_2010	118	0.118

Adding these 3 treatment variables to the original set used to derive the second batch of 20 models did not result in any improvement of percent variance explained.

Landscape Metrics

To calculate landscape metrics, the original twelve classes from the 2011 NAIP landcover classification were collapsed as follows: Sagebrush 0-5% and Sagebrush 6-10% to Grassland; Sagebrush 11-15%, Sagebrush 16-20%, Sagebrush 21-25%, Sagebrush 26-30% and Sagebrush 30% and greater to Shrubland; the remaining classes (Water, Bare Ground, Riparian, Conifer and Agriculture) were kept unchanged.

Sampling points were buffered (15m radius) to emulate sampling plots and extract reclassified NAIP pixels, each one of the 218 plots becoming its own "landscape". Metrics were computed in Fragstats v4.2 (McGarigal et al. 2012). Although it is possible to generate many metrics at different scales (patch, class, and landscape), 23 landscape-scale metrics characterizing each "landscape" were computed (Table 10).

Table 10. Landscape metrics computed with Fragstats for each plot. For detailed descriptions, refer to https://www.umass.edu/landeco/research/fragstats/documents/fragstats.help.4.2.pdf

NP	Number of Patches
PD	Patch Density
LPI	Largest Patch Index
LSI	Landscape Shape Index
AREA_MN	Mean Patch Area
AREA_SD	Standard Deviation of Patch Area
SHAPE_MN	Mean Shape

FRAC_MN	Mean Fractal Dimension Index
PARA_MN	Mean Perimeter-Area Ratio
CIRCLE_MN	Mean Related Circumscribing Circle
CONTIG_MN	Mean Contiguity Index
CONTAG	Contagion Index
COHESION	Patch Cohesion Index
DIVISION	Landscape Division Index
PR	Patch Richness
PRD	Patch Richness Density
SHDI	Shannon's Diversity Index
SIDI	Simpson's Diversity Index
MSIDI	Modified Simpson's Diversity Index
SHEI	Shannon's Evenness Index
SIEI	Simpson's Evenness Index
MSIEI	Modified Simpson's Evenness Index
AI	Aggregation Index

Values for each metric were added to the dataset of variables and the R script run again; but only two metrics (Largest Patch Index and Simpson's Diversity Index) were selected among the 15 most important variables, with LPI in only two out of 1,000 models and SIDI in only one.

CONCLUSIONS

2019 was a very wet year, with an explosion of sweet yellow clover that may explain the increased grasshopper biomass in 2020 compared to previous years. Despite the lack of correlation between most variables and arthropod biomass, and the absence of fine-scale variables 9especially climatic ones), randomForest models still explained about a third of variance, and the top variables (maximum winter temperature, elevation, and winter precipitation as snow) make ecological sense in terms of overwinter survival; as does the only vegetation variable retained, litter.

Effects of Sage-Grouse Initiative Grazing Management on Invertebrate Biomass

Summary

Our study was not designed to test the effects of Sage-Grouse Initiative grazing management (SGI) on invertebrate biomass. But we wanted to explore the relationship between invertebrate biomass and the grazing management variables found important from the modeling effort above. Invertebrate biomass was consistently lower in the non-SGI category for all SGI predictors (see below). But we did not find significant relationships between SGI predictors and invertebrate biomass. Sample sizes were relatively low in certain categories (Table 4) which affected our ability to detect differences among categories.

Generating Sampling Locations

We included several vegetation metrics when building the first iteration of the predictive spatial model to determine which ones were important and would be kept in the model. Please see the above report prepared by Claudine Tobalske from the Spatial Analysis Laboratory at the University of Montana. Preliminary analyses from data collected during 2012-2017 on this project and the sage-grouse grazing project showed that invertebrate abundance and sage-grouse chick habitat use were correlated with percent bare ground cover; thus, we initially used this variable to stratify our sampling locations across the study area (see above) during 2018-2019. However, we did not find a relationship of percent bare ground cover with invertebrate biomass in the model that was built with the 2018-2019 data. During 2019-2020, we stratified our sampling sites by areas with greater uncertainty, and expanded sampling to gain more complete coverage of the study area (see above).

We also sampled invertebrates at sage-grouse locations and songbird survey locations, in addition to the above sampling used to build the predictive spatial model, to validate the predictive model. We sampled bird locations one week after they were located and tried to minimize the time between location and sampling to no longer than a week. In other words, we tried to obtain an invertebrate sample that reflected, as closely as possible, the food available at each location when birds were sampled without disrupting bird sampling.

Data Collection

Sampling occurred during the day, when both sage-grouse and songbirds were more likely to be active and foraging. We attempted to collect both ground-dwelling and above ground invertebrates, because sage-grouse and songbirds eat both. In 2018, we used the five methods from Tronstad et al. (2018) to collect ground-dwelling as well as above-ground invertebrates (see *Invertebrate Sampling* below). However, data from 2018-2019 showed that the sweep net sampling technique, which mainly samples above-ground invertebrates, was the most reliable and consistent collection method. The other sampling methods resulted in invertebrate counts that were too low to support predictive distribution modeling. Thus, we only used sweep net samples in our modeling effort, which may bias our models. We also collected a suite of vegetation metrics at each sampling site during 2018-2019 to analyze how these conditions affected invertebrate biomass (see above). There was no evidence of a strong relationship between any vegetation metrics and invertebrate biomass. As the vegetation metrics require a considerable amount of

time to collect, we did not collect vegetation metrics in 2020, and instead put the effort into additional invertebrate sampling across the study areas.

Vegetation Metrics. At each sampling site, we set up a 30m x 30m plot using the site coordinates as the center of the plot, with two metric tapes bisecting the plot in the center. The vegetation metrics we collected during 2018-2019 are the same as those collected for our sage-grouse grazing study and are summarized in Smith et al. (2018). In addition to metrics collected at these plots, we used metrics from remotely sensed layers (see above).

Invertebrate Sampling. Please see the above report by Tobalske et al. on how stratified random sampling locations were generated. We sampled invertebrates using five methods based on protocols from Tronstad et al. (2018): counting ant mounds, flushing grasshoppers, collecting shrub samples, sampling litter, and sweep net sampling. Ant mounds and grasshopper flushes were counted while systematically traversing a plot. Four shrub and litter samples were collected per plot at the shrub closest to the 5m mark on the two measuring tapes delineating the plot. During 2019, we tried a modified version of Tronstad et al.'s (2018) method for sampling invertebrates on shrubs: we used a hand-held vacuum/aspirator to vacuum invertebrates from the shrub and the ground beneath the shrub, which were collected in a cup attached to the vacuum. To avoid invertebrates escaping, we placed a mesh enclosure around the shrubs and a white sheet on the ground beneath the shrub before using the aspirator. For the sweep net technique, we used a sweep net to take 200 sweeps per plot: 100 sweeps along the North-South tape, and 100 sweeps along the East-West tape. During this process, a net with a 3-ft handle and a 12-in diameter bag was swept back and forth through the vegetation along the tape to collect invertebrates. The invertebrates from each sampling technique were transferred to a ziploc bag and stored in a freezer until processing. Samples were dried and sorted, and then identified and weighed according to their phylogenetic Order.

Analyses

Invertebrate biomass was used as a response variable in models that relate predictor variables including vegetation metrics, weather, and SGI grazing management variables to invertebrate biomass (see above). The predictive model was generated using a random forest model (see above). Several random forest models were run to determine which predictors were most influential on biomass and should be kept for the final predictive model. But this method only identified which predictors may be important, not their effects on biomass. We conducted further analyses on predictors identified as important through this process. Three SGI grazing management variables were identified as influential on invertebrate biomass: treatments 2016, 2017, and 2019 (see above). Treatments including whether a pasture was enrolled in the Sage-Grouse Initiative were included separately in random forest models by year for each pasture. Thus treatment 2016 may be due to an effect of SGI grazing management or year, and further analyses were needed to determine the effect of this predictor on biomass. There were predictors representing specific treatments by pasture related to the timing of grazing and how many times a pasture was grazed each year. However, the sample size

Sage-Grouse Initiative (SGI) predictors were included in random forest models used to create the predictive model, detailed in the Tobalske report above. Some were found to be influential, so we further analyzed these variables with linear regression models in program R 4.0.0 (R Core Team 2020) using package *lme4* (Bates et al. 2015). We used biomass data collected during 2012-2020. The sampling was not designed to specifically test the effects of our SGI predictors on invertebrate biomass. Additional invertebrate data collected for this project during 2012-2015 was used to test the relationship of SGI with invertebrate diversity and abundance (Goosey et al. 2019). However, these data could not be used to determine invertebrate food availability for our bird models. The invertebrate spatial layer, however, could be used to predict invertebrate biomass at any of our bird sampling locations, and the layer became our primary goal for the remainder of the project. But we did attempt to assess the influence of SGI grazing management variables on invertebrate biomass with the data we had (raw biomass data, not the biomass predicted from the model for the spatial layer). These data were skewed towards zero, so we log-transformed the data to give it a normal distribution. We used the log-transformed biomass as the response variable in all regression models. We explored the effect of the SGI on log-transformed bug biomass from three perspectives:

1. **'sgi'** – First, we considered whether the pasture was enrolled in SGI grazing and the grazing was implemented during the year the pasture was sampled, or the pasture was not enrolled (binary predictor variable).
2. **'sgi2'** – Categorical predictor variable with 3 factor levels: 'no', 'pre', and 'post' – The pasture was not enrolled in SGI ('no'). If the pasture was enrolled, it was sampled before SGI grazing was implemented ('pre' – SGI grazing occurred in years subsequent to the year the pasture was sampled), or after SGI grazing was implemented ('post' – grazing occurred in years prior to the year the pasture was sampled).
3. **'sgi3'** – Categorical predictor variable with 4 factor levels: 'no', 'pre', 'during', and 'post' – The pasture was not enrolled in SGI ('no'). If the pasture was enrolled, it was sampled before SGI grazing was implemented ('pre' – SGI grazing occurred in years subsequent to the year the pasture was sampled), during SGI grazing implementation ('during' – grazing occurred during the year the pasture was sampled), or after SGI grazing was implemented ('post' – grazing occurred in years prior to the year the pasture was sampled).

The first perspective, 'sgi', was intended to evaluate immediate, direct effects of SGI grazing strategies, whereas the last two perspectives, 'sgi2' and 'sgi3', were intended to evaluate delayed or cumulative effects of SGI grazing. We also used the total number of days a pasture was grazed each year ('grdays') as a predictor variable.

We were also interested in quantifying the time-varying components of each three-year grazing regime. These components included variation in the intensity, duration, timing, and frequency of grazing. We originally planned to use animal units per month (AUMs) to represent grazing intensity, but these data were only available for approximately 25% of our pastures. Thus, we did not include AUMs. To quantify grazing timing and frequency, we divided the grazing periods into categorical "treatments." We defined

these treatments based on seasonal periods of importance to both vegetative habitat components and sage-grouse life stages, and the specific treatments were the factor levels of predictor 'trtmt_current' used in models (Figure 2). We also used the predictor 'trtmt_prev' with the same treatments as factor levels to represent the previous year's SGI grazing management. FWP staff developed treatment categories in collaboration with range scientists at Montana State University. Treatments are categorized as follows:

1. **Treatment 1:** April 1-July 15: Vegetation growing season and the nesting season for sage-grouse.
2. **Treatment 2:** July 16-September 15: The end of growth and reproduction for vegetation and the brood-rearing season for sage-grouse; grazing during this season can affect plant reproduction and seed-set.
3. **Treatment 3:** September 16-March 31: Vegetation is dormant; grazing during this season removes residual vegetation that may otherwise be used for hiding cover during the following nesting season.
4. **Treatment 4:** No grazing occurred for an entire year.

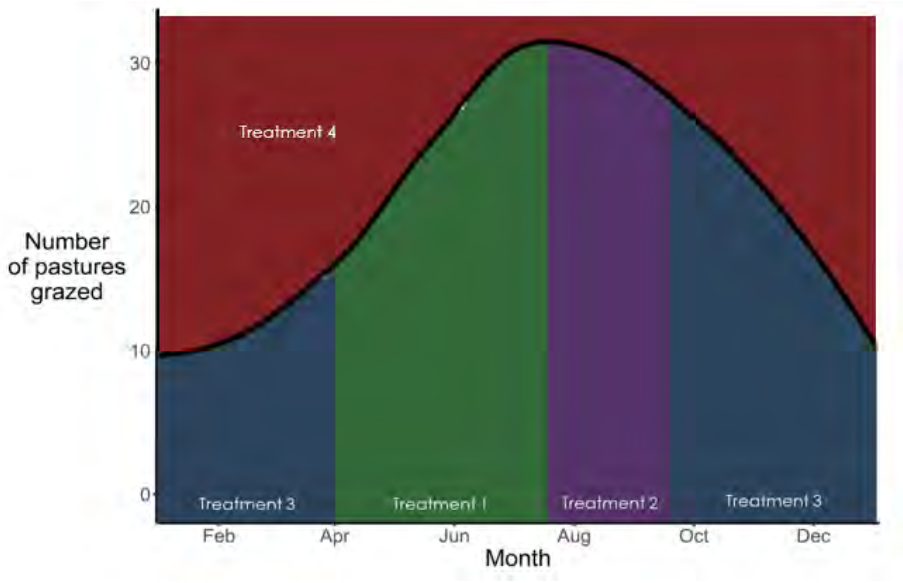

Figure 2. A schematic diagram showing the timing of the four main grazing treatments in relation to the time of year.

But some pastures were grazed multiple times per year, had wildfires, or were managed as crops. We established distinct treatment categories for these as well:

5. **Treatment 5:** Grazing data unknown.
6. **Treatment 6:** Cropland.
7. **Treatment 7:** Burned due to wildfire.
8. **Treatment 8:** Grazed during two treatment periods (from treatments 1, 2, or 3) during the year.
9. **Treatment 9:** Grazed during all three grazing treatment periods (treatments 1-3) during the year.

Treatments 8 and 9 could be further broken down by which two or three specific treatments, respectively, were grazed that year, but we did not separate these for this report. These treatments were applied to both SGI enrolled pastures and pastures that were not enrolled. We also modeled biomass as a function of the SGI grazing management the previous year, utilizing the same categories as above. We did not have enough samples to model both current year and previous year treatments together.

We modeled log-transformed biomass in linear mixed models. We tested 'year' and 'ranch' as random effects to account for variation in biomass that we did not measure. 'Ranch' is a categorical variable grouping pastures that were managed together as a ranch. We compared models using Akaike's Information Criterion for small sample sizes (AIC_c) in R package *AICcmodavg* (Mazerolle 2020), and model selection was based on minimization of AIC_c and AIC_c weights (Burnham and Anderson 2002). We considered predictor variables to be uninformative if $\Delta AIC_c < 2.0$ for models that differed by one variable, or if 95% confidence intervals overlapped 0 (Arnold 2010). We computed 95% confidence intervals and p-values using the *effects* (Fox and Weisberg 2019) and *parameters* (Lüdecke et al. 2020) packages in program R, respectively.

RESULTS & DISCUSSION

We evaluated null models with 'year' and 'ranch' as random effects separately and together. Using the variance to assess the importance of the random effects, ranch only accounted for 1.1% of the total variation of the random effects, so we did not include ranch in models going forward. Year accounted for 62.8% of the total variation of the random effects, showing that mixed modeling was appropriate for these data and that year should be included as a random effect in further modeling efforts. This is consistent with results from a simple linear regression of invertebrate biomass as a function of year; biomass varied significantly from year to year ($F_{8, 572}=25.26$, $p<0.001$; Table 1).

Table 1. Results of linear regression modeling invertebrate biomass collected at sites in central Montana (Golden Valley and Musselshell Counties) with sweep nets during 2012-2020 as a function year. Asterisks (*) denote level of significance, with more asterisks indicating the factor was more significant.

Model	**β**	**SE**	**95% CI**	**p-value**
Biomass ~ year				
Intercept (reference year=2012)	2.23	0.55	1.16, 3.30	< 0.001 ***
2013	0.93	0.80	-0.65, 2.51	0.25
2014	-1.30	0.75	-2.77, 0.17	0.08
2015	-1.33	1.00	-3.28, 0.63	0.18
2016	-1.90	0.73	-3.33, -0.47	0.01 *
2017	-1.78	0.73	-3.21, -0.35	0.01 *
2018	-5.60	0.60	-6.79, -4.42	< 0.001***
2019	-3.93	0.55	-5.02, -2.85	< 0.001***
2020	-1.18	0.55	-2.27, -0.09	0.03 *

All models performed better than the null model when comparing AIC_c scores (Table 2). The model that included the 'sgi2' and 'grdays' predictors performed best, with an $\Delta AIC_c < 2.0$. The next best model included 'sgi3' and 'grdays' as predictors, and its ΔAIC_c value was very close to the criteria for minimizing ΔAIC_c at 2.07 (Table 2). This model had an AIC_c score reflecting that it was similarly parsimonious to the top model. However, the confidence intervals for the parameters overlapped 0, and the variance

Table 2. Model selection results for linear mixed regression modeling invertebrate biomass collected at sites in central Montana (Golden Valley and Musselshell Counties) with sweep nets during 2012-2020 as a function of variables describing Sage-Grouse Initiative systems that included livestock grazing prescriptions. The number of parameters (*K*), Akaike's Information Criterion adjusted for small sample sizes (AIC_c) values, ΔAIC_c values, model weights (wi), cumulative weights (AIC_c Wt), and log-likelihoods (LL) are reported.

Model	***K***	**AIC_c**	**ΔAIC_c**	**AIC_c Wt**	**Cum.Wt**	**LL**
biomass ~ sgi2 + grdays + (1|year)	6	886.08	0.00	0.69	0.69	-436.85
biomass ~ sgi3 + grdays + (1|year)	7	888.14	2.07	0.25	0.94	-436.82
biomass ~ grdays + (1|year)	4	891.70	5.62	0.04	0.98	-441.76
biomass ~ sgi + grdays + (1|year)	5	893.08	7.01	0.02	1.00	-441.41
biomass ~ trtmt_prev + grdays + (1|year)	11	899.43	13.35	0.00	1.00	-438.10
biomass ~ trtmt_current + grdays + (1|year)	12	903.30	17.22	0.00	1.00	-438.92
biomass ~ trtmt_prev + (1|year)	10	1299.11	413.03	0.00	1.00	-639.23
biomass ~ trtmt_current + (1|year)	11	1301.18	415.10	0.00	1.00	-639.20
biomass ~ sgi2 + (1|year)	5	1756.34	870.26	0.00	1.00	-873.11
biomass ~ sgi + (1|year)	4	1756.92	870.84	0.00	1.00	-874.42
biomass ~ sgi3 + (1|year)	6	1757.76	871.68	0.00	1.00	-872.79
biomass ~ 1 + (1|year) - NULL MODEL	3	2113.28	1227.20	0.00	1.00	-1053.62

explained is very small compared to year-to-year variation, so the biological effect size of the SGI grazing management is relatively small (Table 3). The first model assessed delayed and cumulative effects of SGI grazing management, and shows that SGI pastures had more invertebrate biomass, particularly post-implementation. The fixed effects in the top two models accounted for only 0.02 of the variation in invertebrate biomass (marginal $R^2 = 0.02$). In addition, the confidence intervals for all predictors overlapped 0.

Table 3. Results for the top two models from AIC_c model selection. These are linear mixed regressions modeling invertebrate biomass collected at sites in central Montana (Golden Valley and Musselshell Counties) with sweep nets during 2012-2020 as a function of 'sgi2', 'sgi3', and 'grdays' variables describing Sage-Grouse Initiative systems that included livestock grazing prescriptions. The β estimate, standard error (SE), 95% confidence intervals (95% CI), and p-values are reported.

Model	**β**	**SE**	**95% CI**	**p-value**
biomass ~ sgi2 + grdays + (1|year)				
Sgi2: no (reference level)	-0.20	0.78	-1.61, 1.38	0.801

Sgi2: pre	0.86	1.40	-2.25, 3.75	0.537
Sgi2: post	0.74	0.24	-0.87, 2.12	0.002
grdays	0.001	0.002	-0.002, 0.005	0.483
biomass ~ sgi3 + grdays + (1|year)				
Sgi3: no	-0.92	0.75	-1.67, 1.35	0.216
Sgi3: pre	0.01	1.49	-2.22, 3.77	0.994
Sgi3: during (reference level)	0.69	0.94	-1.06, 2.60	0.467
Sgi3: post	-0.20	0.76	-0.97, 2.10	0.795
grdays	0.001	0.002	-0.002, 0.005	0.487

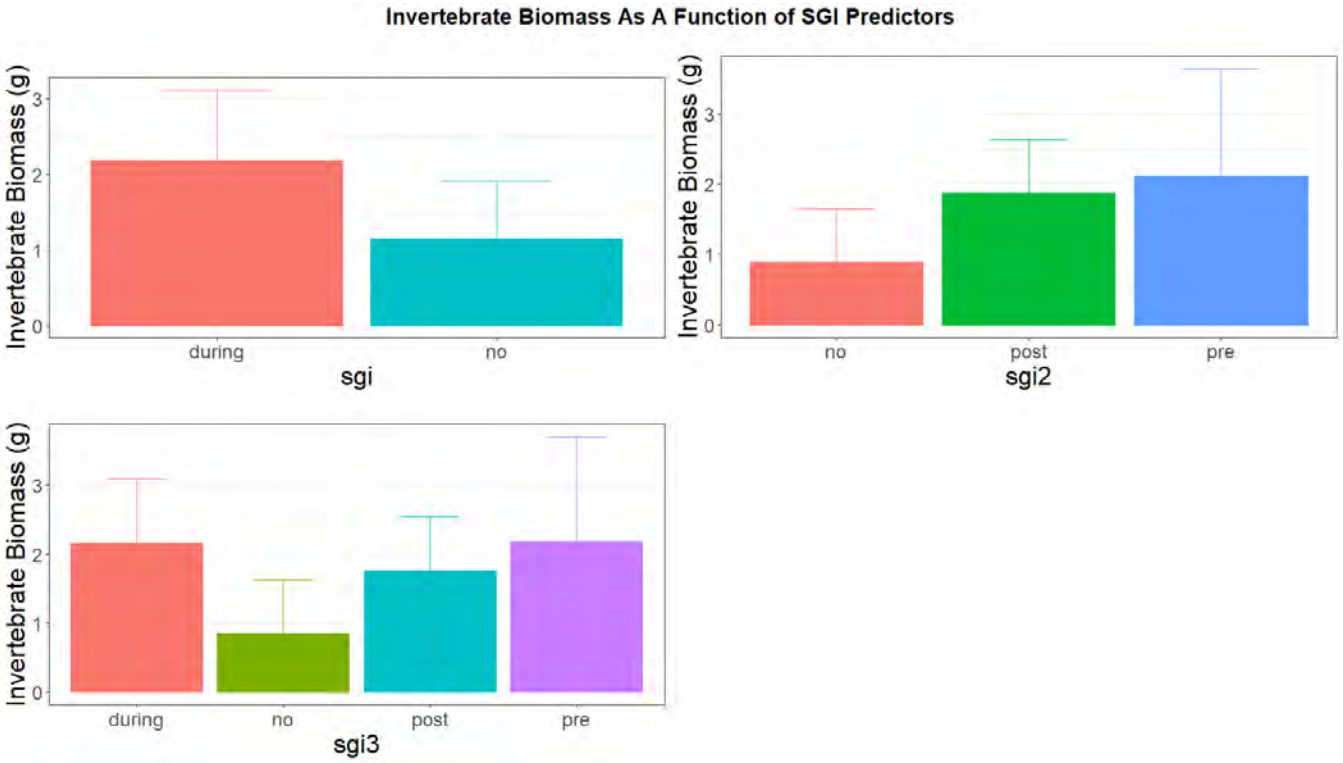

Figure 3. Log of measured invertebrate biomass from sweep net sampling during 2012-2020 in central Montana (Golden Valley and Musselshell Counties).

Looking at a summary of the data, invertebrate biomass was consistently lower in the non-SGI category for all SGI predictors (Figure 3). However, sample sizes were relatively low in certain categories (Table 4) which affects our ability to detect differences among categories.

(Table 4). Our sampling during 2018-2020 was not designed specifically to test for differences

Table 4. Number of sites sampled for invertebrate biomass within factor levels of each SGI variable. Sites were located in central Montana (Golden Valley and Musselshell Counties) during 2012-2020. NA indicates a predictor variable that did not include that factor level.

Factor Level	Variable sample sizes		
	Sgi	Sgi2	Sgi3
No	476	282	282
Pre	NA	3	3
Post	NA	206	191
During	15	NA	15
Unknown	108	108	108

among SGI factor levels, particularly because our goal was to provide data for the sage-grouse and songbird grazing projects (see above). We were able to use 2012-2017 data even though the sampling design was different, but a subsampling design was used (Goosey et al. 2019) which resulted in relatively few independent sample sites and less sampling cover of the study area. In 2018-2020 our goal was to create a predictive spatial layer of invertebrate biomass, and we were able to expand our sampling efforts. However, most of the SGI contracts had ended by 2018 and no 'pre' sites were available to sample. The treatment categories 1-9 representing timing and frequency of SGI and non-SGI grazing management (predictor='trtmt_current') were not correlated with invertebrate biomass and did not perform well when compared against other models in AIC_c model selection (Table 2). We also modeled biomass as a function of the previous year's grazing treatments (predictor='trtmt_prev'), and this model also was not competitive (Table 2).

Results on the effects of grazing on the invertebrate community and avian food availability using data collected during 2012-2015 on our study area compared SGI-enrolled pastures with idle land that was left ungrazed for 10 years (Goosey et al. 2019). This work showed that the communities differed between grazed SGI-enrolled land and ungrazed land, with more abundant and diverse potential avian food invertebrates on grazed land (Goosey et al. 2019). We have reported on the available data, but further research could be designed to specifically compare invertebrate biomass in the SGI factor levels as we have defined them if there is interest in further evaluating delayed and cumulative effects of SGI managed systems on invertebrate biomass in central Montana.

LITERATURE CITED

Aldridge, C. L., and M. S. Boyce. 2007. Linking occurrence and fitness to persistence: habitat-based approach for endangered greater sage-grouse. Ecological Applications 17:508-526.

Arnold, T. W. 2010. Uninformative parameters and model selection using Akaike's Information Criterion. Journal of Wildlife Management 74:1175-1178.

Bates, D., M. Maechler, B. Bolker, and S. Walker. 2015. Fitting Linear Mixed-Effects Models Using lme4. Journal of Statistical Software, 67(1), 1-48. doi:10.18637/jss.v067.i01.

Beck, J. L., J. W. Connelly, and C. L. Wambolt. 2012. Consequences of treating Wyoming big sagebrush to enhance wildlife habitats. Rangeland Ecology and Management 65:444-455.

Beck, J. L., and D. L. Mitchell. 2000. Influences of livestock grazing on sage-grouse habitat. Wildlife Society Bulletin 28:993-1002.

Berkeley, L. I., M. S. Szczypinski, J. Helm, and V. J. Dreitz. 2019. The impacts of grazing on greater sage-grouse habitat and population dynamics in central Montana. Annual progress report to the US Fish and Wildlife Service Grant-in-Aid, or Pittman-Robertson, from Montana Fish, Wildlife, and Parks, Helena, and the University of Montana, Missoula, USA, 40 pp.

Bradford, D. F., S. E. Franson, A. C. Neale, D. T Heggem, G. R. Miller, and G. E Canterbury. 1998. Bird species assemblages as indicators of biological integrity in Great Basin rangeland. Environmental Monitoring and Assessment 49: 1-22.

Braun, C.E., M.F. Baker, R.L. Eng, J.S. Gashwiler, and M.H. Schroeder. 1976. Conservation committee report on effects of alteration of sagebrush communities on the associated avifauna. Wilson Bulletin 88:165-171.

Burnham, K. P., and D. R. Anderson. 2002. Model selection and multimodel inference: a practical information theoretic approach. Second Edition edition. Springer-Verlag, New York, USA.

Casey, D. 2000. Partners in Flight Bird Conservation Plan, Montana, v.1.1. American Bird Conservancy, Kalispell, MT.

Connelly, J. W., and C. E. Braun. 1997. Long-term changes in sage grouse *Centrocercus urophasianus* populations in western North America. Wildlife Biology 3:229-234.

Connelly, J. W., S. T. Knick, M. A. Schroeder, and S. J. Stiver. 2004. Conservation assessment of greater sage-grouse and sagebrush habitats. Unpublished report. Western Association of Fish and Wildlife Agencies, Cheyenne, Wyoming, USA.

Coppedge, B. R., S. D. Fuhlendorf, W. C. Harrell, and D. M. Engle. 2008. Avian community response to vegetation and structural features in grasslands managed with fire and grazing. Biological Conservation 141:1196–1203. doi:10.1016/j.biocon.2008.02.015

Crawford, J. A., R. A. Olson, N. E. West, J. C. Mosley, M. A. Schroeder, T. D. Whitson, R. F. Miller, M. A. Gregg, and C. S. Boyd. 2004. Ecology and management of sage-grouse and sage-grouse habitat. Journal of Range Management 57:2-19.

Dahlgren, D. K., T. A. Messmer, and D. N. Koons. 2010. Achieving better estimates of greater sage-grouse chick survival in Utah. Journal of Wildlife Management 74:1286-1294.

Dahlgren, D. K., M. R. Guttery, T. A. Messmer, D. Caudill, R. D. Elmore, R. Chi, and D. N. Koons. 2016. Evaluating vital rate contributions to greater sage-grouse population dynamics to inform conservation. Ecosphere 7.

Dobkin, D. S., A. C. Rich, and W. H. Pyle. 2008. Habitat and Avifaunal Recovery from Livestock Grazing in a Riparian Meadow System of the Northwestern Great Basin. Conservation Biology 12(1): 209–221., doi:10.1111/j.1523-1739.1998.96349.x.

Doherty, K. E., D. E. Naugle, J. D. Tack, B. L. Walker, J. M. Graham, and J. L. Beck. 2014. Linking conservation actions to demography: grass height explains variation in greater sage-grouse nest survival. Wildlife Biology 20:320-325.

Dreitz, V. J., K. Reintsma, K. Ruth, and L. Berkeley. 2019. Migratory songbird grazing study. Annual progress report to the US Fish and Wildlife Service Grant-in-Aid, or Pittman-Robertson, from the University of Montana, Missoula, and Montana Fish, Wildlife, and Parks, Helena, USA, 25 pp.

Drut, M. S., W. H. Pyle, and J. A. Crawford. 1994. Technical note: diets and food selection of Sage Grouse chicks in Oregon. Journal of Rangeland Management 47:90-93.

Fischer, R. A., K. P. Reese, and J. W. Connelly. 1996. An investigation on fire effects within xeric sage grouse brood habitat. Journal of Rangeland Management 46:194-198.

Fleischner, T. L. 1994. Ecological costs of livestock grazing in western North America. Conservation Biology 8: 629–644.

Fox, J. and S. Weisberg. 2019. An R Companion to Applied Regression, 3rd Edition. Thousand Oaks, CA <https://socialsciences.mcmaster.ca/jfox/Books/Companion/index.html>

Freeman, Elizabeth & Frescino, Tracey & G Moisen, Gretchen. 2019. ModelMap: an R Package for Model Creation and Map Production.

Goosey, H. B., J. T. Smith, K. M. O'Neill, and D. E. Naugle. 2019. Ground-dwelling arthropod community response to livestock grazing: implications for avian conservation. Environmental Entomology 48:1-11.

Gregg, M. A., and J. A. Crawford. 2009. Survival of greater sage-grouse chicks and broods in the northern Great Basin. Journal of Wildlife Management 73:904-913.

Guttery, M. R., D. K. Dahlgren, T. A. Messmer, J. W. Connelly, K. P. Reese, P. A. Terletzky, N. Burkepile, and D. N. Koons. 2013. Effects of landscape-scale environmental variation on greater sage-grouse chick survival. PLOS ONE 8:1-11.

Holechek J. L., R. D. Pieper, and C. H. Herbel. 1998. Range management: principles and practices. 3rd ed. Prentice Hall, Upper Saddle River, New Jersey, USA.Hormay, A. L. 1970. Principles of rest-rotation grazing and multiple-use land management. USDA, Forest Service Training Text. Vol. 4. No. 2200.

Hormay, A. L. 1970. Principles of rest-rotation grazing and multiple use land management. U.S. Forest Service Training Text #4 (2200), U.S. Government Printing Office, 1970, #0-385-056. 25 pp.

Johnson, G. D., and MS Boyce. 1990. Feeding trials with invertebrates in the diet of sage grouse chicks. Journal of Wildlife Management 54:89-91.

Knick, S. T. 1999. Requiem for a sagebrush ecosystem? Northwest Science Forum 73:53-57.

Krausman, P. R., D. E. Naugle, M. R. Frisina, R. Northrup, V. C. Bleich, W. M. Block, M. C. Wallace, and J. D. Wright. 2009. Livestock grazing, wildlife habitat, and rangeland values. Rangelands 31:15-19.

Leu, M., and S. E. Hanser. 2011. Influences of the human footprint on sagebrush landscape patterns. Pages 253-271 *in* S. T. Knick, andJ. W. Connelly, editors. Greater sage-grouse: ecology and conservation of a landscape species and its habitats. Studies in Avian Biology (vol. 38). University of California Press, Berkeley, California, USA.

Londe, D. W., R. D. Elmore, C. A. Davis, S. D. Fuhlendorf, T. J. Hovick, B. Luttbeg, and J. Rutledge. 2021. Fine-scale habitat selection limits trade-offs between foraging and temperature in a grassland bird. Behavioral Ecology <doi:10.1093/beheco/arab012>.

Lüdecke, D., M. Ben-Shachar, I. Patil, and D. Makowski. 2020. Extracting, Computing andExploring the Parameters of Statistical Models using R. Journal of Open SourceSoftware, 5(53):2445. doi: 10.21105/joss.02445 (URL:https://doi.org/10.21105/joss.02445).

Mazerolle, M. J. 2020. AICcmodavg: Model selection and multimodel inference based on (Q)AIC(c). R package version 2.3-1. https://cran.r-project.org/package=AICcmodavg.

McGarigal, K., SA Cushman, and E Ene. 2012. FRAGSTATS v4: Spatial Pattern Analysis Program for Categorical and Continuous Maps. Computer software program produced by the authors at the University of Massachusetts, Amherst. Available at the following web site: http://www.umass.edu/landeco/research/fragstats/fragstats.html

Montana Natural Heritage Program [online]. 2011. Big Sagebrush Steppe. Montana Field Guide. Accessed May 4, 2011. <http://fieldguide.mt.gov/displayES_Detail.aspx?es=5454> > Last accessed Aug 5, 2016.

Montana's State Wildlife Action Plan [MTSWAP]. 2015. Montana. Montana Fish, Wildlife and Parks, Helena, MT. 441 pp.

Naugle, D. E., K. E. Doherty, B. L. Walker, M. J. Holloran, and H. E. Copeland. 2011. Energy development and greater sage-grouse. In S. T. Knick, and J. W. Connelly, editors. Greater sage-grouse: ecology

and conservation of a landscape species and its habitats. Studies in Avian Biology (vol. 38), University of California Press, Berkeley, CA.

Natural Resources Conservation Service (NRCS). 2017. Conservation practice standard: prescribed grazing 528. United Stated Department of Agriculture. < https://www.nrcs.usda.gov/Internet/FSE_DOCUMENTS/stelprdb1255132.pdf > Last accessed Oct 6, 2021.

Open Range Consulting. 2015. Vegetation cover mapping of the Lake Mason, Willow Creek, and North refuges of the Charles M. Russell Wildlife Refuge and the surrounding sage grouse core areas. Report, 16pp.

Paige, C., and S. A. Ritter. 1999. Birds in a sagebrush sea: managing sagebrush habitats for bird communities. Partners in Flight Western Working Group, Boise, ID.

Pal, M., and K. Antil. 2017. Comparison of Landsat 8 and Sentinel 2 data for accurate mapping of built-up area and bare soil.

R Core Team (2020). R: A language and environment for statistical computing. R Foundation for Statistical Computing, Vienna, Austria. URL https://www.R-project.org/.

Rich, T. D., C. J. Beardmore, H. Berlanga, P. J. Blancher, M. S. W. Bradstreet, G. S. Butcher, D. W. Demarest, E. H. Dunn, W. C. Hunter, E. E. Inigo-Elias, J. A. Kennedy, A. M. Martell, A. O. Panjabi, D. N. Pashley, K. V. Rosenberg, C. M. Rustay, J. S. Wendt, and T. C. Will. 2004. Partners in Flight North American Landbird Conservation Plan. Cornell Lab of Ornithology. Ithaca, NY.

Rich, T. D., M. J. Wisdom, and V. A. Saab. 2005. Conservation of priority birds in sagebrush ecosystems. United States Department of Agriculture Forest Service General Technical Report PSW-GTR-191, pp 859-606.

Robinson, N.P., B.W. Allred, W.K. Smith, M.O. Jones, A. Moreno, T.A. Erickson, D.E. Naugle, and S.W. Running. 2018. Terrestrial primary production for the conterminous United States derived from Landsat 30 m and MODIS 250 m. Remote Sensing in Ecology and Conservation. doi:10.1002/rse2.74

Rodewald, P. (Editor). 2015. The Birds of North America: https://birdsna.org. Cornell Laboratory of Ornithology, Ithaca, NY. Last accessed May 2018.

Saab, V. A., and T. D. Rich. 1997. Large-Scale Conservation Assessment for Neotropical Migratory Land Birds in the Interior Columbia River Basin. USDA Forest Service General Technical Report PNW-GTR-399. doi:10.2737/pnw-gtr-399.

Smith, J. T., J. S. Evans, B. H. Martin, S. Baruch-Mordo, J. M Kiesecker, and D. E. Naugle. 2016. Reducing cultivation risk for at-risk species: predicting outcomes of conservation easements for sage-grouse. Biological Conservation 201:10-19.

Smith, J. T., J. D. Tack, L. I. Berkeley, M. Szczypinski, and D. E. Naugle. 2018. Effects of Livestock Grazing on Nesting Sage-Grouse in Central Montana. Journal of Wildlife Management, 82:103-112. doi:10.1002/jwmg.21500.

Thompson, K. M., M. J. Holloran, S. J. Slater, J. L. Kuipers, and S.H. Andersen. 2006. Early brood-rearing habitat use and productivity of Greater Sage Grouse in Wyoming. Western North American Naturalist 66:332-342.

Tronstad, L., G. Jones, M. Andersen, and G. Beauvais. 2018. Modeling and mapping the distribution of invertebrate prey used by Greater Sage-grouse during the early brood rearing period: Report of a pilot project. Report prepared for the Wyoming Landscape Conservation Initiative by the Wyoming Natural Diversity Database, University of Wyoming, Laramie, Wyoming.

U.S. Department of Interior Fish and Wildlife Service (USFWS). 2015. Endangered and Threatened Wildlife and Plants; 12-Month Finding on a Petition To List Greater Sage-Grouse (*Centrocercus urophasianus*) as an Endangered or Threatened Species. Federal Register, pp. 59858–59942.